MONTHLY WEATHER REVIEW

VOLUME 82 NUMBER 1

JANUARY 1954

CONTENTS

U. S. DEPARTMENT OF COMMERCE • WEATHER BUREAU

PUBLICATIONS OF THE U. S. WEATHER BUREAU

As the national meteorological service for the United States, the Weather Bureau issues several periodicals, serials, and miscellaneous publications on weather, climate, and meteorological science as required to carry out its public service functions. The principal periodicals and serials are described on this page and on the inside of the back cover. A more complete listing of Weather Bureau publications is available upon request to Chief, U. S. Weather Bureau, Washington 25, D. C.

Orders for publications should be addressed to the Superintendent of Documents, Government Printing Office, Washington 25, D. C.

MONTHLY WEATHER REVIEW

First published in 1872, the Monthly Weather Review serves as a medium of publication for technical contributions in the field of meteorology, principally in the branches of synoptic and applied meteorology. In addition each issue contains an article descriptive of the atmospheric circulation during the month over the Northern Hemisphere with particular reference to the effect on weather in the United States. A second article deals with some noteworthy feature of the month's weather. Illustrated. Annual subscription: Domestic, $3.50; Foreign, $4.50; 30¢ per copy. Subscription to the *Review* does not include the *Supplements* which have been issued irregularly and are for sale separately.

CLIMATOLOGICAL DATA—NATIONAL SUMMARY

This monthly publication contains climatological data such as pressure, temperature, winds, rainfall, snowfall, severe storms, floods, etc., for the United States as a whole. A short article describing the weather of the month over the United States, tables of the observational data, and a description of flood conditions are supplemented by 15 charts. An annual issue summarizes weather conditions in the United States for the year. More detailed local data are provided in the Climatological Data (by sections) for 45 sections representing each State or a group of States, and Hawaii, Alaska, and the West Indies. Subscription price for either the National Summary or for a Section: $1.50 per year (including annual issue), 15¢ per copy.

(Continued on inside back cover)

The Weather Bureau desires that the *Monthly Weather Review* serve as a medium of publication for original contributions within its field, but the publication of a contribution is not to be construed as official approval of the views expressed.

The issue for each month is published as promptly as monthly data can be assembled for preparation of the review of the weather of the month. In order to maintain the schedule with the Public Printer, no proofs will be sent to authors outside of Washington, D. C.

The printing of this publication has been approved by the Director of the Bureau of the Budget, February 11, 1952.

DEPARTMENT OF COMMERCE
SINCLAIR WEEKS, Secretary

WEATHER BUREAU
F. W. REICHELDERFER, Chief

MONTHLY WEATHER REVIEW

Editor, JAMES E. CASKEY, JR.

Volume 82
Number 1

JANUARY 1954

Closed March 15, 1954
Issued April 15, 1954

THE RATIONAL RELATIONSHIP BETWEEN HEATING DEGREE DAYS AND TEMPERATURE [1]

H. C. S. THOM

Climatological Services Division, U. S. Weather Bureau, Washington 25, D. C.

[Manuscript received December 2, 1953]

ABSTRACT

The probability function of degree days below the base 65° F. is derived from the temperature probability function. Standard statistical analysis is applied to this function to obtain the relationship between mean degree days and mean temperature. This relationship is modified for use with available data and applied in the conversion of a monthly normal temperature for Detroit to the corresponding degree day normal.

INTRODUCTION

Almost from the time that heating degree days first came into use there has been a need for a rational relationship between temperature and degree-day statistics. The lack of such a relationship has always made it necessary to estimate degree-day means or normals from degree-day records which were often not available and tedious to compile. Temperature means, on the other hand, are already available for most stations and if not, are easy to compute from published data. Such a relationship makes degree-day statistics quickly available from any place with a temperature record. It also removes the difficulties associated with the lack of consistency between temperature and degree-day means which has been troublesome in the past. This has made it difficult to adjust degree-day means for a heterogeneous record. In the recent normals revision program of the Weather Bureau, for example, the usual arithmetical procedures could not be applied to obtain degree-day normals because of the numerous heterogeneities in the records at most stations. With a rational conversion formula available, properly adjusted temperature normals may be converted directly to degree-day normals with uniform consistency. More important than this use, perhaps, is the fact that the rational relationship is basic to the full development of the climatological analysis of degree-day data.

The study reported here is another phase [1] in the development of a general climatological analysis for degree days *below* a given base. With proper modification it may also be employed in the analysis of degree days *above* any base. The probability function of degree days derived here from the temperature distribution will form the basis for the later development of methods for obtaining degree-day probabilities.

THE TEMPERATURE FREQUENCY CURVE

In a previous paper [1] it was observed that the average temperatures of a particular day through a series of years have been found to have a normal probability or frequency function, or to be normally distributed. This probability function describes bell-shaped curves like those shown in figure 1 which are normal frequency curves on temperature scale t.

A normal probability function is known to be completely specified by its mean and standard deviation. The mean serves to locate the curve along the t axis while the standard deviation σ determines its scale, or how widely it is spread along the t axis. In figure 1 it is seen that both frequency curves are located by a mean temperature of 60° F. but have different scales or standard deviations. The curve with a standard deviation of 5.0 is spread out widely along the t axis while the curve with a standard deviation of 2.5 is more closely concentrated about the mean.

[1] Paper presented at 127th National Meeting of the American Meteorological Society, New York, N. Y., January 26, 1954.

289649—54——1

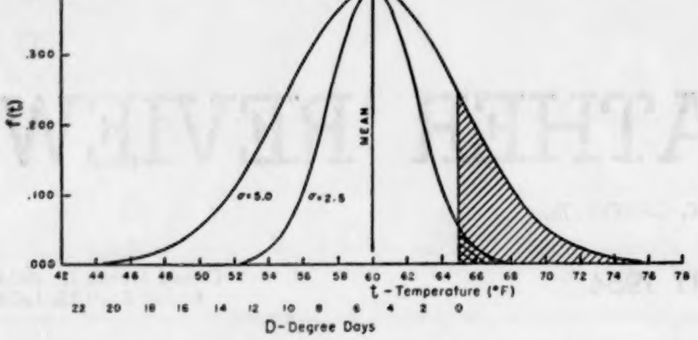

FIGURE 1.—Two examples of normal frequency curves, one for $\sigma=5.0$, the other for $\sigma=2.5$, both with mean temperatures of 60° F. Both the temperature scale t and its transformation by equation (1) to the degree-day scale D, are shown. As t is transformed to D, the distribution of t is transformed into the degree-day distribution. This is the unshaded portion under the temperature frequency curve distributed over the D scale together with an area of probability corresponding to the shaded portion concentrated at zero degree days. The entire distribution of degree days may be represented by the frequency curves shown in figure 2.

It is clear that as a result of these properties two changes may occur in the normal curve and hence in the distribution of temperature: (1) The mean may shift and move the curve to the left or right along the t axis, giving a location at a different value of t. (2) The scale or standard deviation may change causing the curve to spread out or become thinner. These changes are not statistically independent of each other but may be considered as separate component properties. An example of the first type of change is to move the curve $\sigma=2.5$ to the left two degrees of temperature, giving it a new mean of 58° but leaving the scale σ unchanged. The second type of change is represented in figure 1 by a change in scale from $\sigma=2.5$ to $\sigma=5.0$. This spreads the frequency curve without change in its location or mean. Also both types of change could occur together, giving a curve which is spread out as well as displaced along the t scale.

While the discussion of location and scale changes as climatic factors is a subject in itself, it will assist in our explanation of the degree-day distribution to have some understanding of climatic location and scale changes in the temperature distribution. The general principle observed over a wide range of climatic conditions is that the location of the temperature distribution increases as the scale decreases and conversely. This is in contrast to bounded elements such as precipitation where the location, as measured by the mean, varies directly as the scale. Since the location of the temperature distribution varies seasonally, as well as climatically, such variations are reflected in the seasonal march at a given station as well as from station to station for the same season.

The location and scale of the temperature distribution are best measured by the mean and standard deviation of the distribution. These parameters can therefore be related through the general principle. Although the variation of mean temperature with geographic position is not precise, there is, of course, a very marked tendency for it to decrease with increasing distance from the equator. Since the mean and standard deviation vary inversely, the standard deviation increases with increasing distance from the equator. In general then, the mean decreases with latitude while the standard deviation increases with latitude. Similarly in seasonal variation the mean is higher in summer and lower in winter and hence the standard deviation is lower in summer and higher in winter.

Large bodies of water have a great effect on the relation between location and scale of the temperature distribution. The pronounced effects of decreasing the rate of change of mean temperature with latitude and the narrowing of the range between summer and winter are well known. The effect on the standard deviation is even more pronounced. As a consequence, standard deviations are stabilized over extended areas along seacoasts and through the seasons in such areas. For example, the standard deviation for January along the east coast of the United States is almost uniform from Maine to Florida while in the interior it is three times larger in Minnesota than in Louisiana. Seasonal variation in the standard deviation is also smaller along the coasts, some stations having nearly the same standard deviation the year around. This occurs particularly along the west coast where the effect is more pronounced because of the prevailing winds off the ocean.

THE DEGREE-DAY FREQUENCY CURVE

These location and scale changes in the temperature frequency distribution produce corresponding changes in the associated degree-day distribution. They may be illustrated by transforming temperature to degree days by the well-known relationship

$$D=65-t, \quad D\geq 0 \tag{1}$$

where D is the degree-day value for a day and t is the day's average temperature in ° F. The inequality on the right is especially to be noted for it is an essential feature of the transformation which converts the t scale to the D scale of figure 1. As t is transformed to D, the distribution of t is transformed into the degree-day distribution. This is the unshaded portion under the temperature frequency curve distributed over the D scale together with an area or probability corresponding to the shaded portion concentrated at zero degree-days. Thus the probability of having degree days greater than zero on a particular day is equal to the unshaded portion below the temperature frequency curve and the probability of having zero degree days is the shaded portion. The manner in which these shaded and unshaded areas vary with the temperature distribution is clearly the key to the relation between temperature and degree-day statistics. Such variations may be interpreted in terms of the location and scale changes discussed above.

Since the degree-day base is fixed at 65° F., all location and scale changes occur in relation to it. With fixed scale or standard deviation, shifts in the mean produce

important changes in the size of the shaded area. As the mean temperature increases, the temperature frequency curve moves toward the right and the shaded area of the curve is increased while the unshaded area is decreased. This produces an increase in the probability of zero degree days and both a decrease in probability of degree days and an increased concentration of the probability at the lower degree-day values. The overall effect is to decrease the mean degree days. For a decrease in mean temperature the shaded portion of the curve decreases while the unshaded portion increases. This produces a decrease in the probability of zero degree days and an increased concentration of probability at higher degree days with a consequent increase in degree days. As the temperature mean moves to low values on the left, the amount of shaded area becomes negligible and the degree-day mean approaches $65-E(t)$ where $E(t)$ is the mean temperature. Thus, as has long been known, the degree-day mean increases as the temperature decreases and at low values is a function of the mean temperature alone. At higher values of mean temperature the shaded area becomes important and must be accounted for through use of both the mean and standard deviation since the size of the shaded area is a function of both parameters.

Variations in the degree-day mean produced by varying the temperature scale or standard deviation are not as easily depicted as those resulting from variation in the mean. With a fixed mean temperature, an increase in standard deviation increases the probability of zero degree days but also spreads the distribution to higher degree days. These changes have opposite effects on the degree-day mean so the effect of scale change is not a simple one and must be accounted for by an analytical relationship. Nevertheless, it is clear that changes in the temperature scale produce marked changes in the degree-day mean and hence must be accounted for in any relationship between degree days and temperature. As will be seen later, the scale or standard deviation is an important variable in the rational relationship.

THE PROBABILITY FUNCTION OF DEGREE DAYS

From the previous discussion it appears that the probability or frequency function of degree days consists of the portion of the temperature frequency curve below 65° and a probability concentrated at zero degree days equal to the probability of temperatures being above 65°. The former is the unshaded portion of the temperature frequency while the latter is equal to the shaded portion of the curve but concentrated at zero degree days. The unshaded portions of the frequency curves are truncated normal distributions which, when compounded with the probability densities at zero degree days, form mixed distributions which are the degree-day distributions. In sampling from such a distribution for a day on which zero degree days may occur, that day will have degree days greater than zero with a probability equal to the

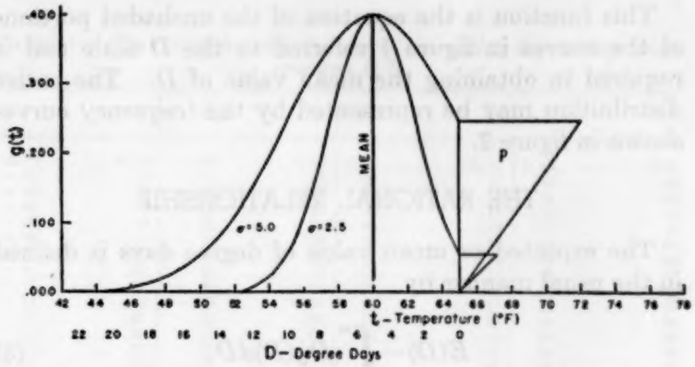

FIGURE 2.—Representation of the entire distribution of degree days, D, for two examples, corresponding to the two temperature frequency curves of figure 1 for which the standard deviations of temperature are 5.0 and 2.5, respectively, and mean temperature is 60° F. Note the area of probability, p, concentrated at zero degree days.

unshaded area of the frequency curve and zero degree days with a probability equal to the shaded portion of the curve. When degree-day values are greater than zero they will be further distributed according to the truncated probability function, the unshaded portion of the curve. They are not further distributed in the shaded portion of the curve, for here they always take the value zero.

The truncated normal distribution has been thoroughly investigated by several statisticians and most of the results we need have been reported in the literature (see [2, 3, 4, and 5]). There remains only to adapt the theory to cover the mixed distribution described above.

Let $F(t)$ be the normal distribution function of the average temperature for a day defined by

$$F(t)=\int_{-\infty}^{t} f(x)dx \tag{2}$$

where $f(x)$ is the normal probability function as shown in figure 1. Evidently $F(t)$ is the probability that an average temperature is less than t, and hence the probability that the average temperature is above the degree-day base is $p=1-F(65)$ and below the base is $q=F(65)$. Performing the transformation to degree days by equation (1), the distribution of degree days is

$$G(D|D\geq 0)=p+qF(65-t|t\leq 65) \tag{3}$$

where G gives the probability of less than D degree days and F is the normal distribution truncated at 65° (c. f. [2]). It will be noted that $G(0)=p$ which is the probability of the average temperature being 65° or greater, and hence is the probability of zero degree days. When $D\geq 0$, G is equal to p plus the probability of temperature being between 65° and some assigned lower value.

The probability function for degree days is the derivative of (3) which is

$$g(D|D\geq 0)=qf(65-t|t\leq 65). \tag{4}$$

This function is the equation of the unshaded portions of the curves in figure 1 referred to the D scale and is required in obtaining the mean value of D. The entire distribution may be represented by the frequency curves shown in figure 2.

THE RATIONAL RELATIONSHIP

The expected or mean value of degree days is defined in the usual manner by

$$E(D)=\int_0^\infty Dg(D)dD. \tag{5}$$

Applying this operation to the right hand side of equation (4) it is found that [2, 3]

$$E(D)=q[65-E(t)+\lambda\sigma]. \tag{6}$$

Here $E(t)$ is the mean temperature, σ is the standard deviation [1], and $\lambda=f(65)/F(65)$. Tables of the reciprocal of this function have been prepared by Pearson [4]. Assuming that t is normally distributed, (6) is the exact relationship between mean temperature and mean degree days. Since $E(t)$ and σ completely define the normal distribution which in turn determines q and λ, the mean value of D is easily found when $E(t)$ and σ are known. Values of F and f are given as functions of the argument $(t-E(t))/\sigma$ in any table of the normal probability function. q and λ are evaluated at $t=65$ and for convenience we designate $(65-E(t))/\sigma$ as h.

For $\sigma=5.0$ and $E(t)=60$ as shown in figure 1, it is seen that the base 65 is one standard deviation above the mean so, from tables of the normal distribution, $q=0.841$ and $\lambda=0.242/0.841=0.288$. Hence the degree-day mean for a day with $\sigma=5.0$ and $E(t)=60$ is

$$E(D)=.841[65-60+(0.288)5]=5.4.$$

APPLICATION OF THE RATIONAL RELATIONSHIP

The rational relationship applies to the means of daily degree days. However our interest is primarily in monthly means so the relationship will be adjusted to give these di-

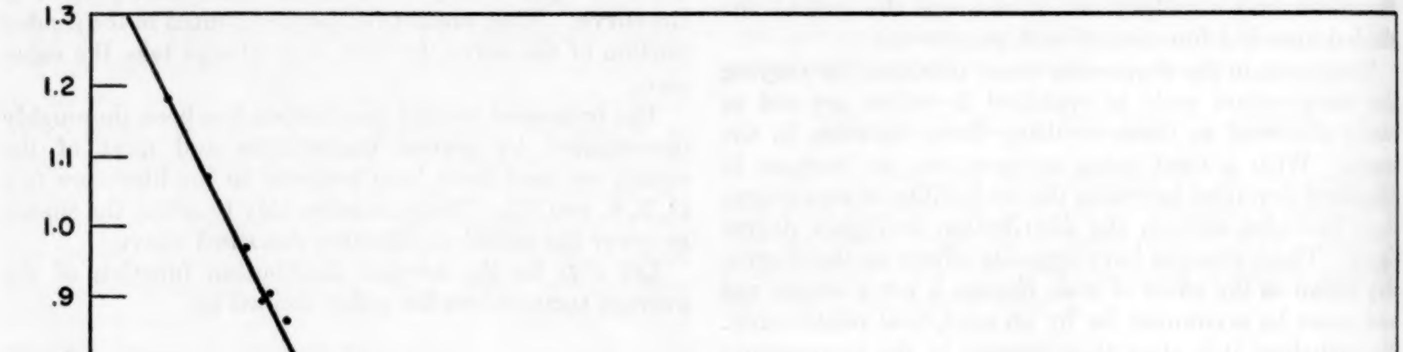

FIGURE 3.—The empirical relationship of l vs. h. The dots are observed values of l against h.

rectly. A simple way of doing this is to determine the relationship for a hypothetical average day of the month and multiply the resulting degree days by the number of days in the month. This average day is not a real day on which any particular average occurs, but a hypothetical day whose mean and standard deviation are such that when the conversion is made to degree days and the result multiplied by the number of days in the month the result is the mean degree days for the month.

In adjusting the relationship to obtain monthly statistics it was found convenient to use the standard deviation of monthly average temperature which is a function of the daily standard deviation and much easier to obtain. If σ is the standard deviation for the average day as above, σ_m the standard deviation of the monthly average, and r the mean correlation between all days for a month of N days, it may be shown [5] that

$$\sigma=\frac{\sqrt{N}\sigma_m}{\sqrt{1+(N-1)r}}$$

Since the factor $(1+Nr)$ is not known but does not seem to vary greatly from station to station, we let it be accounted for in the overall proportional adjustment to the rational relationship by assuming

$$\sigma=\sqrt{N}\sigma_m. \tag{7}$$

Since σ for a single day is known only proportionally, q, which is a function of h, will also be known only proportionally. The approximation we need may be obtained by rearranging the rational relationship (6) in the form

$$\lambda-\frac{E(D)}{\sigma}\frac{(1-q)}{q}=\frac{E(D)-65+E(t)}{\sigma} \tag{8}$$

Substituting $\sqrt{N}\sigma_m$ for σ and l for the term on the left, we find

$$l=\frac{E(D)-65+E(t)}{\sqrt{N}\sigma_m} \tag{9}$$

Since all of the variables in (8) are functions of h, l will also be a function of h. Solving (9) for $NE(D)$, the mean monthly degree days, gives

$$NE(D)=N(65-E(t)+l\sqrt{N}\sigma_m). \tag{10}$$

Next, l can be established as a function of h by plotting observed values of l against h. These values were computed from 30-year records at 30 stations representing all climatic conditions in the United States. The data which are for all of the 12 months are shown plotted on figure 3 together with the empirical l vs. h relationship. It is to be noted that the relationship is independent of climate and season and is only dependent on the parameters of the temperature frequency distribution. In this respect the l-function is general, like the λ-function, in that it is also dependent only on h. It is also similar in shape to the

TABLE 1.—*The factors h and l, for use in computing degree days from equation (10)*

h	l	h	l	h	l	h	l
−0.70	0.70	−0.32	0.39	0.05	0.17	0.42	0.05
−.69	.70	−.31	.38	.06	.17	.43	.05
−.68	.69	−.30	.38	.07	.16	.44	.04
−.67	.68	−.29	.37	.08	.16	.45	.04
−.66	.67	−.28	.36	.09	.15	.46	.04
−.65	.66	−.27	.36	.10	.15	.47	.04
−.64	.65	−.26	.35	.11	.14	.48	.04
−.63	.64	−.25	.34	.12	.14	.49	.03
−.62	.63	−.24	.34	.13	.13	.50	.03
−.61	.62	−.23	.33	.14	.13	.51	.03
−.60	.61	−.22	.32	.15	.13	.52	.03
−.59	.60	−.21	.32	.16	.12	.53	.03
−.58	.59	−.20	.31	.17	.12	.54	.03
−.57	.58	−.19	.30	.18	.11	.55	.03
−.56	.58	−.18	.30	.19	.11	.56	.02
−.55	.57	−.17	.29	.20	.11	.57	.02
−.54	.56	−.16	.29	.21	.10	.58	.02
−.53	.55	−.15	.28	.22	.10	.59	.02
−.52	.54	−.14	.27	.23	.10	.60	.02
−.51	.53	−.13	.27	.24	.09	.61	.02
−.50	.53	−.12	.26	.25	.09	.62	.02
−.49	.52	−.11	.25	.26	.09	.63	.02
−.48	.51	−.10	.25	.27	.08	.64	.02
−.47	.50	−.09	.24	.28	.08	.65	.01
−.46	.50	−.08	.24	.29	.08	.66	.01
−.45	.49	−.07	.23	.30	.07	.67	.01
−.44	.48	−.06	.23	.31	.07	.68	.01
−.43	.47	−.05	.22	.32	.07	.69	.01
−.42	.47	−.04	.22	.33	.07	.70	.01
−.41	.46	−.03	.21	.34	.06	.71	.01
−.40	.45	−.02	.20	.35	.06	.72	.01
−.39	.44	−.01	.20	.36	.06	.73	.01
−.38	.44	.00	.19	.37	.06	.74	.01
−.37	.43	.01	.19	.38	.06	.75	.01
−.36	.42	.02	.18	.39	.05	.76	.01
−.35	.41	.03	.18	.40	.05	.77	.01
−.34	.41	.04	.17	.41	.05	.78	.00
−.33	.40						

For $h \geq 0.78$, $l=0$
For $h \leq -0.70$, $l=-h$

λ-function and has analogous limiting properties, e. g., $l=-h$ for large values of $-h$, and $l=0$ for $h\geq 0.78$. Values read from figure 3 have been entered in table 1 for convenience in use.

In order to use (10) to compute normal monthly degree days, a set of manuscript charts has been prepared showing isolines of monthly standard deviations, s_m. Using the appropriate value of s_m and the normal value of the temperature, $\bar{t}$, as estimates of σ_m and $E(t)$, h may be readily calculated. Entering the table or graph with this value of h one finds the proper value of l. Substituting this together with $\bar{t}$ and s_m in (10) and multiplying by N, the number of days in the month, gives the degree-day normal $N\overline{D}$ a statistical estimate of $NE(D)$.

As an example, for September at Detroit we find the normal temperature $\bar{t}=64.3$ and the standard deviation $s_m=2.7$. Then h is easily found to be $(65-64.3)/(5.48)(2.7)=0.047$. For this value of h table 1 gives $l=0.17$ and hence $\sqrt{N}ls_m=(5.48)(2.7)(0.17)=2.51$. Substituting in (10) gives

$$N\overline{D}=30(65-64.3+2.51)=96$$

This is Detroit's degree-day normal for September.

REFERENCES

1. H. C. S. Thom, "Seasonal Degree-day Statistics for the United States", *Monthly Weather Review*, vol. 80, No. 9, Sept. 1952, pp. 143–149.

2. Harold Cramér, *Mathematical Methods of Statistics*, Princeton University Press, Princeton, 1946, pp. 247–248.
3. R. A. Fisher, "Sampling Error of Estimated Deviates", etc., British Association, *Mathematical Tables*, vol. 1, 1931, p. xxxiii.
4. Karl Pearson (Editor), *Tables for Statisticians and Biometricians*, Part II, Cambridge University Press, London, 1931, pp. xxx and 11.
5. John F. Kenney, *Mathematics of Statistics*, Part II, D. Van Nostrand Co., New York, N. Y. 1939, p. 101.

PRESSURE DROP IN A DUST DEVIL

ROY E. WYETT

Weather Bureau Regional Office, Salt Lake City, Utah

[Manuscript received January 8, 1954]

At about 1620 MST on August 12, 1953, the Airways Operations Specialist on duty at St. George, Utah, stepped out the door of the CAA Communications Station to begin the 1628 MST observation. Swirling directly toward him was a rising column of dust, sand, paper and other debris, rising to an estimated height of 50 feet—a dust devil, quite common to these semiarid valleys of the Intermountain Region during hot, dry days. This particular dust devil was unusual, however, in that it was about 200 yards south to south-southeast of the station's microbarograph (standard Weather Bureau equipment with a double dashpot), and was traveling directly toward that instrument. (See fig. 1.)

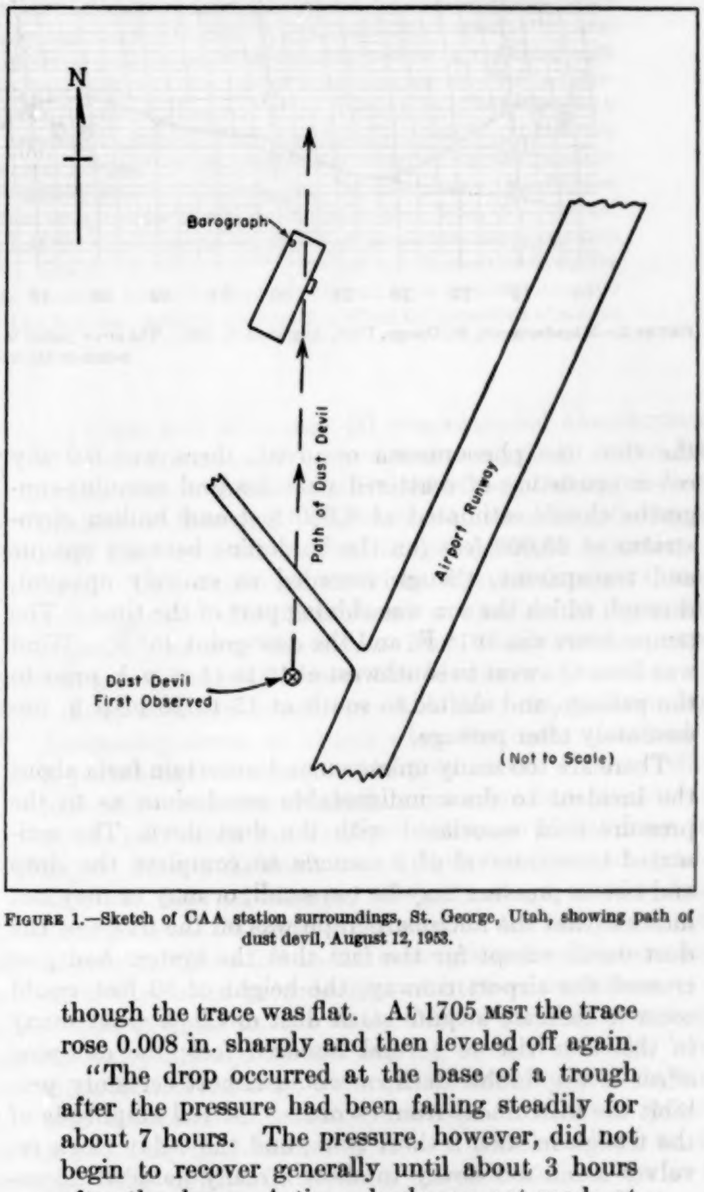

FIGURE 1.—Sketch of CAA station surroundings, St. George, Utah, showing path of dust devil, August 12, 1953.

Proceeding with the observation, the observer had returned to the office when the dust devil passed over the building. Windows and doors on the east-southeast side of the building were all open, and as the cloud of dust and sand swirled into the office and as papers began scattering throughout the building, the observer's attention was drawn to the microbarograph, which had just begun to fall rapidly. Its downward traverse halted sharply, then reversed, leaving a vertical line the width of the pen-point, with an amplitude of 0.04 inch of mercury. The total time elapsed during this fall and rise was estimated to be 3 seconds.

The dust devil proceeded northward after passing over the station, as indicated in figure 1. From the estimated line of travel, it appears that the microbarograph was 8 to 10 feet to the left of center of the dust devil and could not have reacted to the lowest pressure within the storm. The diameter of the system was roughly estimated to be 50 to 60 feet.

The microbarogram showing the pressure drop with the passage of the dust devil is reproduced in figure 2. The following analysis of the barogram was made in the Scientific Services Division of the Central Office:

"Examination of the 4-day microbarograph trace from St. George, Utah (CAA) for August 12, 1953 shows an apparently instantaneous drop and rise in pressure of 0.040 in. at approximately 1625 MST. This drop was preceded at 1610 MST by a slight drop of 0.005 in. in 5 minutes and a rise at 1615 MST of 0.010 in. in 10 minutes. The trace was unsteady from 1625 until about 1705 MST, showing amplitudes of the order of 0.005 in. although the trace was flat. At 1705 MST the trace rose 0.008 in. sharply and then leveled off again.

"The drop occurred at the base of a trough after the pressure had been falling steadily for about 7 hours. The pressure, however, did not begin to recover generally until about 3 hours after the drop. A time check was not made at (or about) 1800 MST as was the pattern of the rest of the chart. The drop-off itself is rather indistinguishable from most of the time checks made on the trace."

The weather throughout the day had been partly cloudy to cloudy, with occasional thunderstorms in the area. At

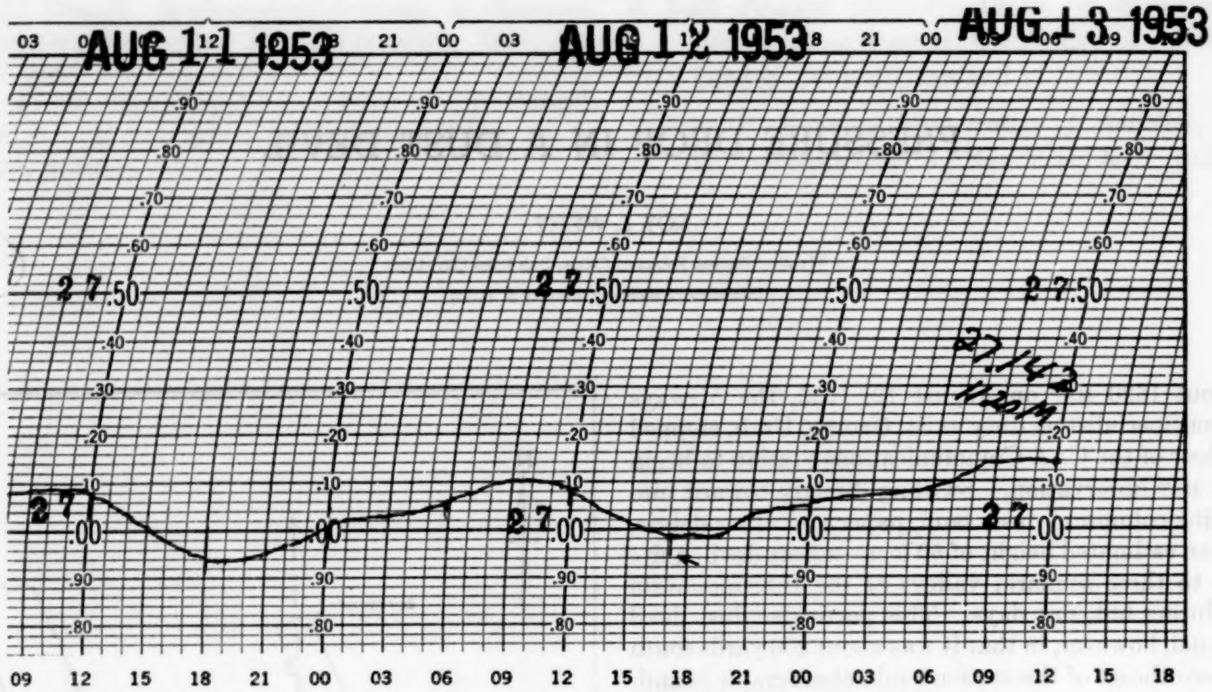

FIGURE 2.—Microbarogram, St. George, Utah, August 11–13, 1953. The arrow points to the pressure drop trace of the dust devil, August 12, 1953. Similar vertical marks at other points on the trace are time checks.

the time the phenomenon occurred, there was 0.9 sky cover consisting of scattered cumulus and cumulus-congestus clouds estimated at 8,000 feet and broken cirrostratus at 25,000 feet (on the borderline between opaque and transparent, though recorded as entirely opaque), through which the sun was shining part of the time. The temperature was 101° F. and the dew point 45° F. Wind was from the west to southwest at 10 to 14 m. p. h. prior to the passage, and shifted to south at 15 to 20 m. p. h. immediately after passage.

There are too many unknown and uncertain facts about the incident to draw indisputable conclusions as to the pressure field associated with the dust devil: The estimated time interval of 3 seconds to complete the drop and rise in pressure may be too small, or may or may not indicate that the microbarograph was on the fringe of the dust devil; except for the fact that the system had just crossed the airport runway, the height of 50 feet would seem to indicate a quite small dust devil—a great many in this area rise to several hundred feet; the damping effect of the double dashpot would almost certainly prohibit the instrument from recording the full amplitude of the trough in such a short time; and the 4-day clock revolves much too slowly to allow a really detailed microanalysis of the barogram.

Despite these indefinite items, it was interesting to note the amount of pressure drop actually recorded; it should prove even more interesting if a systematic dust-devil-observing project could be accomplished, utilizing undamped barographs with accelerated clocks stationed at intervals of perhaps 50 yards across (or around) areas known to produce frequent dust devils, and predetermined observing criteria for size and height of phenomena, direction and speed of movement, and possibly temperatures at one-foot intervals up to 15 or 20 feet above the ground.

ACKNOWLEDGMENTS

The author wishes to express his appreciation to Dr. Morris Tepper of the Scientific Services Division for his interest in the original Field Aide report, and for his suggestion that this note be written for publication; to Mr. W. A. Hass of the Scientific Services Division for his analysis of the barogram; and to Mr. Thomas F. Janik, Airways Operation Specialist and Weather Observer at St. George, Utah, for his clear, concise notes on Form WBAN-10 CAA and his later, more detailed description of the occurrence of the dust devil.

SOME OBJECTIVE QUANTITATIVE CRITERIA FOR SUMMER SHOWERS AT MIAMI, FLORIDA

ROBE B. CARSON

Weather Bureau Airport Station, Miami, Fla.

Original manuscript received June 23, 1952; final revision received October 28, 1953

ABSTRACT

A brief review of previous efforts in Florida and elsewhere to cope with the problem of summer air mass showers is followed by a new attempt to apply to the Miami problem empirical methods of determining the combined effect of several often contradictory shower parameters. Employing the hypothesis that criteria differ seasonally, geographically, and diurnally, this study classifies Miami summer soundings into four rainfall producing types for each of the two diurnal periods and presents averaged dry bulb, wet bulb, and dew point temperatures by 50-mb. intervals to 450 mb. for each type. In addition the heights of the 700-mb. surface and of the freezing level, together with corresponding changes by half days up to three days, are recorded by types. From these and related data, inductive reasoning suggests mechanisms for endemic shower types, and parameters are selected for determining precipitation during the 12-hour period following either sounding. Probability curves that represent also quantitative rainfall are drawn from four summer seasons' data. Contingency tables are given for the dependent objective data, two seasons' independent objective data, and one season of corresponding 12-hour forecasts. In terms of skill score the subjective forecasts are found to be inferior at 1500 GMT and slightly superior at 0300 GMT. Principal conclusions include the finding that Miami showers are more closely related to the absolute humidity through a broad layer centered near 800 mb. than to moisture in higher or in surface levels, and that heavier showers may be inhibited by excessive absolute humidity above 650 mb.

CONTENTS

THE MIAMI SHOWER PROBLEM

It is now well known by weathermen that their middle latitude tools are of little use in the Tropics. A central problem of tropical meteorology therefore is to find suitable methods and techniques for analysis and prediction. Among the few low latitude map features that have been seriously appraised for diagnostic and forecasting value, perhaps the best known are the 24-hour isallobaric pattern and the easterly wave. However, Byers and Rodebush [1] found traveling synoptic features "too rare or remote to account for typical weather patterns over the [Florida] peninsula." Similar conclusions have been reached by others, and some difficulties in using easterly waves as forecasting aids have been reported by Folling [2] and by Durham et al [3].

Palmer and Ellsaesser [4] recommended abandonment of conventional surface pressure analysis in lower latitudes, even in those of the United States, and urged direct analysis of the wind field, which can be observed directly with less error where the diurnal pressure variation is large. Unfortunately, the kind of streamline microanalysis suggested is difficult and subjective at best, and especially so over the oceans from which much summer convective activity crosses the Florida east coast.

Despite these handicaps, it is easy to produce high forecasting scores at Miami when these are measured as a percentage of rain-no rain predictions. These reflect generally monotonous and unusually fine weather in which conditions can be depended on to repeat for a few days. It is a different story when forecasts are graded only on days of change; the percentage correct drops close to zero. More as a rule than as the exception, rains of 6 to 10 inches fall on the same generalized shower forecasts that often precede days of little or no rain.

The complex nature of the Miami problem was noted several years ago by Abrams [5], who wrote that "aside from frontal showers, Miami is affected by both daytime and nocturnal convective activity . . . shower periods are *usually* detectable if a careful watch is kept on the sounding which will show up the *characteristic rise in the height of the moist layer*" (italics mine). A study by the United States Weather Bureau [6] has shown that between 0000 and 0600 EST Miami has more summer thunderstorms than any other part of peninsular Florida except Key West; that between 0600 and 1200 EST Miami leads in

thunderstorm activity; while in the period 1200–2400 EST Miami has fewer thunderstorms than any other part of peninsular Florida except Key West. Despite this, the majority of Miami thunderstorms occur in the afternoon. A later study by Bovinett [7] of July thunderstorms at Weather Bureau Office, Miami (1945 through 1948) also shows that these are far more common between the hours of 1100 and 1700 EST.

Two local rainy season shower types have been described by Thomas [8]. The first is associated with a deep easterly current which produces showers and thunderstorms mostly at night and during the forenoon; the second has shallow southerly winds veering to southwest below 10,000 feet, producing afternoon thundershowers which develop over land southwest of the airport. "In both cases," he states, ". . . relatively little activity is to be expected if a stable layer and dry air are present below 8000 feet." Bovinett's study showed that in July 1946 and 1947 southwesterly winds at 850 mb. produced thunderstorms only in the afternoon; south and southeasterly winds, at any hour but chiefly between 1200 and 1600 EST; easterly winds, only between 0700 and 1100 EST (except rarely between 1600 and 2000 EST). Other directions gave few or no thunderstorms.

The role of classical parameters in these showers has been obscure. Hurley [9], in a study of summer thunderstorms at Banana River, Fla., noted that (1) the surface to 650-mb. average lapse rate for thunderstorm days differed from that for other days by only 1.2° C., (2) there was no reliable correlation between positive and negative energy areas and thunderstorm frequency, (3) there appeared to be no correlation between wind shear and thunderstorm frequency, (4) a relatively thick layer of moist air—3,000 to 4,000 meters—was necessary for widespread thunderstorm activity. The last observation, singularly in agreement with others noted above, offered perhaps the best clue for identification of thundery days. A few years later Baum [10] concluded that occurrence or nonoccurrence of Florida thunderstorms could not be determined by purely thermodynamic considerations, even when the moisture content was taken into account. A study by the United States Weather Bureau [6] reported average lapse rates to be coincident for those stations reporting showers and/or thunderstorms and those not doing so, and Chalker [11] obtaining similar results concluded that the effect of the lapse rate is greatly overshadowed by the role of relative humidity in many cases. Beebe [12] reported from Atlanta the abandonment of the parcel method as a forecasting tool. Further evidence that criteria for air mass thunderstorms were not everywhere in accord with classical concepts came from a study by Means [13], who found a relationship between thunderstorms and "cross pattern" trends in the central United States; charts presented in support of this relationship show plainly that the large May-July increase in thunderstorm activity in northwestern Florida is unrelated to this factor.

The work of Gentry [14] offered for the first time a systematic analysis of the Miami showers as related to the wind field, humidity, and convergence at selected levels. A test of his method in 1950 at the Miami Flight Advisory Weather Service Unit showed that it offered improvement over current forecasts, particularly on a skill basis. A disadvantage of the method was the subjectivity inherent in streamline analysis. Nevertheless, the paper demonstrated, after the methods of Brier [15], Thompson [16] and others, an effective means of solving empirically the old riddle of the group effect of many and contradictory rain parameters.

As results to be presented in this study often can be interpreted in terms of diurnal convergence patterns, some findings of recent studies of this factor should be kept in mind. In 1948 Byers and Rodebush [1], seeking a sounder theory of Florida thunderstorm activity, discovered a pronounced 1600 EST diurnal maximum of convergence at 1,000 feet at the centroid of a wind triangle made up of Jacksonville, Miami, and Tampa, produced by afternoon sea breezes entering the peninsula from both sides. Along the Gulf coast, where the double effect did not operate, both convergence and thunderstorm activity were halved. Day [17] has shown that (for July and August 1951) the diurnal convergence pattern over much of southeast Florida is related to but not identical with that reported by Byers and Rodebush for interior Florida. The 1,000-foot convergence maximum occurs instead at 1000 EST, with divergence beginning at 4,000 to 5,000 feet.[1] A daily daytime trigger appears to exist in this part of the State too, but it is much less pronounced and intense, and probably effective only if upper air moisture distribution is just right. Thus if large scale diurnal vertical movement must be taken into account in understanding the showers of the peninsular interior, it seems that smaller scale but regular vertical motion is also a factor to be reckoned with in understanding the conditions of summer showers along the lower east coast. Individual standards of critical moisture distribution may exist over different parts of the peninsula: over the interior, where the strongest afternoon lift is felt, the air rising into the 500-mb. level would be subject to warming by latent heat found at 1000 EST near 650 or 700 mb., while near Miami a higher level, say 550 or 600 mb. would often affect late afternoon positive areas. (Evidence that just such levels at Miami are critical in the production of heavier afternoon showers will be presented in fig. 10c).

Day's data show that at 2200 EST divergence is the rule below 5,000 feet in the area studied. We are then in need of a unique explanation of the troublesome showers that occur in the early hours after midnight. Forecasting of these almost invariably has depended on the forecaster's night vision and observational alertness rather than on sophisticated techniques.

A few other research findings will be mentioned because

[1] The diurnal variation in convergence at these levels explains a local empirical rule regarding a rather dependable failure of middle clouds to persist through the afternoon.

they dovetail into the Miami data to be reported below. According to Showalter [18] tornadoes require, among other things, a layer of moist air near the surface usually extending upward to a level below 10,000 feet, where a distinct dry tongue is favorable. Tillotson [19], comparing the relationship of Denver showers to both the 700-mb. mixing ratio and the averaged value from the surface to 700 mb., reported the *lower* values as better related to thunderstorm activity. Means [13] states "thunderstorm activity seems to be damped *under the warm lid aloft at 700 mb.* in areas where the greatest advance of isotherms at that level has occurred." Lastly, we note that Malkus [20, 21], Stommel [22] and others of the Woods Hole Oceanographic Institution have observed that trade cumulus do not show the well defined, classical columns of unsaturated, warm air rising from deep in the layer of air under the cloud. This group has constructed a tentative model of these clouds showing entrainment of drier air into their windward *sides*. (All italics mine).

THE PROBLEM REAPPROACHED

Data compiled by the United States Weather Bureau [6] presented evidence suggesting that shower criteria are not uniform in space and time. Thunderstorm-producing soundings for July 1942 at Oklahoma City showed slightly lower mixing ratios below 850 mb., with markedly higher values between 800 and 400 mb. at both 1100 and 2300 EST. At Washington, however, such thundery soundings showed considerably higher mixing ratios at all levels below 400 mb. at 1100 EST and differed hardly at all from non-thunderstorm soundings at 2300 EST. These findings are neither particularly consistent with each other nor with such uses as Miami forecasters have learned to make of the Miami sounding. Among the several possible explanations of this fact the following idea has been adopted as a working hypothesis in the preparation of this paper: *shower criteria differ geographically, diurnally, and seasonally.*

In the belief that an investigation was warranted in the Miami area, a detailed study of the Miami soundings for July and August 1950 was made by the author. Confinement of the present approach to the Miami shower problem to these narrow limits appears to be justified, although the following objections might be raised: (1) no account is taken of the wind field, which is of great importance in determining when and if showers will occur at Miami, (2) radiosonde data are not representative of anything more than a very limited section of time and space and cannot be assumed reliable on this account, (3) radiosonde data are themselves subject to large enough errors to nullify efforts to use them, and (4) 2 months is a relatively short period on which to base a study.

Objection (1) is met in part by the following considerations: Although the wind field is a basic source of weather, its direct analysis over oceanic areas is highly subjective. There is a possibility of getting equivalent results from close study of the sounding itself, since it is a product of the wind field. Because low level convergence through a deep layer results in high moisture content, a conservative factor like the mixing ratio may be taken as an index of this convergence, one that has the great advantage of being objective. Similarly, changes in lapse rate may be considered a function of the wind field and hence to some extent a measure of it. It is far from the purpose of this paper to urge that raob analysis be substituted for careful appraisal of the winds aloft; the analysis should instead be added to it. Indeed the ideal solution, one far beyond the time resources of the author, would incorporate additional wind and other parameters to provide for scientific appraisal of all the important shower indices. The present study was limited to raob factors because these must be separately analyzed if we are ever to learn their significance.

Objection (2) has already been considered in part in the discussion of objection (1). Is it likely that the diurnal convergence cycle shown by Day to exist near the centroid and probably generally within an equilateral triangle over 200 miles on its side would often be operative in Opa Locka but not in Coral Gables? Or that the 700-mb. height falls to be studied would often be found over Miami Beach but not Hialeah? This objection amounts to asserting that these conditions are commonplace. With regard to our primary purpose—determining some of the conditions of our *heavier* showers—it seems reasonable to assume that such conditions are rare.

Objection (3) leads us to note that all radiosond observations used were taken after the introduction of lithium chloride hygrometers of less lag than the mechanical type, and after the introduction of instruments less subject to solar radiation. Of course, even the newer instruments are less than perfect, as are observers. Nevertheless, according to the United States Weather Bureau [23], compatibility tests (sponsored by the Air Coordinating Committee) of the several types of radiosondes in use in the United States showed that for all constant-pressure levels up through 400 mb., 61 percent of plotted temperature points agreed within 1° C. and 91 percent within 2° C., and 90 percent of relative humidity points agreed within 10 percent. These tolerances even if aggravated by transmissional errors, are not such as to invalidate practical use of radiosonde data, especially in a study like the present one in which average values are used. The evidence rather indicates that instrumental and observational techniques have already surpassed professional skill in using observational data.

Objection (4) is not pertinent to the purposes of the present study. On the contrary, the relatively short period of 2 months was chosen deliberately. Within this period was a series of several wet and dry spells of the kind forecasters are expected to identify and foresee. If statistical differences are not plainly evident in the soundings of this short period, doubt must attach to

their use at all in day-to-day shower forecasting, since any statistical defects inherent in a 60-day period are multiplied many times over in the shorter period of 1 day.

These considerations seemed to justify the detailed study of the Miami soundings for July and August 1950, and the investigation was started in the fall of 1950. Soundings associated with hurricanes, missing data, or frontal weather (rare in summer) were eliminated. At first, 0300 and 1500 GMT values were lumped together, with tantalizing results that merely suggested that improvement could be had by separating the two diurnal types. These results together with the following consideration led to the final plan to study separately the 0300 GMT and 1500 GMT soundings: It is basic to know precisely what type sounding is required for immediate rain (other factors assumed favorable). If we lack such basic knowledge, any attempt to forecast from trends in either soundings or wind field seems futile. A corollary of this principle: we will have to learn to anticipate these heavy showers by 5 hours before we can hope to do so for 5, or for 30, days.

Soundings for the 2 times were classified into 4 groups according as they produced a total rainfall of zero, trace through 0.05 in., 0.06 through 0.99 in., or $\geq$1.00 in. at the Miami Weather Bureau Office and Weather Bureau Airport Station, combined within the 12-hour period beginning shortly after the sounding was made. (Periods were not quite coincident, being 0130 to 1330 EST and 1330 to 0130 EST at WBAS, and 0000 to 1200 EST and 1200 to 2400 EST at WBO.) The four types will be referred to as D, W, WW, and WWW soundings. Data recorded were dry bulb temperature, wet bulb temperature, and dew point at 50-mb. intervals from 1000 through 450 mb. In addition, the height of the 700-mb. surface, together with the corresponding tendency for periods of 12, 24, 36, 48, 60, and 72 hours preceding were recorded, as well as the pressure in millibars of the freezing level and similar tendency increments up to a period of 72 hours.

Inclusion of the freezing level resulted from a study of the August 1–5, 1950 soundings, which revealed a diurnal pattern in freezing level movement which changed phase by one-half day 36 hours before a heavy rain. This and other evidence suggested that the soundings themselves sometimes offer evidence of vertical movement that would be most difficult to detect in other ways. Just how much of these temperature changes may be due to advection, how much to daytime temperature error, and how much to vertical movement would be a considerable problem in itself, but it seems reasonable to assume that under stagnant summer conditions, at least, no small part of it represents vertical movement.

In classifying the soundings it was noted that WBO and WBAS rainfall closely paralleled each other most of the time. Although these stations are some five miles apart, classifications would have been essentially the same had either WBO or WBAS rainfall been used separately (with standards halved) instead of totally. The chief reason for using figures from both offices was to provide a more representative coverage in space.

THE 0300 GMT SOUNDINGS

SHOWER CHARACTERISTICS

Principal findings will be presented in a few selected tables and figures. We might expect to find significant differences in rainfall-producing ability of the soundings if we compare mixing ratios. In figure 1a we see such a comparison, from 1,000 through 500 mb., for WWW types only, with the 0300 GMT values as the arbitrary standard, and 1500 GMT values shown on a horizontal scale in gm/kg. deviation from the standard. For example, at 950 mb. we see that 1500 GMT WWW soundings averaged 1.9

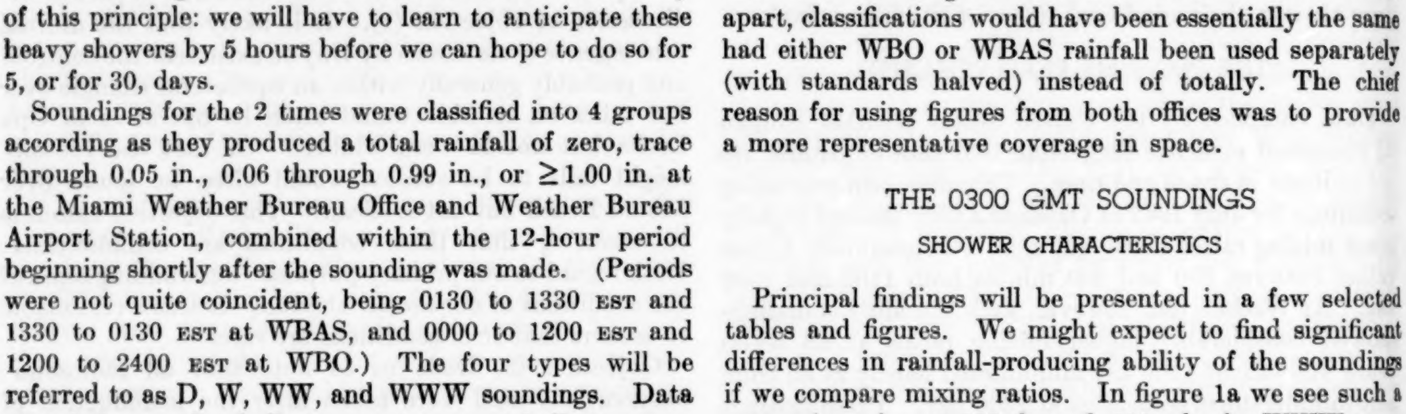

FIGURE 1.—(a) Departure of average mixing ratio (gm/kg) at 1500 GMT from that at 0300 GMT for WWW type soundings. Miami, Fla., July and August 1950. (b) 0300 GMT average change in freezing level pressure (mb.) for various time increments for each of the four shower types. Negative ordinates indicate fall in height (rise in pressure), positive ordinates indicate rise in height (fall in pressure). Miami, Fla., July and August 1950. (c) 0300 GMT average 700-mb. height change (ft.) for various time increments for each of the four shower types. Height falls are negative, rises positive. Miami, Fla., July and August 1950.

gm/kg. higher in moisture than did 0300 GMT WWW ascents. This extra moisture in low levels, together with the relative dryness at 600 and 650 mb. shown by 1500 GMT soundings, suggests that deep convective instability, particularly in low levels, distinguishes afternoon from early morning shower types. From Day's data [17], we note that ordinarily divergence prevails in low levels at 0300 GMT, which would render ineffective from a rainfall-producing standpoint any extra moisture in these low levels. At 1500 GMT however, convergence prevails in these levels, and we see from figure 1a that extra moisture in the low levels is indeed associated with the heaviest rains.

Figure 1b depicts the freezing level tendencies shown by the four shower types at 0300 GMT. Considering the WWW type, it is read in this way: on an average, WWW showed a 12-hour fall in freezing level of 12 mb. (−12, as from 600 to 612 mb.); a 24-hour fall of −1; a 36-hour fall of −22; etc. For the 72-hour change it will be noted that only D soundings had an average rise (+7) while both W and WW averaged no change, and WWW showed large falls of −25 mb. The 3-day freezing level tendency appears, then, to offer possibilities in separating shower types. (Note the diurnal movement apparent especially in WW values; this may be partly due to temperature errors caused by radiational warming of the instrument at 1500 GMT.)

Figure 1c shows similar data for the 700-mb. heights at 0300 GMT. Here the diurnal tendencies are even more pronounced. Changes for 72 hours again offer the best separation, with D, WW, W, and WWW lined up in that order, and with appreciable separation of D from WWW.

In table 1 are average temperatures (°C.) for the four types at 0300 GMT for levels from 1,000 to 450 mb. If these values are plotted on a suitable thermodynamic chart, we see that D, W, and WW lapse rates effectively coincide; that WWW differs in presenting steeper lapse rates above the level of 800 mb., fanning out to a difference of about 2° C. at 450 mb. Steep lapse rates are associated only with the heaviest showers.

TABLE 1.—*0300 GMT average temperatures (° C.) at 50-mb. pressure intervals for the four shower types. Miami, Fla., July and August, 1950*

Pressure \ Type	WWW	WW	W	D
(mb.)	(°C.)	(°C.)	(°C.)	(C.)*
450	−14.0	−11.7	−12.2	−12.3
500	−8.8	−6.8	−7.2	−6.9
550	−4.2	−3.0	−2.7	−2.8
600	−.2	.6	1.0	.7
650	3.4	4.4	4.4	4.3
700	6.8	8.1	8.2	8.0
750	10.4	11.0	11.3	11.3
800	13.6	14.0	14.2	14.4
850	16.4	17.2	17.2	17.5
900	19.6	20.0	20.3	20.3
950	22.4	22.6	22.9	23.1
1,000	25.8	26.0	25.8	26.0

TABLE 2.—*0300 GMT average wet-bulb temperatures (° C.) at 50-mb, intervals for the four shower types. Miami, Fla., July and August 1950*

Pressure \ Type	WWW	WW	W	D
(mb.)	(°C.)	(°C.)	(°C.)	(°C.)
500	−11.4	−10.2	−10.5	−10.8
550	−7.2	−6.3	−6.3	−7.3
600	−3.5	−3.2	−2.6	−3.6
650	0	.1	.5	−.6
700	3.5	4.0	3.9	3.1
750	6.2	7.1	7.3	6.6
800	10.0	10.6	10.5	10.0
850	13.5	14.2	13.6	13.4

Table 2 shows corresponding wet bulb data. These too must be plotted to be evaluated; we are then in a position to compare convective stability. Contrasting D with W, we see appreciable contrasts only in the level from 550 to 500 mb.; W against WW shows no appreciable difference; and WWW, as contrasted to WW, shows great stability differences between 600 and 500 mb. only. We may conclude that light showers following 0300 GMT soundings are associated with slight decreases in convective stability between 550 and 500 mb.; that the factors causing light showers to become moderate are related principally to other considerations; and lastly that the heaviest showers again require further decreases in convective

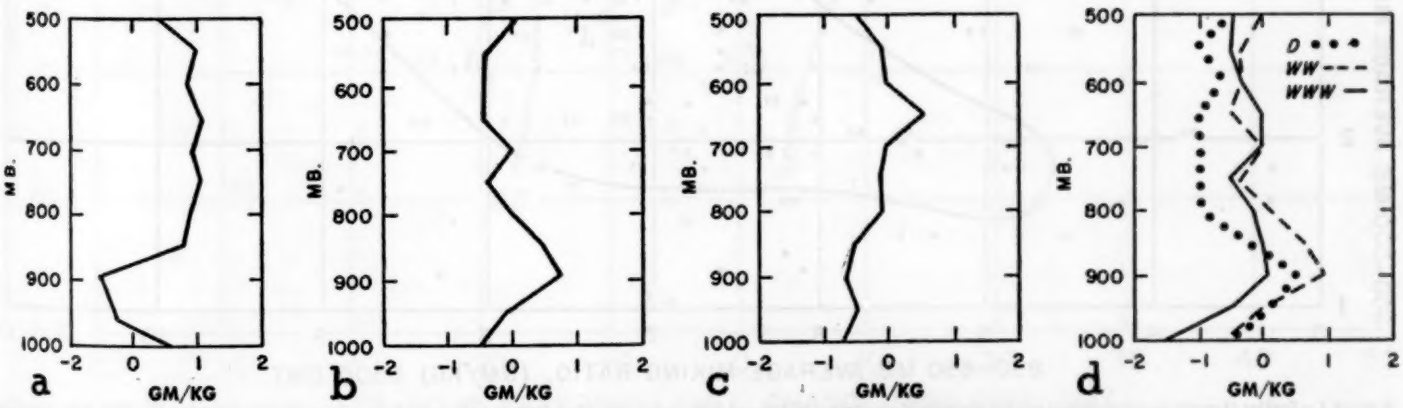

FIGURE 2.—Comparisons between average mixing ratios (gm/kg) for the four types of soundings for 0300 GMT, Miami, Fla., July and August 1950. (a) deviation of W type from D type, (b) deviation of WW type from W type, (c) deviation of WWW type from WW type, and (d) deviation of D, WW, and WWW types from W type (combination of data from figs. a, b, and c).

TABLE 3.—*0300* GMT *average dewpoints (° C.) at 50-mb. intervals for the four shower types. Miami, Fla., July and August 1950*

Pressure \ Type	WWW	WW	W	D
(mb.)	(°C.)	(°C.)	(°C.)	(°C.)
450	−22.5	−21.0	−21.6	−23.0
500	−18.8	−16.0	−16.2	−18.3
550	−12.2	−11.8	−10.4	−14.5
600	−7.8	−7.7	−6.9	−9.3
650	−3.2	−4.5	−3.3	−6.4
700	.7	.6	.5	−1.8
750	3.5	3.8	4.2	2.6
800	8.2	8.7	8.4	6.7
850	11.8	12.5	11.8	11.0
900	14.8	15.7	14.8	15.5
950	18.2	18.7	18.7	19.0
1,000	20.5	21.3	21.8	21.4

TABLE 4.—*0300* GMT *average freezing level (mb.) and average 700-mb. height (ft.) for the four shower types. Miami, Fla., July and August 1950*

Type	Freezing level	700-mb. height
	Mb.	*Feet*
D	587	10,547
W	585	10,497
WW	591	10,524
WWW	602	10,510

stability through a deeper layer from 600 to 500 mb. Returning again to Day's data we are not surprised to note that control of these early morning showers rests in fairly high levels. With normal divergence at 0300 GMT in low levels, it is believed these night showers would ordinarily have to develop within the more flexible layers of 14,000 to 18,000 feet.

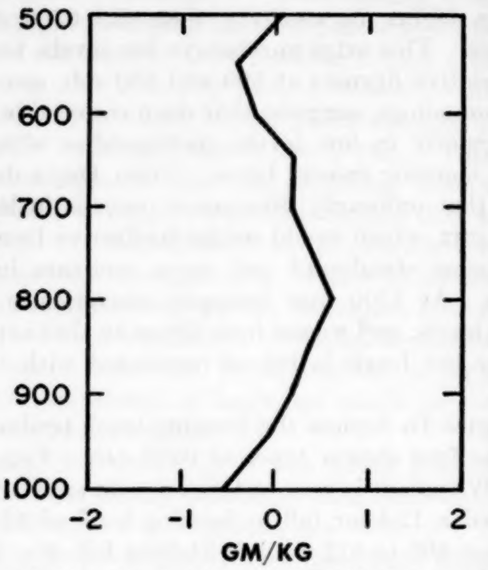

FIGURE 3.—0300 GMT deviation of average mixing ratio (gm/kg) for shower type sounding (W, WW, WWW combined) from that for D type. Miami, Fla., July 1951.

Table 3, presenting dewpoint data, is conveniently analyzed by converting to mixing ratio and plotting on a relative scale where differences can be magnified. In

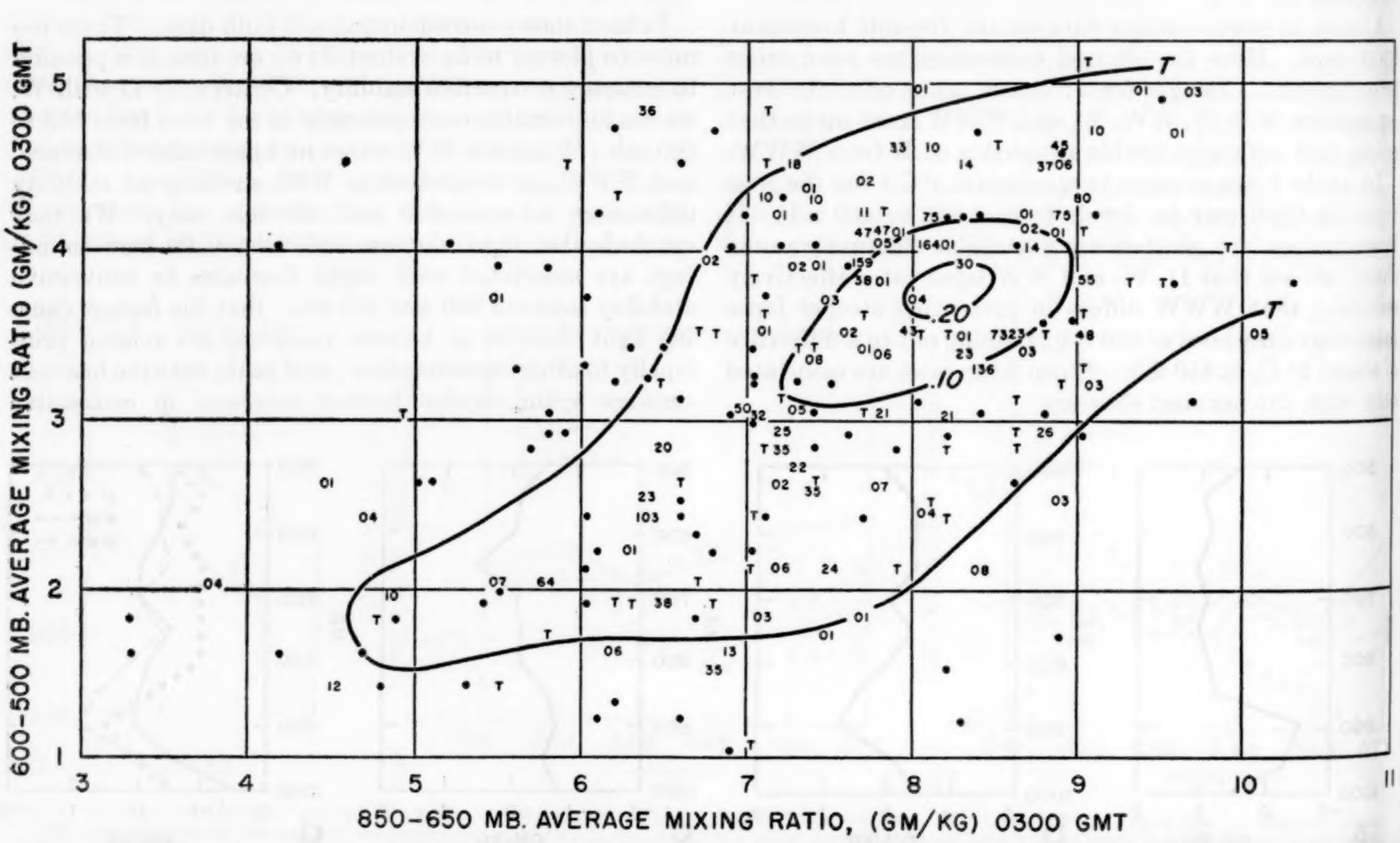

FIGURE 4.—Scatter diagram showing plots of rainfall (average of amounts at WBO and WBAS, Miami, Fla.) during the 12-hour period immediately following the 0300 GMT sounding from which the mixing ratio coordinate values were taken. Dot indicates no rain; T, a trace; and number, a measurable amount (in hundredths of an inch). The empirical curves are isograms of median values of rainfall amounts but may also be interpreted as rainfall frequency: ≥0.20 in. represents a frequency of 85%, and ≤trace a frequency of <50%. Dependent data: July and August 1948–51.

figure 2a, this is done for D and W. Evidently a surge of absolute humidity in the deep layer between 850 and 550 mb. is a characteristic difference in these types. Of particular interest is the "bite" removed at and below 900 mb., which emphasizes that these levels have little to do with producing rain at this time of day when divergence prevails here.

In figure 2b WW is similarly compared with W. As the mixing ratio difference (centered near 700 mb.) between D and W (fig. 2a) is augmented in lower levels—i. e. 900 mb.—the light showers become moderate. Again we note the heavy "bite" in very low levels, which are still plainly unrelated to shower activity.

Figure 2c similarly compares WWW and WW. Here the middle level increase in mixing ratio is augmented at 650 mb., just above the original (fig. 2a) center at 700 mb., producing a mixing ratio surge in the deep layer from 900 to 650 mb. capable of producing heavy showers. In figure 2d, figures 2a, b, and c are combined into a single diagram, with W as the arbitrary standard. This was used because we are aiming chiefly at finding the features that distinguish light showers from heavy showers. Of great interest is the relative drying at 500, 550, and 600 mb. associated with the heavier showers. This indicates that convective instability is a factor in producing the heaviest showers, a fact previously noted.

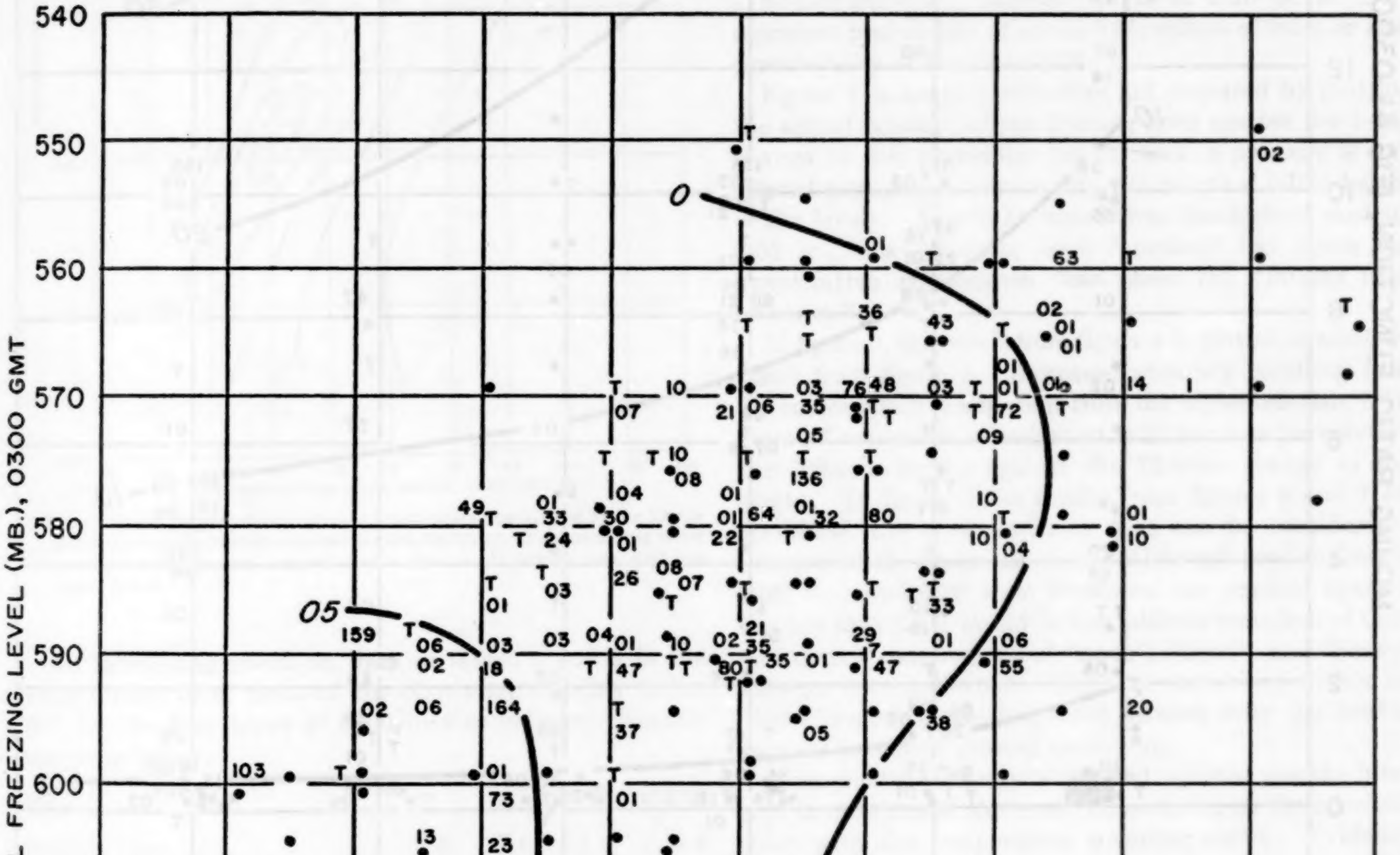

FIGURE 5.—Scatter diagram showing plots of Miami rainfall (as in fig. 4) during the 12-hour period following the 0300 GMT sounding to which the freezing level and freezing level change coordinates correspond. Negative abscissa indicates a fall in height (rise in pressure); positive, a rise in height (fall in pressure). Isograms are interpreted as in figure 4. Dependent data: July and August 1948–51.

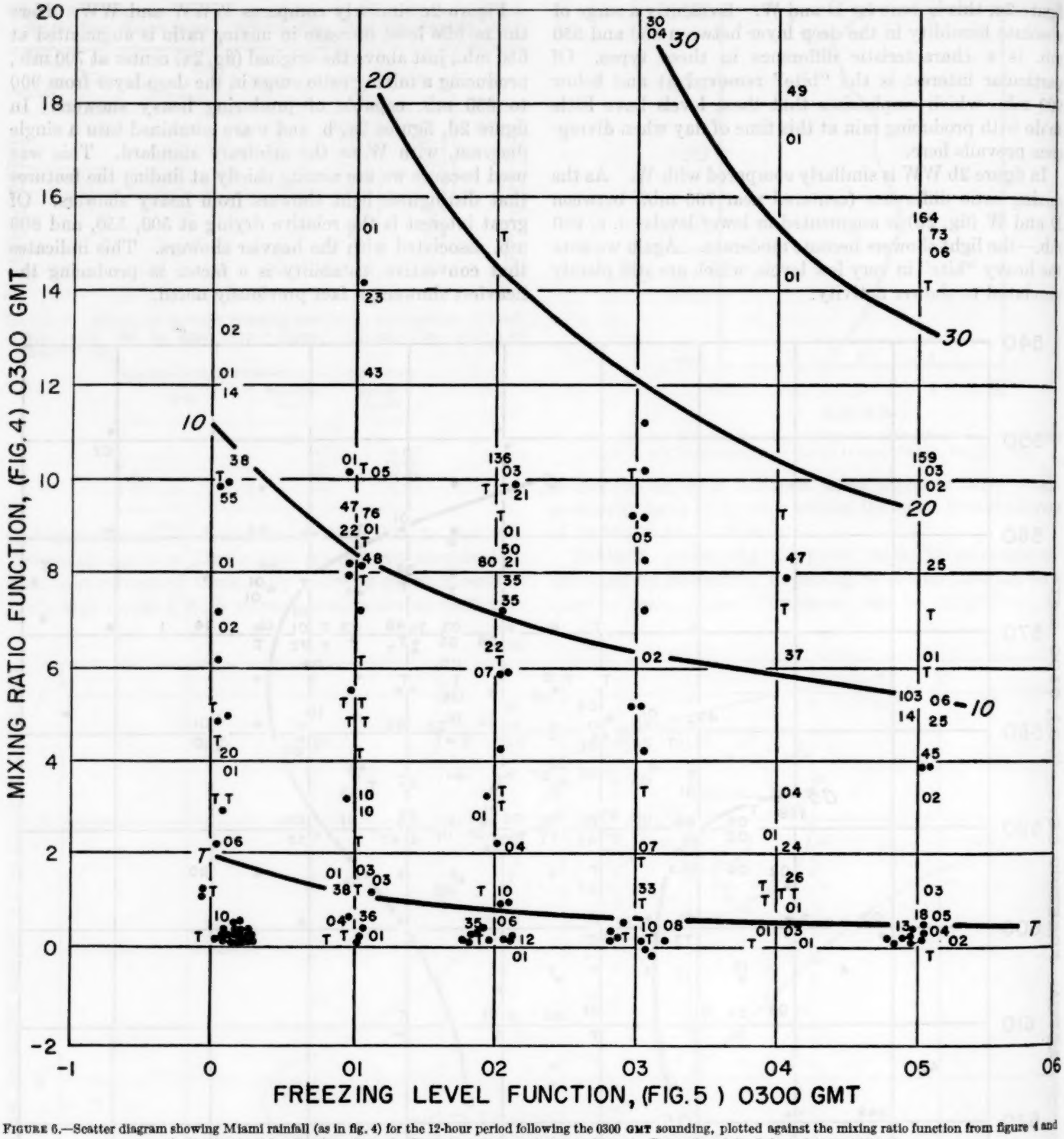

FIGURE 6.—Scatter diagram showing Miami rainfall (as in fig. 4) for the 12-hour period following the 0300 GMT sounding, plotted against the mixing ratio function from figure 4 and the freezing level function from figure 5. Isograms are interpreted as in figure 4. Dependent data: July and August 1948–51.

Table 4 presents, by types, the freezing level and 700-mb. height averages. Note that the heaviest showers had the lowest freezing levels (i. e. highest pressure) with W, WW, and WWW lining up in that order. The 700-mb. heights also, except for the anomalous position of W, present a pattern of increasing shower activity with lowering heights.

In figure 3 is presented evidence from a different year (July 1951) as a check on the validity of the relative drying noted in figure 2d. Data in figure 3 present all shower types in a single group contrasted with non-shower types. The principal difference consists in an 800-mb. mixing ratio surge, together with the relative drying at 550 and 600 mb.

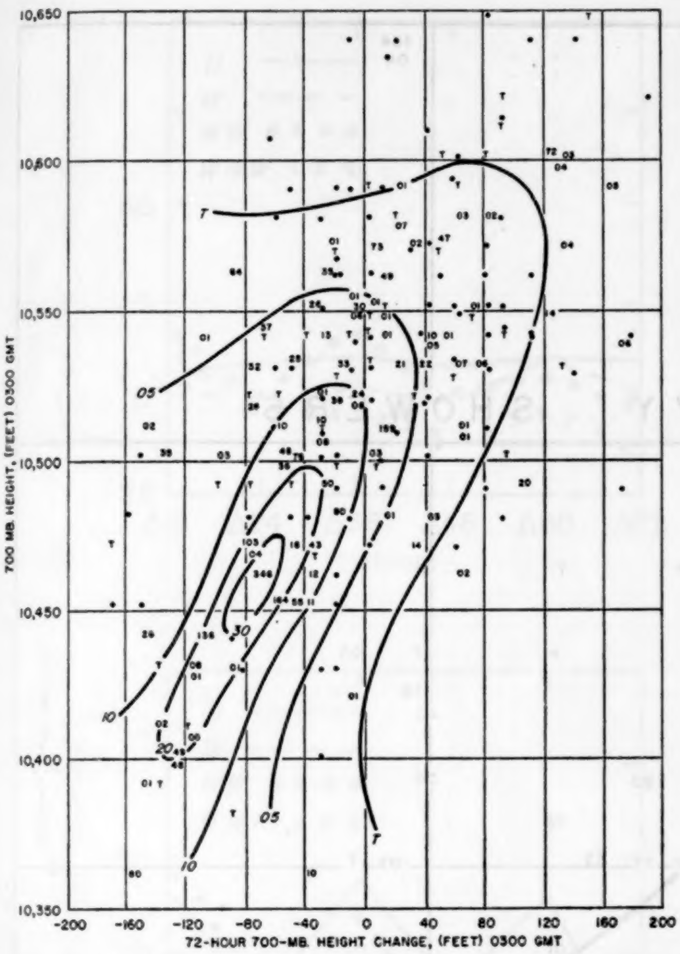

FIGURE 7.—Scatter diagram showing plots of Miami rainfall (as in fig. 4) for the 12-hour period following the 0300 GMT sounding to which the 700-mb. height coordinate values correspond. Isograms are interpreted as in figure 4. Dependent data: July and August 1948–51.

An interesting check on data in tables 1 and 3 is the computation from them of the Showalter stability index [24] for the four types of 0300 GMT soundings. Results are given below:

Type	D	W	WW	WWW
Stability index	2.6	2.0	2.0	0.9

The quantitative value of the index is obvious. We may also note that 0300 GMT summer values are usually much less than the 3.00 generally considered suspect for shower activity.

OBJECTIVE FORECASTING AID

Figure 4 is an objective forecasting aid based on differences noted in the 0300 GMT soundings. The forecast period is of course limited to that used in defining the shower types—the 12-hour period beginning immediately after the sounding is completed. The empirical curves incorporate data from three additional years—1948, 1949, and 1951— making in all four summer seasons. Although raobs have been made at Miami since 1941, some doubt attaches to temperatures given by daytime soundings made before 1947, which means that for best accuracy in 0300 and 1500 GMT data comparisons the period used is almost as long as data presently available will permit. Abscissas represent mixing ratio in the layer from 850 to 650 mb., averaged graphically.[2] Ordinates represent a similarly determined average for the layer 600–500 mb. Isograms drawn are median values for the 12-hour rainfall resulting (an average of Weather Bureau Airport Station and Weather Bureau Office). As a check, rainfall probability values were also entered at various points on the original scatter diagrams. These values were so closely related to the quantitative values that it seemed possible to let a single set of curves serve a double purpose. Median values of 0.20 in. or more represent probability of about 0.85; values of trace or less, a probability of less than 0.50.

Figure 5 is another objective aid prepared by plotting the actual pressure of the freezing level against the 3-day change in this parameter (an increase in pressure is considered negative, corresponding to a physical fall in height of the level). As will be noted from the highest median, 0.05 in., this "freezing level function" has much less quantitative significance than does the "mixing ratio function."

In figure 6, the result from figure 4 is plotted against the result from figure 5. Increased accuracy resulting from the combination is apparent from the higher median, 0.30. Figure 7 represents a fresh start with two new parameters, the 700-mb. height against the 72-hour change in this height. In figure 8 the results from figures 6 and 7 are combined into a single index that can be considered a function of the six parameters. Although median lines of 0.05, 0.10 and 0.20 were drawn on the original figure it was felt that there would be less misinterpretation of these meanings if only regions of "none", "light", and "heavy" showers were indicated. Also, the variability within the "light" region is much greater because only the heavier showers represent general conditions.

A parameter that was tested and rejected was the intercept in millibars of the $-10°$ C. isotherm on the adiabatic chart with the temperature sounding curve. Evidently the *observed* lapse rate in these levels is less important than the *impending* one.

THE 1500 GMT SOUNDINGS

SHOWER CHARACTERISTICS

Figure 9a presents the freezing level movements for the four shower types. These data offer little help in identifying types—certainly less than was seen in figure 2 for 0300 GMT.

[2] A small transparent ruler is laid on the adiabatic chart with its edge parallel to the constant specific humidity lines and crossing the dew-point curve near the middle of the layer. From extremities of the layer, perpendiculars are dropped from the dewpoint to the ruler which is then moved left or right without altering its slope until a point is found such that the sum of the areas enclosed by the ruler edge, the perpendicular and the mixing ratio curve on the left equals that on the right. If the curve is a straight line, the average can be taken, for practical purposes, to be the value at 750 mb.

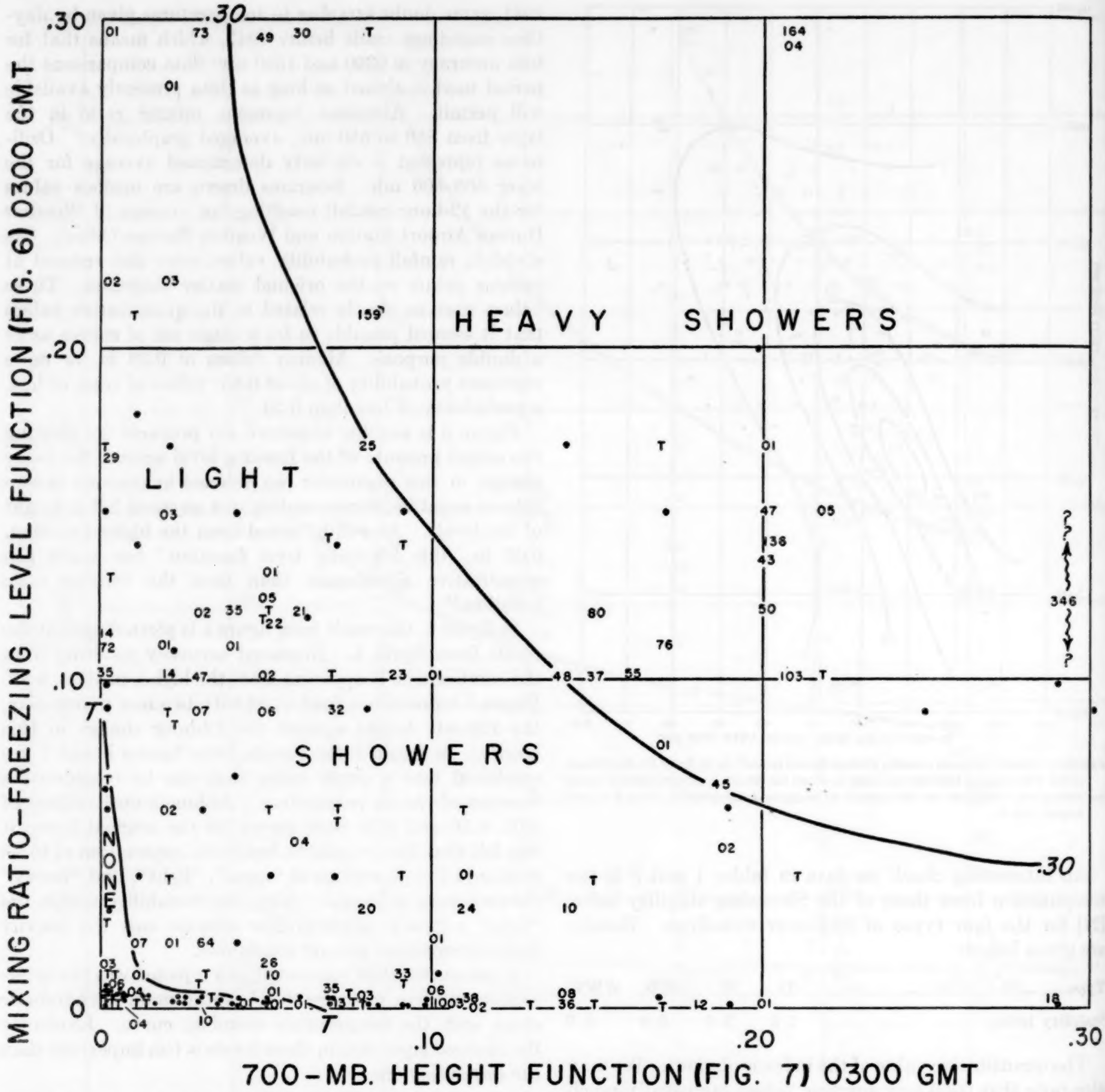

FIGURE 8.—Scatter diagram showing Miami rainfall (as in fig. 4) for the 12-hour period following the 0300 GMT sounding, plotted against the mixing ratio-freezing level function from figure 6 and the 700-mb. height function from figure 7. Isograms, now a function of six parameters, are interpreted as in figure 4. Dependent data: July and August 1948–51.

Figure 9b is of interest when compared to figure 1c, which it resembles only slightly. The zigs of one are the zags of the other. Again we note that 3-day falls tend to distinguish WWW but this time with less suggestion of continuous quantitative significance (D falls between W and WW). The overall downward slope of WWW to the right is perhaps meaningful; note that these heaviest showers occurred just after 12-hour rises of 50 feet and 72-hour falls of 25 feet—that is, on a strong rise following a gradual 3-day fall. This fits accepted patterns of easterly waves, with maximum convergence just after wave crest passage. However a test of this slope as a parameter proved disappointing. Probably a few large values affected the averages in figure 9b enough to suggest qualities less typical than exceptional.

Table 5 gives temperature averages for the four type 1500 GMT soundings. Plotted on an adiabatic chart they show the following contrasts: W lapse rates, as com-

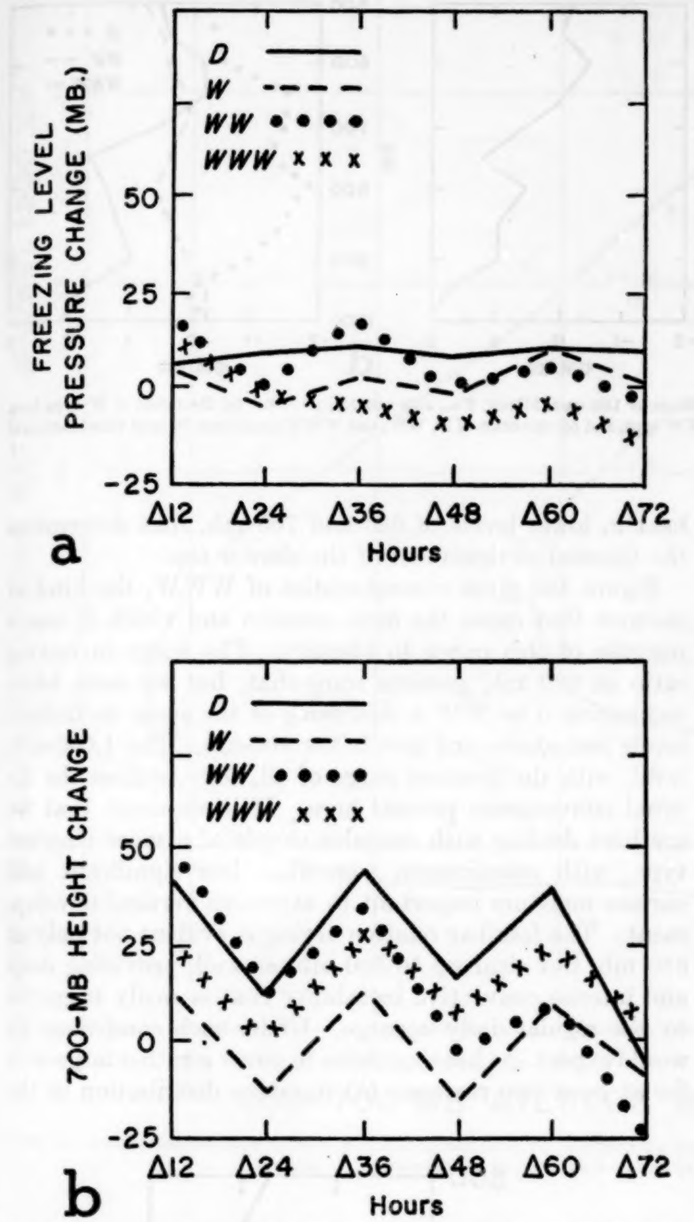

FIGURE 9.—(a) 1500 GMT average change in freezing level pressure (mb.) for various time increments for each of the four shower types. Negative ordinates indicate fall in height (rise in pressure); positive ordinates indicate rise in height (fall in pressure). Miami, Fla., July and August 1950. (Compare with fig. 1b for 0300 GMT soundings.) (b) 1500 GMT average 700-mb. height change (ft.) for various time increments for each of the four shower types. Height falls are negative, rises positive. Miami, Fla., July and August 1950. (Compare with fig. 1c for 0300 GMT soundings.)

pared to D, are slightly steeper from 1,000 to 850 mb., nearly identical from 850 to 600 mb., and again slightly steeper from 600 to 500 mb. Considering W as against WW, temperature curves are about a degree apart up to 600 mb., with the paradox of stabler lapse rates for WW between 600 and 550, and with nearly identical curves above this. One way of partially separating these types on a basis of temperature distribution is to mark the level of intersection of $\theta = 343.5°$ with the temperature curve; this gives 700, 750, and 820 mb. for D, W, and WW, respectively, and 770 mb. for WWW. Thus an intercept of 750 mb. or lower is associated with showers, and this

TABLE 5.—*1500* GMT *average temperatures (° C.) at 50-mb. intervals for the four shower types. Miami, Fla., July and August 1950*

Pressure \ Type	WWW	WW	W	D
(mb.)	(° C.)	(° C.)	(° C.)	(° C.)
450	−11.7	−11.6	−11.9	−11.7
500	−6.8	−6.8	−7.2	−6.4
550	−2.8	−2.2	−2.8	−2.4
600	1.8	.5	1.4	1.5
650	5.0	4.1	5.1	5.5
700	8.2	7.5	8.6	8.8
750	11.2	10.4	11.6	12.3
800	14.5	13.6	14.6	15.3
850	17.5	16.6	17.3	18.1
900	21.0	19.6	20.3	21.0
950	23.8	22.6	23.7	23.7
1,000	27.5	26.0	27.3	27.1

TABLE 6.—*1500* GMT *average wet-bulb temperatures (° C.) at 50-mb. intervals for the four shower types. Miami, Fla., July and August 1950*

Pressure \ Type	WWW	WW	W	D
(mb.)	(° C.)	(° C.)	(° C.)	(° C.)
500	−9.5	−9.2	−10.6	−10.7
550	−5.5	−5.9	−6.2	−7.0
600	−2.8	−2.3	−2.4	−3.4
650	.7	.9	1.2	−.3
700	4.8	3.9	4.1	3.0
750	8.5	6.9	6.8	6.0
800	12.0	10.6	10.4	9.2
850	14.8	13.8	13.5	12.6

relationship is partly quantitative. This intercept was used as a forecasting parameter.

Table 6 similarly presents wet-bulb temperatures. Plotting these we get, for D against W, considerably greater convective instability for W between 650 and 500 mb. For W against WW the curves are about identical except between 550 and 500 mb., where WW oddly shows greater stability. Comparing WW and WWW, much greater instability is manifest for WWW between the 750 and 600-mb. levels. Important differences shown by wet-bulb temperatures between 0300 and 1500 GMT soundings seem to include a requirement for deep convective instability through a layer from 750 to 500 mb. for afternoon rains, while night showers require instability in a higher layer, at 600 mb. and above. Because of the 0300 GMT divergence near the surface, night showers are controlled principally in higher levels. (A paper by Gentry and Moore [25] offers evidence that most of these night showers do not, as is often suggested, form over the Gulf Stream and move inland, but instead begin over sections well west of the coastline.)

Table 7 gives the 1500 GMT dewpoint values. Reducing these as before to mixing ratios and contrasting D and W in figure 10a, we note that a mixing ratio surge of between one and two gm/kg. in the deep layer between 900 and 650 mb. distinguishes the two types. The "bite" at 950 mb. and below is of interest, particularly since we cannot this time explain it as associated with low level divergence. There may exist in the atmosphere a level of maximum moisture transportability—that is, a level where day-to-day mixing ratio changes are at a maximum.

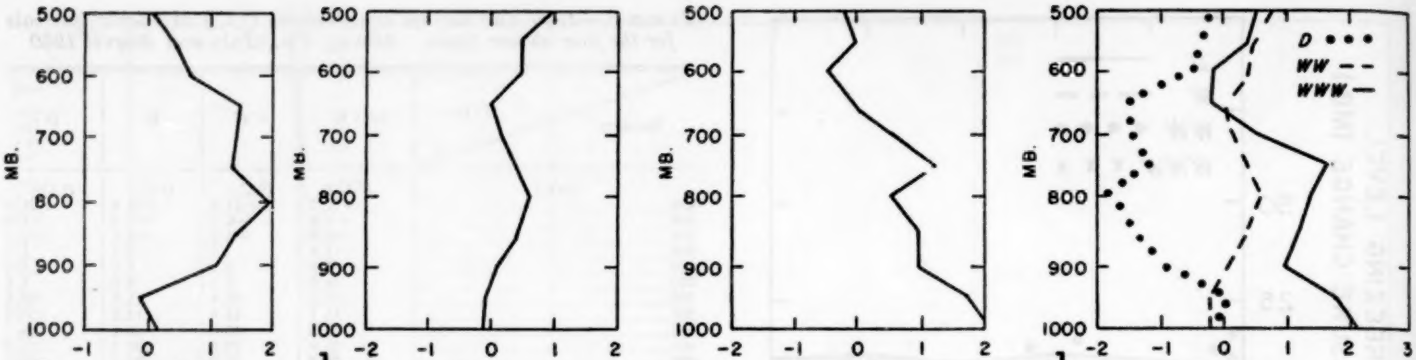

FIGURE 10.—Comparisons between average mixing ratios (gm/kg) for the four types of soundings for 1500 GMT, Miami, Fla., July and August 1950. (a) Deviation of W type from D type, (b) deviation of WW type from W type, (c) deviation of WWW type from WW type, and (d) deviation of D, WW, and WWW types from W type (combination of data from figs. a, b, and c.)

TABLE 7.—*1500* GMT *average dew points (° C.) at 50-mb. intervals for the four shower types. Miami, Fla., July and August 1950*

Pressure \ Type	WWW	WW	W	D
(mb.)	(°C.)	(°C.)	(°C.)	(°C.)
450	−18.5	−18.2	−21.8	−23.6
500	−13.5	−12.3	−17.2	−18.5
550	−9.0	−9.6	−11.4	−14.4
600	−8.0	−6.4	−7.7	−10.5
650	−3.0	−2.2	−2.6	−7.1
700	2.0	.9	−.3	−3.2
750	6.5	3.8	2.7	−.3
800	9.8	8.7	7.5	3.6
850	13.0	11.9	11.4	9.3
900	16.2	15.3	15.1	13.3
950	20.0	18.0	18.2	18.4
1,000	22.5	20.3	20.6	20.4

In low levels, more source moisture is available, but due to surface friction it is less free to be carried about, while in higher levels available moisture falls off as wind speed increases. Thus a point of maximum efficiency could be shown to exist. Or perhaps the fact that the principal differences in figure 10a appear near the 800-mb. level—a point almost exactly halfway between the surface and the freezing level—is of significance because it is in the middle of this important layer. The fact of the relative unimportance of surface levels to the development of trade cumulus has been recognized by the group at Woods Hole [20–22] in developing the concept of entrainment, as discussed previously.

Figure 10b contrasts W and WW. The surge at 800 mb. continues, but with an important qualification: at 650 mb. there is no increase. This relative drying effect has been encountered and discussed before. Since at 1500 GMT there is normally low level convergence, it is evident that a very large column of air is gently rising, and our smaller shower cell is simply rising more rapidly than is the surrounding air—a situation that could still allow much relative motion between the parcel and its surroundings. Hence there appears a need to consider positive area from a standpoint not of *observed* 1500 GMT 500-mb. temperatures but rather of *later* temperatures, say at 2000 GMT, when the daily upsurge (and shower activity) has almost reached its peak. It is at this time that our smaller parcel will enter these levels, and it will sometimes be the latent heat in lower levels of 650 and 700 mb. that determines the thermal environment of the shower top.

Figure 10c gives characteristics of WWW, the kind of showers that cause the most concern and which it was a purpose of this paper to identify. The surge in mixing ratio at 800 mb. persists somewhat, but we note when comparing it to WW a *thickening* of the surge to include levels just above and just below 800-mb. The 1,000-mb. level, with the greatest surge of all, fully utilizes the diurnal convergence present here. It is apparent that we are here dealing with cumulus clouds of a more classical type, with entrainment somewhat less significant and surface moisture important to extensive vertical development. The familiar relative drying is evident not only at 650 mb. but clear up to 500 mb. as well, providing deep and intense convective instability that is easily triggered by the regular daily upsurge. Under such conditions we would expect the heaviest rains to cover a rather large area for at least two reasons: (*a*) moisture distribution in the

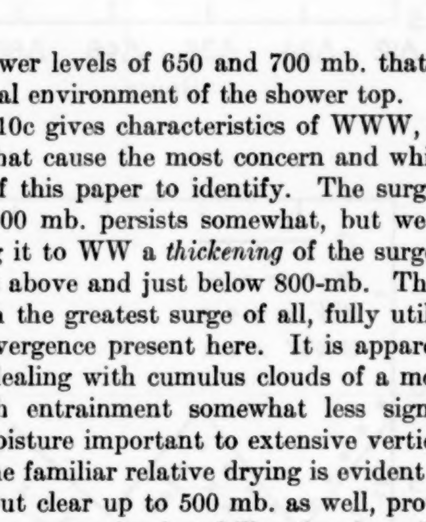

FIGURE 11.—1500 GMT deviation of average mixing ratio (gm/kg) for shower type soundings (W, WW, WWW combined) from that for D type. Miami, Fla., July 1951.

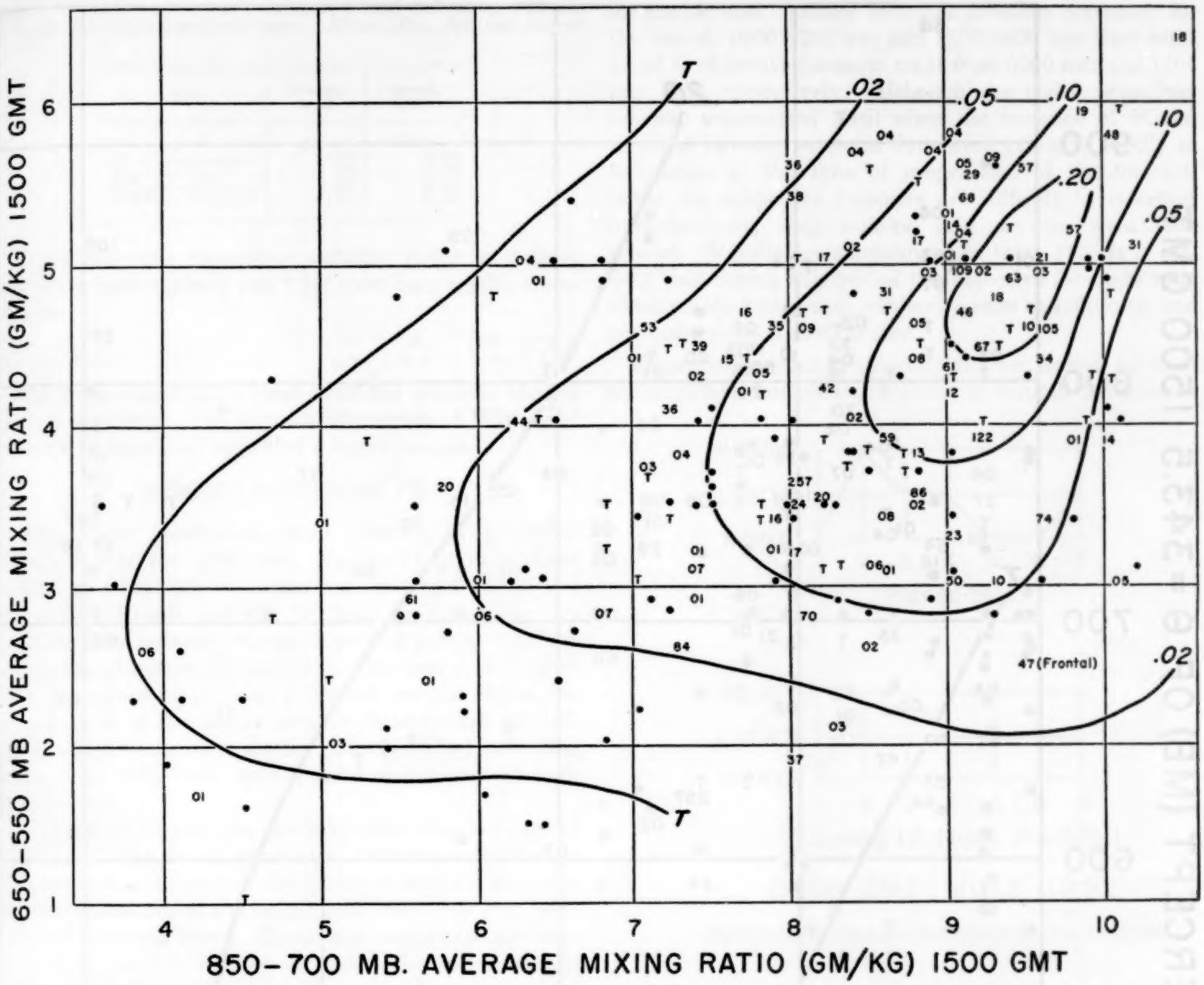

FIGURE 12.—Scatter diagram showing plots of Miami rainfall (as in fig. 4) during the 12-hour period immediately following the 1500 GMT soundings from which the mixing ratio coordinate values were taken. Isograms are interpreted as in figure 4. Dependent data: July and August 1948–51.

sounding is a function of a wind field common to most of southeast Florida, (*b*) the diurnal low level convergence is a product of land-sea contrast likewise common to most of southeast Florida.

Figure 10d sums up the previous three figures for convenience in comparing all four types. It will be noted that the 750- and 800-mb. levels provide the best overall index of shower intensity. Also we see that only the heaviest showers are related to low level mixing ratio. (This is a weakness of the forecasting parameter to be used, which considers only the 850- to 700-mb. layer). Relative drying in high levels seems to intensify the showers, and too much moisture in these levels inhibits them. This offers an explanation of an old idea that it is safe to forecast improvement once it has rained hard for a few minutes—that is, after the cumulonimbus has fanned out enough moisture in higher levels to abruptly alter the convective stability of the much larger, gently rising column that constitutes its environment. Also, of course, great expanses of middle clouds sharply retard surface insolation. Each large shower thus eventually signs its own death warrant. Can anyone recall *two* successive cloudbursts in southern Florida in a single half day?

In table 8 are presented freezing level and 700-mb. data for 1500 GMT corresponding to those of table 4 for 0300 GMT. Interesting as some of these values are, none seems to offer enough skill to warrant use as a parameter. In figure 11 are presented independent data from July 1951 as a check on the reality of the relative drying near 600 mb. associated with heavier showers. As in its counterpart figure 3, all shower types were considered as one type and compared to dry averages.

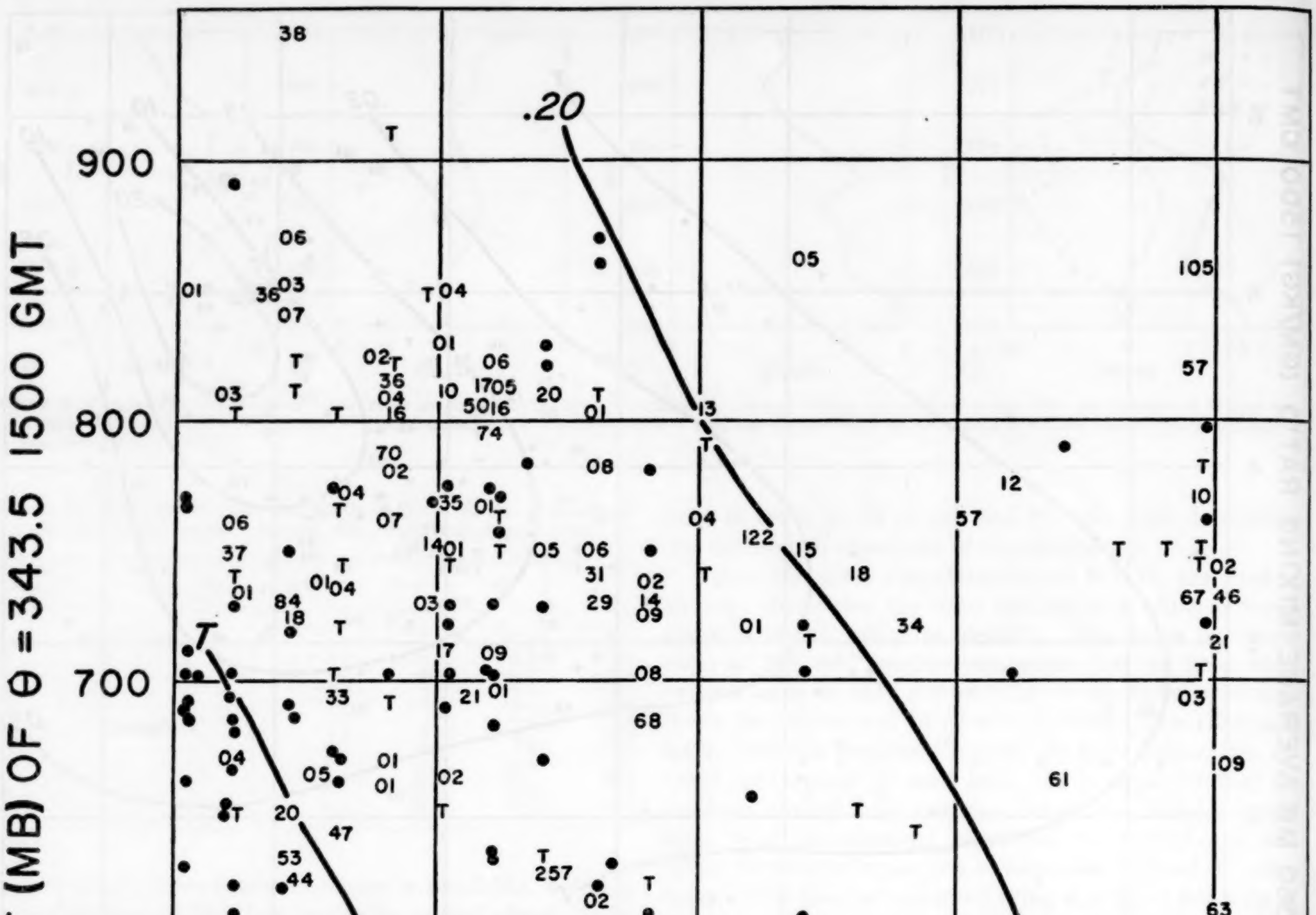

FIGURE 13.—Scatter diagram showing Miami rainfall (as in fig. 4) for the 12-hour period following the 1500 GMT sounding, plotted against the 1500 GMT pressure intercept of $\theta = 343.5°$ and the mixing ratio function from figure 12. Isograms, now a function of three parameters, are interpreted as in figure 4. Dependent data: July and August 1948–1951.

TABLE 8.—*1500* GMT *average freezing level (mb.) and average 700-mb. height (ft.) for the four shower types. Miami, Fla., July and August 1950*

Type	Freezing level	700-mb. height
	Mb.	*Feet*
D	581	10,555
W	583	10,545
WW	590	10,542
WWW	575	10,527

Computing the Showalter stability index as before, with data from tables 5 and 7 for 1500 GMT, results are as follows:

Type	D	W	WW	WWW
Stability Index	4.2	2.3	2.8	1.6

Again the quantitative relation of the index to shower type is apparent. The anomalous position of WW could perhaps be improved by use of a larger sample.

OBJECTIVE FORECASTING AID

Only three parameters were selected in preparing objective aids for 1500 GMT. Figure 12 gives 12-hour rainfall as a function of mixing ratio averages in the two layers 850–700 mb. and 650–550 mb. In comparing this to figure 4 we note agreement on several points: (1) there is a region of maximum rainfall, (2) the contours suggest that the effect of increasing beyond certain limits the mixing ratio in the higher stratum is to reduce rainfall, (3) the highest medians are the same (0.20 in.) indicating comparable skill from mixing ratio parameters at both times of day.

In figure 13 we combine the value gotten from figure 12 with the "lapse rate" parameter, defined as the height (expressed in millibars) of the lowest reasonable intercept (highest pressure) of $\Theta=343.5°$ with the 1500 GMT temperature sounding curve. (In cases of marked temperature inversions, use the highest intercept (lowest pressure); with an irregular temperature curve smooth as necessary.) The curves of figure 13 give a final quantitative estimate for ensuing 12-hour rainfall.

The limitations in the criteria employed in the objective forecasting aids have already been considered in the discussion of objections to limiting this study to the use of radiosonde data. Another kind of objection might be made at this point: the chances of hitting on the most effective combination of six parameters as used for 0300 GMT data are slim, as there are 45 possible ways to combine them as in this paper. It is here that theory can be of much help in suggesting logical relationships and eliminating the need for testing meaningless combinations.

VERIFICATION

Several tests of the objective aids were made. Results for dependent data are summarized in contingency tables in table 9, and for independent data in table 10. Corresponding subjective forecasts regularly issued by the Miami WBAS during July and August 1952 were graded for comparison. Miami terminal aviation forecasts for the periods 0000–1200 EST and 1200–2400 EST were compared to objective forecasts made from 0300 GMT and 1500 GMT data respectively. Although the coded soundings are not transmitted until after the issuance of Miami terminal forecast, essential data were available locally to forecasters at the time of preparation of the forecast. Since the subjective forecasts are difficult to interpret quantitatively, only rain–no rain aspects were considered. Results are summarized in table 11. It is evident that during this period the objective forecasts were considerably better than subjective ones at 1500 GMT, and not quite as good at 0300 GMT.

Figure 14 presents graphically the correlation between the objective forecasts and observed rainfall for selected

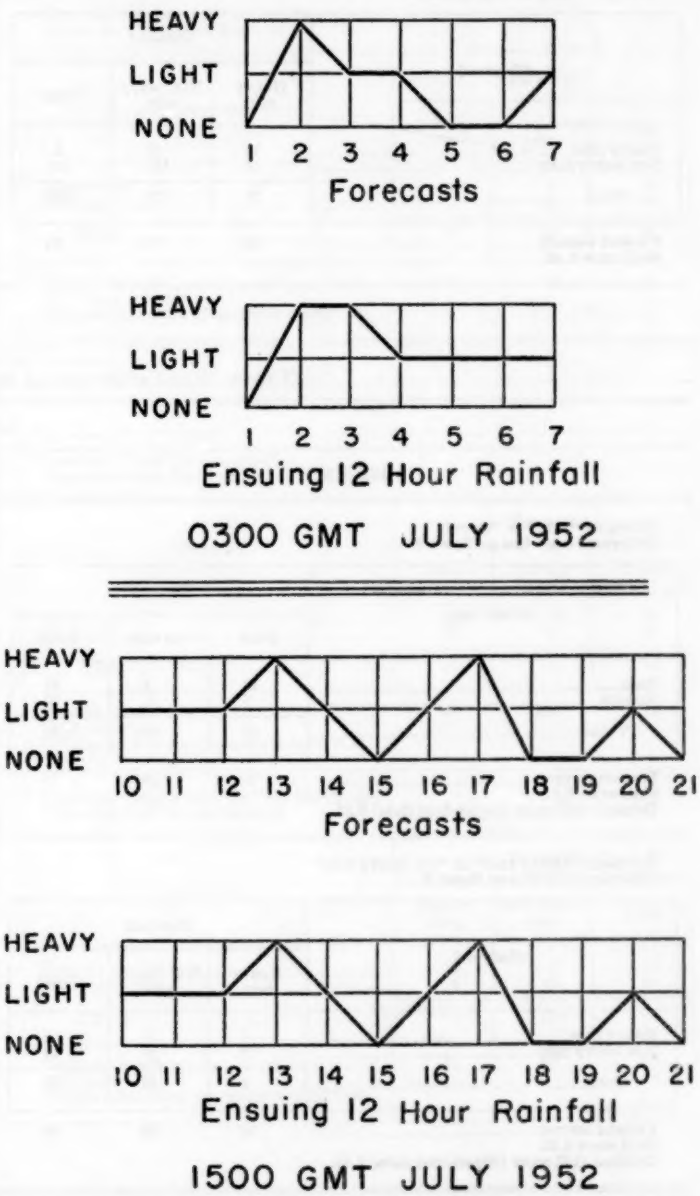

FIGURE 14.—Graphical comparison between objective forecasts and observed rainfall at Miami, Fla. for selected periods in July 1952. Abscissas are dates; ordinates, shower types as defined in figures 8 and 13.

TABLE 9.—*Verification of objective forecasts, dependent data*

July and August, 1948-51

0300 GMT

Forecast: "rain" or "no rain"
Criterion: trace line on figure 8

Observed	Forecast: Rain	Forecast: No rain	Forecast: Total
Rain	107	16	125
No rain	42	41	83
Total	149	57	206
Percent correct	72	72	72

Skill score 0.37.

Forecast: "heavy rain" or "not heavy rain"
Criterion: 0.30 line on figure 8

Observed	Forecast: Heavy rain	Forecast: Not heavy rain	Forecast: Total
Heavy rain	15	11	26
Not heavy rain	13	167	180
Total	28	178	206
Percent correct	53	94	88

Skill score 0.49.

1500 GMT

Forecast: "rain" or "no rain"
Criterion: trace line on figure 13

Observed	Forecast: Rain	Forecast: No rain	Forecast: Total
Rain	127	13	140
No rain	52	38	90
Total	179	51	230
Percent correct	71	75	72

Skill score 0.36.

Forecast: "heavy rain" or "not heavy rain"
Criterion: 0.20 line on figure 13

Observed	Forecast: Heavy rain	Forecast: Not heavy rain	Forecast: Total
Heavy rain	14	20	34
Not heavy rain	20	176	196
Total	34	196	230
Percent correct	41	90	83

Skill score 0.31.

TABLE 10.—*Verification of objective forecasts, independent data*

July 1952

0300 GMT

Forecast: "rain" or "no rain"
Criterion: trace line on figure 8

Observed	Forecast: Rain	Forecast: No rain	Forecast: Total
Rain	16	5	21
No rain	3	7	10
Total	19	12	31
Percent correct	84	58	74

Skill score 0.44.
Original skill score (dependent data) 0.37.

Forecast: "heavy rain" or "not heavy rain"
Criterion: 0.30 line on figure 8

Observed	Forecast: Heavy rain	Forecast: Not heavy rain	Forecast: Total
Heavy rain	1	1	2
Not heavy rain	2	27	29
Total	3	28	31
Percent correct	34	96	90

Skill score 0.33.
Original skill score (dependent data) 0.49.

1500 GMT

Forecast: "rain" or "no rain"
Criterion: trace line on figure 13

Observed	Forecast: Rain	Forecast: No rain	Forecast: Total
Rain	16	0	16
No rain	9	6	15
Total	25	6	31
Percent correct	64	100	71

Skill score 0.40.
Original skill score (dependent data) 0.36.

Forecast: "heavy rain" or "not heavy rain"
Criterion: 0.20 line on figure 13

Observed	Forecast: Heavy rain	Forecast: Not heavy rain	Forecast: Total
Heavy rain	3	1	4
Not heavy rain	2	25	27
Total	5	26	31
Percent correct	60	96	90

Skill score 0.62.
Original skill score (dependent data) 0.31.

TABLE 10.—*Verification of objective forecasts, independent data*—Continued

August 1952

0300 GMT

Forecast: "rain" or "no rain"
Criterion: trace line on figure 8

Observed	Forecast: Rain	Forecast: No rain	Forecast: Total
Rain	14	4	18
No rain	7	6	13
Total	21	10	31
Percent correct	67	60	65

Skill score 0.25.
Original skill score (dependent data) 0.37.

Forecast: "heavy rain" or "not heavy rain"
Criterion: 0.30 line on figure 8

Observed	Forecast: Heavy rain	Forecast: Not heavy rain	Forecast: Total
Heavy rain	0	0	0
Not heavy rain	6	25	31
Total	6	25	31
Percent correct	0	100	81

Skill score 0/0.
Original skill score (dependent data) 0.49.

1500 GMT

Forecast: "rain" or "no rain"
Criterion: trace line on figure 13

Observed	Forecast: Rain	Forecast: No rain	Forecast: Total
Rain	18	0	18
No rain	8	5	13
Total	26	5	31
Percent correct	69	100	74

Skill score 0.42.
Original skill score (dependent data) 0.36.

Forecast: "heavy rain" or "not heavy rain"
Criterion: 0.20 line on figure 13

Observed	Forecast: Heavy rain	Forecast: Not heavy rain	Forecast: Total
Heavy rain	0	6	6
Not heavy rain	2	23	25
Total	2	29	31
Percent correct	0	79	74

Skill score −0.13.
Original skill score (dependent data) 0.31.

July and August 1952 combined

0300 GMT

Forecast: "rain" or "no rain"
Criterion: trace line on figure 8

Observed	Forecast: Rain	Forecast: No rain	Forecast: Total
Rain	30	9	39
No rain	10	13	23
Total	40	22	62
Percent correct	75	59	69

Skill score 0.34.
Original skill score (dependent data) 0.37.

Forecast: "heavy rain" or "not heavy rain"
Criterion: 0.30 line on figure 8

Observed	Forecast: Heavy rain	Forecast: Not heavy rain	Forecast: Total
Heavy rain	1	1	2
Not heavy rain	8	52	60
Total	9	53	62
Percent correct	11	98	85

Skill score 0.13.
Original skill score (dependent data) 0.49.

1500 GMT

Forecast: "rain" or "no rain"
Criterion: trace line on figure 13

Observed	Forecast: Rain	Forecast: No rain	Forecast: Total
Rain	34	0	34
No rain	17	11	28
Total	51	11	62
Percent correct	67	100	73

Skill score 0.41.
Original skill score (dependent data) 0.36.

Forecast: "heavy rain" or "not heavy rain"
Criterion: 0.20 line on figure 13

Observed	Forecast: Heavy rain	Forecast: Not heavy rain	Forecast: Total
Heavy rain	3	7	10
Not heavy rain	4	48	52
Total	7	55	62
Percent correct	43	87	82

Skill score 0.25.
Original skill score (dependent data) 0.31.

TABLE 11.—*Verification of subjective forecasts of "rain" or "no rain" for July and August 1952. Compare with corresponding contingency table in table 10.*

0300 GMT

Observed	Forecast: Rain	Forecast: No rain	Forecast: Total
Rain	29	10	39
No rain	8	15	23
Total	37	25	62
Percent correct	78	60	71

Skill score 0.39.
Skill score for comparable objective forecasts 0.34.

1500 GMT

Observed	Forecast: Rain	Forecast: No rain	Forecast: Total
Rain	25	9	34
No rain	14	14	28
Total	39	23	62
Percent correct	64	61	63

Skill score 0.24.
Skill score from comparable objective forecasts 0.41.

periods in July 1952. That the agreement was not this good most of the time is evident from the skill scores; however, the fact that it was possible for any forecasts to stay so closely in phase with rapidly changing weather for even this short period is encouraging.

Since the preparation of the original manuscript, verification data for July, August, and September 1–20, 1953 have been compiled. These additional independent data have been combined with the independent data for July and August 1952 and are summarized in table 12.

CONCLUSIONS

Principal findings of this study may be summarized briefly as follows:

(1) The Showalter stability index is of quantitative value in the Miami area.

(2) Low level (1,000–900 mb.) mixing ratios are valueless in predicting summer showeriness at Miami following 0300 GMT, but are of value following 1500 GMT.

(3) Miami summer showers following 0300 GMT require an initial surge of absolute humidity from 850 to 550 mb., and these showers become heavier as this surge is intensified at 900 mb. and lessened at 750–550 mb.

(4) Miami summer showers following 1500 GMT require an initial surge of absolute humidity from 900 to 650 mb. and centered on 800 mb., and these showers become heavier as this surge is thickened and intensified (mostly at 750 and 1,000 mb.) and lessened at 650–500 mb.

(5) Three-day freezing levels and tendencies at 0300 GMT are of some quantitative value in summer shower forecasting at Miami.

TABLE 12.—*Verification of objective forecasts, independent data, July and August 1952, July, August, and September 1–20, 1953*

0300 GMT

Forecast: "rain" or "no rain"
Criterion: trace line on figure 8

Observed	Forecast: Rain	Forecast: No rain	Forecast: Total
Rain	73	18	91
No rain	25	26	51
Total	98	44	142
Percent correct	75	59	70

Skill score 0.32.
Original skill score (dependent data) 0.37.

Forecast: "heavy rain" or "not heavy rain"
Criterion: 0.30 line on figure 8

Observed	Forecast: Heavy rain	Forecast: Not heavy rain	Forecast: Total
Heavy rain	3	5	8
Not heavy rain	14	120	134
Total	17	125	142
Percent correct	18	96	87

Skill score 0.17.
Original skill score (dependent data) 0.49.

1500 GMT

Forecast: "rain" or "no rain"
Criterion: trace line on figure 13

Observed	Forecast: Rain	Forecast: No rain	Forecast: Total
Rain	72	6	78
No rain	43	18	61
Total	115	24	139
Percent correct	63	75	65

Skill score 0.23.
Original skill score (dependent data) 0.36.

Forecast: "heavy rain" or "not heavy rain"
Criterion: 0.20 line on figure 13

Observed	Forecast: Heavy rain	Forecast: Not heavy rain	Forecast: Total
Heavy rain	8	16	24
Not heavy rain	14	101	115
Total	22	117	139
Percent correct	36	86	78

Skill score 0.22.
Original skill score (dependent data) 0.31.

(6) Three-day 700 mb. heights and tendencies at 0300 GMT are of similar value.

Of greatest interest perhaps is the relationship between slight high level relative drying and intensified shower activity. Although convective instability has been related to tornado activity, there has been to my knowledge no suggestion that this is also related to ordinary air mass showers.

It is also significant that in summer the Showalter stability index values as computed from the Miami data are practically always within the range usually considered thundery. Nevertheless perhaps half our summer days are quite dry. A value of 1 or 2 is needed here to produce the activity gotten by 3 or 4 elsewhere, and our night criteria are a little different from daytime ones. This is offered as evidence in support of the hypothesis proposed early in this paper. Such an idea, indeed, is implicit in the writings of experienced forecasters like Hallenbeck [26], who stated "I am convinced that the only way in which any appreciable improvement in the accuracy of weather forecasts can be attained is to assign each forecaster to a limited territory . . . *and keep him there*" (italics his). If this hypothesis stands, there appears a need to inhibit the nomadic tendencies of forecasters and to provide them with time and incentives to explore and record for their successors the peculiarities of their own regions.

In the approach to the Miami shower problem presented here, the surface has only been scratched and more work is needed. It would be desirable to incorporate wind parameters and raob criteria into a single system, to extend the 1500 GMT mixing ratio parameter down to the 1,000-mb. level, and to improve the accuracy of the curves as time and additional data permit.

ACKNOWLEDGMENTS

Thanks are due Mr. Stanley Day for his interest and help. Valuable advice and help was also provided by Mr. R. C. Gentry, Mr. Wilmer L. Thompson, and Mr. Jack C. Thompson.

REFERENCES

1. H. R. Byers and H. R. Rodebush, "Causes of Thunderstorms of the Florida Peninsula," *Journal of Meteorology*, vol. 5, No. 6, Dec. 1948, pp. 275–280.
2. N. D. Folling, "Troughs in the Easterlies and the Use of Winds Aloft in Forecasting Tropical Weather," July 1948, reproduced by Pan American World Airways.
3. C. O. Durham et al., A Study of "Waves" in the Easterlies, AAF Weather Research Station, Institute of Tropical Meteorology, University of Puerto Rico, Rio Piedras, P. R. 1945 (Reviewed by H. Riehl, *Bulletin of the American Meteorological Society* vol. 29, No. 4, Apr. 1948, pp. 196–198.)
4. C. E. Palmer and H. W. Ellsaesser, "Notes on Tropical Meteorology," 2143d Air Weather Wing, *Technical Bulletin*, vol. 1, 1949, pp. 1–49.
5. David Abrams, "Introductory Notes on Forecasting for the Miami Section" (reproduced 1945 by Pan American World Airways), p. 21.
6. U. S. Weather Bureau, "Thunderstorm Rainfall," *Hydrometeorological Report No. 5*, Waterways Experiment Station, Vicksburg, Miss. 1947, 331 pp. (Part 1) +155 figs. (Part 2). (See especially figs. 6, 8, 15, 17, 92, 93, 94.)
7. L. R. Bovinett, Thundershower Activity in the Miami Area During the Summer Months, Nov. 1952. (Unpublished, on file at Miami Weather Bureau Office.)
8. Phillip D. Thomas, Forecasting Manual, Miami, Fla. Section. (Unpublished, on file Miami Weather Bureau Airport Station.)
9. John C. Hurley, Thunderstorms at Banana River Naval Air Station from May 1 to September 30, 1943. (Unpublished, on file Miami Weather Bureau Airport Station.)
10. W. A. Baum, "On the Utilization of Radiosonde Data in the Study of Thunderstorm Thermodynamics," *Report to the U. S. Weather Bureau on Research performed by the University of Chicago, Dept. of Meteorology in connection with the Thunderstorm Project, Oct. 1, 1946–June 30, 1947*, Part IV–A. University of Chicago, Aug. 1947.
11. W. R. Chalker, "Vertical Stability in Regions of Air Mass Showers," *Bulletin of the American Meteorological Society*, vol. 30, No. 4, Apr. 1949, pp. 145–147.
12. Robert G. Beebe, "Thunderstorm Forecasting in the Atlanta, Ga., Area," *Monthly Weather Review*, vol. 80, No. 4, Apr. 1952, pp. 63–69.
13. Lynn L. Means, "On Thunderstorm Forecasting in the Central United States," *Monthly Weather Review*, vol. 80, No. 10, Oct. 1952, pp. 165–189. (See especially figs. 8, 9, 11, 12.)
14. R. C. Gentry, "Forecasting Local Showers in Florida During the Summer," *Monthly Weather Review*, vol. 78, No. 3, Mar. 1950, pp. 41–51.
15. G. W. Brier, "A Study of Quantitative Precipitation Forecasting in the TVA Basin," U. S. Weather Bureau *Research Paper*. No. 26, Washington, D. C., 1946, 40 pp.
16. J. C. Thompson, "A Numerical Method for Forecasting Rainfall in the Los Angeles Area," *Monthly Weather Review*, vol. 78, No. 7, July 1950, pp. 113–124.
17. Stanley Day, "Horizontal Convergence and the Occurrence of Summer Precipitation at Miami, Fla.," *Monthly Weather Review*, vol. 81, No. 6, June 1953, pp. 155–161.
18. A. K. Showalter and J. R. Fulks, *Preliminary Report*

on Tornadoes, U. S. Weather Bureau, Washington, D. C., 1943.
19. Kenneth C. Tillotson, "An Objective Aid for Forecasting September Thunderstorms at Denver, Colo.," *Monthly Weather Review*, vol. 79, No. 2, Feb. 1951, pp. 27–34. (See p. 31.)
20. Joanne S. Malkus, "Recent Advances in the Study of Convective Clouds and Their Interaction with the Environment," *Tellus*, vol. 4, No. 2, May 1952, pp. 71–87.
21. Joanne S. Malkus, "Aeroplane Studies of Trade-Wind Meteorology," *Weather*, vol. 8, No. 10, Oct. 1953, pp. 291–300.
22. Henry Stommel, "Entrainment of Air into a Cumulus Cloud," *Journal of Meteorology*, vol. 4, No. 3, June 1947, pp. 91–94.
23. U. S. Weather Bureau, *Radiosonde Compatibility Tests, Made at Oklahoma City June 4–20, 1951*, Washington, D. C., March 1952, 273 pp.
24. A. K. Showalter, "A Stability Index for Thunderstorm Forecasting," *Bulletin of the American Meteorological Society*, vol. 34, No. 6, June 1953, pp. 250–252.
25. R. C. Gentry and P. L. Moore, The Relation of Sea Breeze and General Wind Interaction to Time and Location of Air Mass Showers, 1953. (Unpublished.)
26. Cleve Hallenbeck, "Why Weathermen Make Mistakes," *The American Scholar*, Spring 1949.

THE WEATHER AND CIRCULATION OF JANUARY 1954 [1]

A Low Index Month With a Pronounced Blocking Wave

ARTHUR F. KRUEGER

Extended Forecast Section, U. S. Weather Bureau, Washington, D. C.

MONTHLY MEAN CIRCULATION

During January 1954 the monthly mean zonal index (35° N.–55° N.) at 700 mb. for the Western Hemisphere averaged below its normal value for the first time since April 1953 [1]. This is indicated in figure 1, which shows the observed and normal monthly zonal indices for the past 10 months. The index reached its highest monthly average and also its greatest positive deviation from normal in the period from mid-November to mid-December 1953, and thereafter experienced a steady decline to speeds that were weaker than normal. Five-day mean values for December and January show that the index dropped from 13.7 m/sec late in December to a minimum of 8.4 m/sec early in January, followed by a recovery to a value (11.1 m/sec) near the normal later in the month. As can be seen from figure 2 these changes were accompanied by shifts in the latitude of the maximum westerlies, southward from about 50° N. on December 27 to about 37° N. on January 8 and then northward. At the end of January the westerlies were shifting southward for the second time once more accompanied by a falling zonal index.

During the southward shift of the westerlies, sea level pressures increased at high latitudes. North of 40° the average pressure over the Western Hemisphere was well above normal for the month, as may be seen in figure 3. At lower latitudes, on the other hand, pressures averaged below normal, so that the polar anticyclones grew at the expense of the subtropical high pressure cells, a condition considered typical of low index [2].

Corresponding to the low index state, the monthly mean position of the belt of maximum westerlies at 700 mb was south of normal in the Pacific and western and central North America (fig. 4a). As a result wind speeds averaged above normal north and northwest of the Hawaiian Islands and along the Pacific coast of the United States (fig. 4b). They were also above normal along a second-

[1] See charts I–XV following p. 41 for analyzed climatological data for the month.

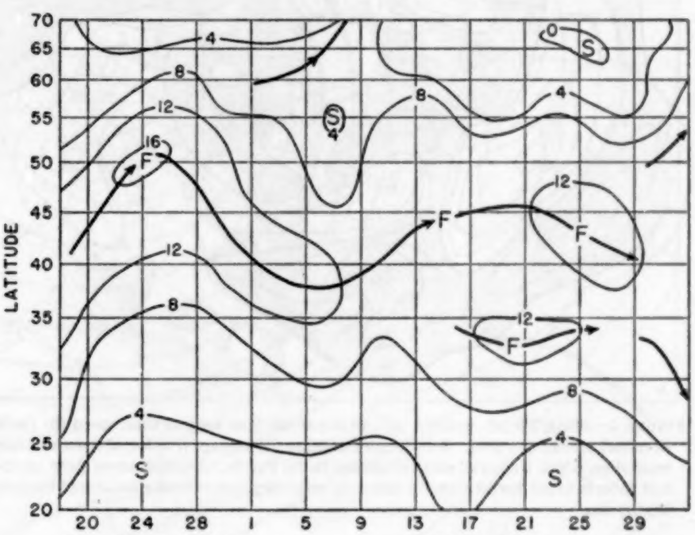

FIGURE 2.—Time-latitude section of 5-day mean 700-mb. zonal wind speed (m/sec) in the Western Hemisphere for period December 18, 1953, to February 2, 1954. Heavy arrowed lines mark latitude of axes of maximum wind speed. Notice the latitudinal variation of the maximum westerlies during late December and January.

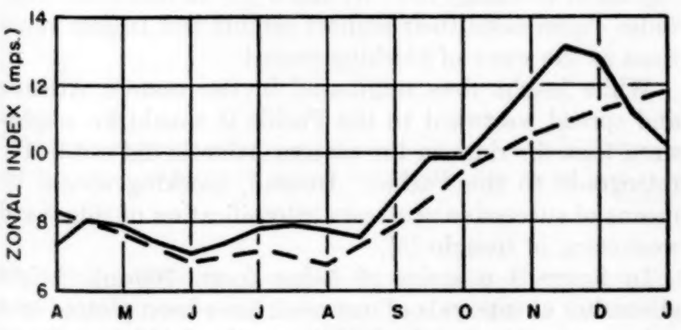

FIGURE 1.—Variations of the mean monthly zonal index at 700 mb. for the Western Hemisphere in the latitude belt 35°–55° N. from April 1953 to January 1954 with normal index dashed. Notice the 8-month period during which the index was above normal.

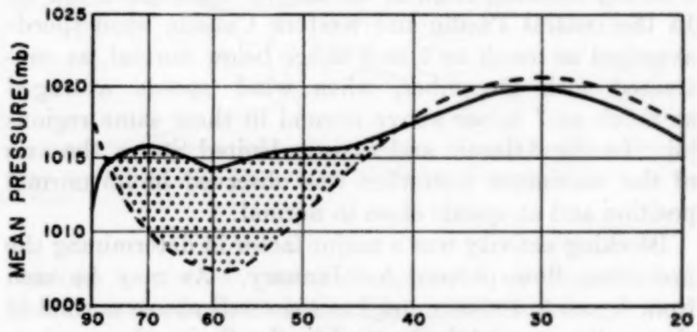

FIGURE 3.—Mean sea level pressure profile in the Western Hemisphere for January 1954 with normal profile dashed. Pressures were above normal north of 40° N. (shaded area).

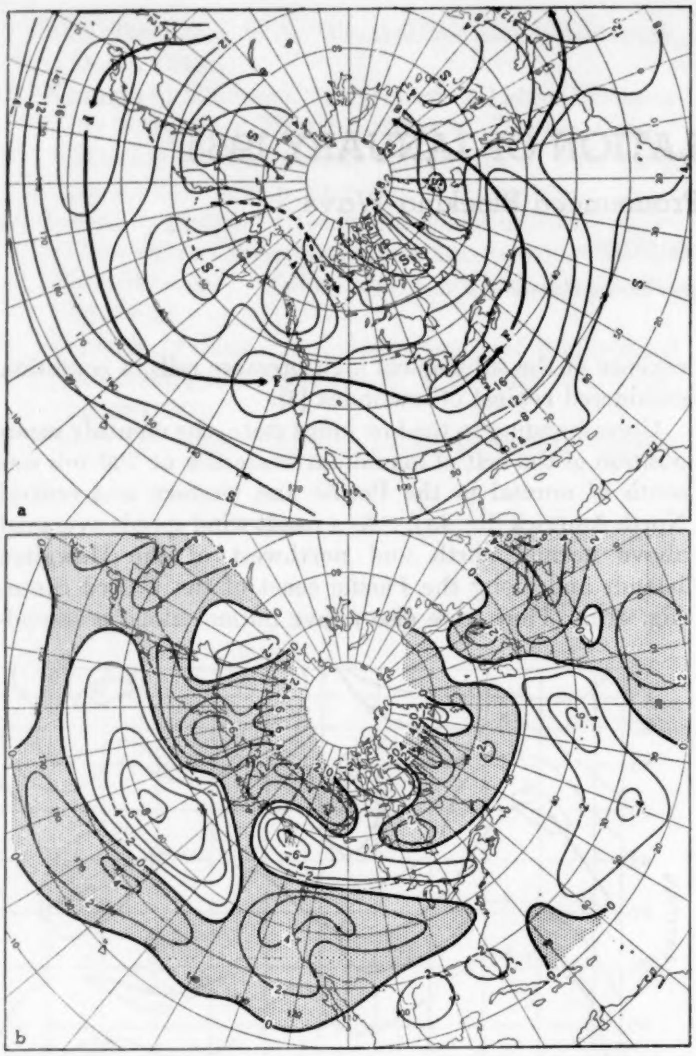

FIGURE 4.—Mean 700-mb. isotachs (a) and departure from normal wind speed (b) (both in m/sec) for January 1954. Solid arrows indicate the average position of the maximum westerlies, which were well south of normal in the Pacific. Dashed arrow from northeast Siberia to northwest Canada indicates secondary axis of westerlies around block in Bering Sea.

ary axis of maximum winds from Kamchatka to the Yukon, where the westerlies were forced to flow around a strong blocking High in the Bering Sea (figs. 4 and 5). In the central Pacific and western Canada wind speeds averaged as much as 6 to 8 m/sec below normal, as contrasted with December, when wind speeds averaged as much as 7 m/sec above normal in these same regions [3]. In the Atlantic and eastern United States the axis of the maximum westerlies was observed in its normal position and at speeds close to normal.

Blocking activity was a major factor in determining the prevailing flow pattern for January. As may be seen from figure 5, 700-mb. heights were well above normal in the northeastern Atlantic and in the Bering Sea, regions which are frequent sites for blocks [4]. In response to the strong ridge in the Bering Sea very cold air was driven southward into western Canada and the eastern Pacific, resulting in frequent cyclogenesis and subnormal heights off the coasts of Washington, Oregon, and British Columbia. An abnormally deep Low in the Sea of Okhotsk was also related to the blocking inasmuch as strong cyclones were blocked by the ridge. Across the United States flow at 700 mb. was nearly zonal despite the fact that the zonal index from 0° westward to 180° averaged below normal. These regional variations in index are frequently observed, and point up the danger of using a hemispheric index to define a regional circulation pattern.

BEHAVIOR OF THE BLOCK

A major feature of blocking as given by Namias [5] is that a regional retardation of the westerlies progresses slowly westward. This feature was conspicuous during January, as figure 6, showing time-variation of regional zonal indices, clearly indicates. An index minimum was reached about the first of January in the eastern Atlantic, the 5th in the western Atlantic, the 10th in North America, the 20th in the eastern Pacific, and finally about the 31st in eastern Asia. The average rate of westward motion of the index minimum during this period was 52° of longitude per week. This rate, however, was not uniform, varying from about 30° of longitude per week in the Pacific to 70° per week in the Atlantic and North America.

It is noteworthy that both these average and sectional rates compare closely with rates computed for a similar blocking case observed during January 1944 by Namias [5].

The changes that took place at various longitudes as blocking spread westward are shown in figures 7 and 8. Figure 7 shows the changes in 700-mb. heights computed at 60° N. from 5-day mean charts 1 week apart. Large rises originated in the eastern Atlantic about 20° W. and spread westward during the month, reaching 160° W. about January 10 and 120° E. about January 31. The long-period trends occurring at most longitudes are striking. For example, strong height rises at 160° W. (Alaska) after January 5 continued for 2 weeks, followed by falls during the remainder of the month. Of interest also is the large magnitude of the changes in the two favorite regions of blocking (160° W. and 0°). In fact most longitudes experienced their highest heights and largest variations as the wave of blocking passed.

While height rises originated in the eastern Atlantic and spread westward to the Pacific it should be emphasized that the ridge in the eastern Atlantic did not bodily retrograde to the Pacific. Instead, blocking spread by means of successive upstream intensification of ridges and weakening of troughs [5].

In figure 8 a series of 5-day mean 700-mb. height anomalies at intervals of one week have been plotted on a polar projection for the regions north of 40° N. Figure 8A shows the block in the eastern Atlantic shortly after it was established, as indicated by an anomaly of +850 ft. at 55° N., 20° W. During the next week (fig. 8B) the anomaly maximum retrograded to 30° W. with height rises

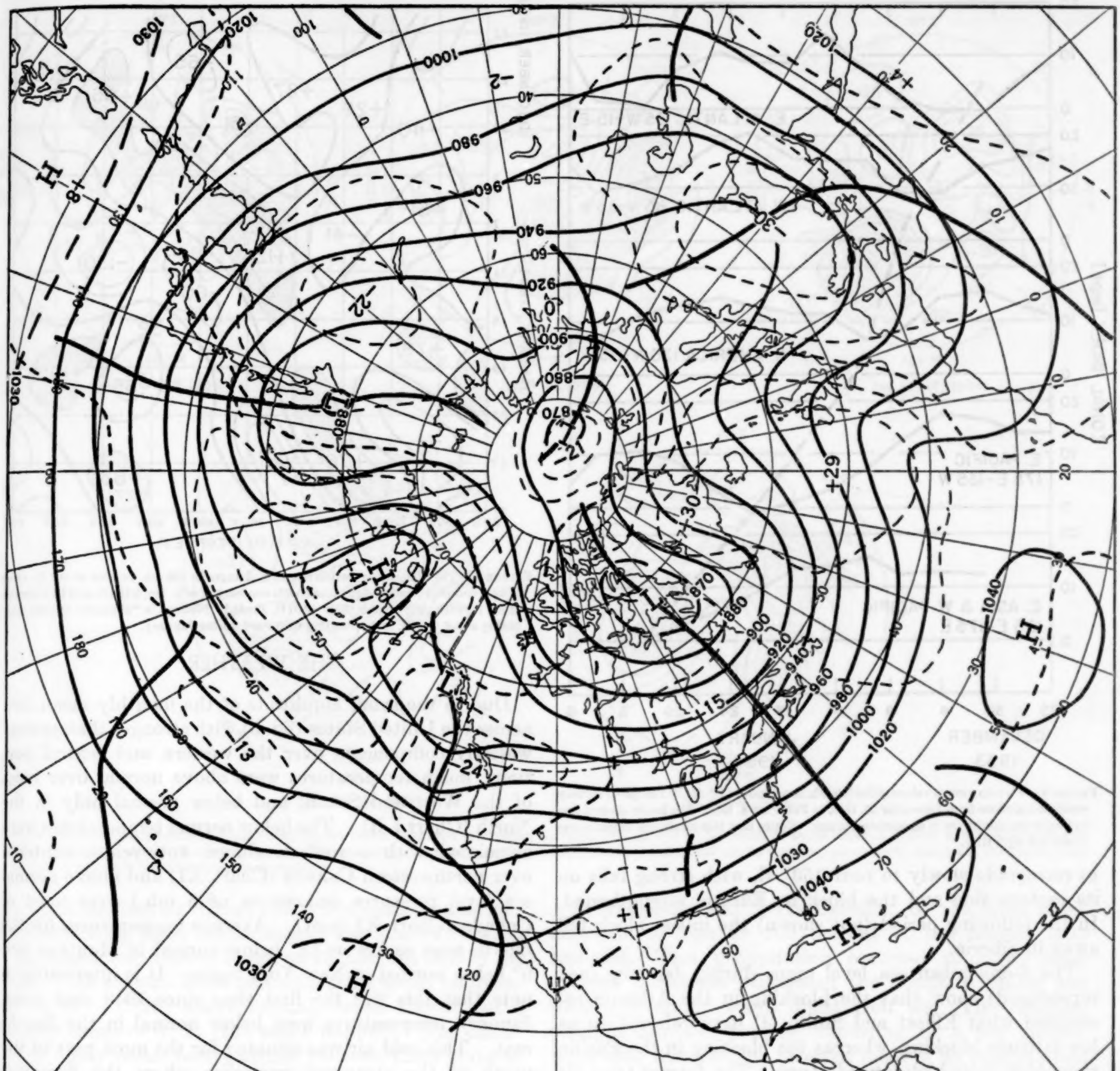

FIGURE 5.—Mean 700-mb. height contours and departure from normal (both in tens of feet) for January 1954. Above normal heights prevailed north of 50° N. in the Western Hemisphere.

spreading westward from this center, as shown by the large positive anomalies extending to about 120° W., where a week earlier heights had been below normal. The following week (fig. 8C) the block became well established over the eastern Pacific with maximum departures of +900 feet around 55° N., 165° W., while heights fell away over Canada. In the Atlantic the blocking condition almost disappeared as strong zonal flow became re-established. Figure 8D indicates a very slow retrogression of the block. To its east abnormally cold air was advected over the Gulf of Alaska accompanied by strong cyclogenesis. Meanwhile, on the other side of the hemisphere another block developed in Eurasia. During the next week (fig. 8E) the Pacific block continued

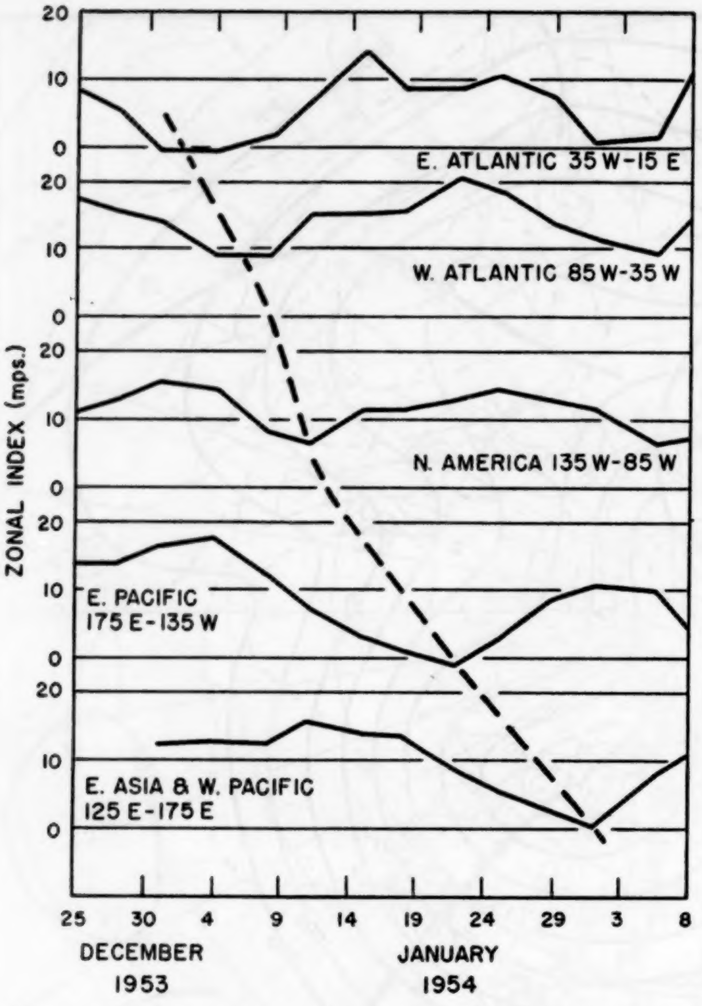

FIGURE 6.—Five-day mean values of the 700-mb. zonal index (35°–55° N.) for progressively westward sections from December 25, 1953, to February 8, 1954. The heavy dashed line indicates the minimum in successive sections. Notice how this minimum index moves westward with time.

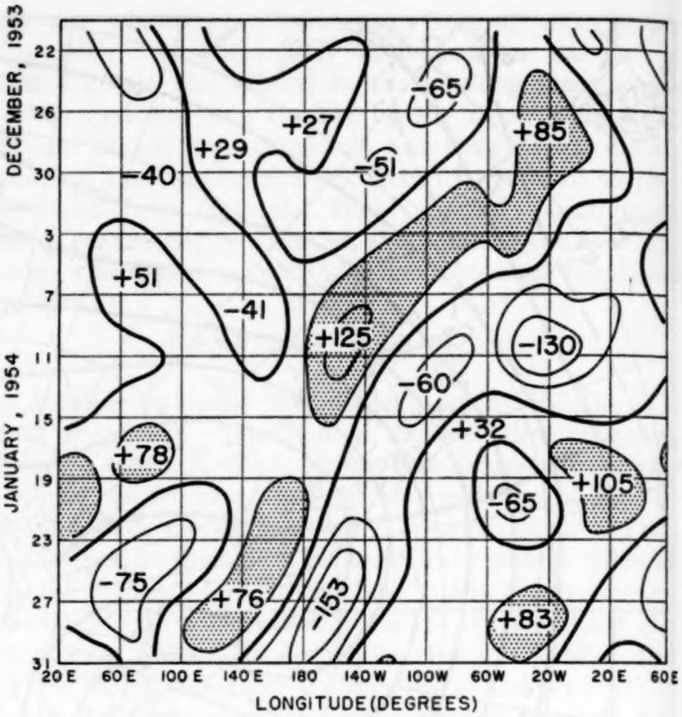

FIGURE 7.—Time-longitude section showing changes in 700-mb. heights at 60° N. (tens of feet) computed from 5-day mean charts one week apart. Isopleths drawn for intervals of 500 ft. with rises greater than +500 ft. shaded. Notice the "channel" of rises originating about 20° W. and spreading westward during January.

to retrograde slowly to near 150° E. with strong falls on its eastern side and the block in Eurasia strengthened. In the following period (not shown) the initial block fell away in Siberia.

The 5-day mean sea level maps during January (not reproduced) show that the blocking in the Atlantic resembled what Elliott and Smith [4] have referred to as low-latitude blocking, whereas the blocking in the Pacific resembled their high-latitude type. The former type "is characterized by a northward extension of the subtropical high cell where the connection with this cell is not broken; any trapped low-pressure centers being formed well to the east of the blocking high cell." On the other hand, their high-latitude type is "characterized by a high-pressure cell far to the north and trapped low-pressure areas along the southern periphery." The behavior of the blocking also seems consistent with their findings and with Yeh's theoretical results on differential rate of energy dispersion at high and low latitudes [6] since the Atlantic block, being of the low-latitude type, extended its influence westward more rapidly than the Pacific block.

THE WEATHER

Due to the small amplitude of the monthly mean flow across the United States (fig. 5) with stronger than normal westerly components over the western and central portions, mean temperatures were above normal over most of the West and South, and below normal only in the North (Chart I-B). The below normal temperatures were associated with a well developed anticyclone centered over northwestern Canada (Chart XI) and above normal sea level pressures (maximum of 8 mb.) over most of Canada (Chart XI inset). Average temperatures for the month were as low as 13° below normal in Montana and 6° below normal in New York State. It is interesting to note that this was the first time since 1948 that mean January temperatures were below normal in the Northeast. This cold air was situated for the most part to the north of the strongest westerlies where the flow was weaker than normal (fig. 4b). It appears that this cold air could not penetrate farther south in the mean due to the containing action of the fast westerlies [7].

In the Plains States the finger of below normal temperatures extending southward corresponds with the prevailing path of polar anticyclones entering the United States from Canada (Chart IX). These polar outbreaks, while frequent, were shallow and were therefore rapidly modified and swept out into the Atlantic in response to the zonal flow aloft.

In the northern Rocky Mountain States an unusually strong contrast was observed between warm Pacific air

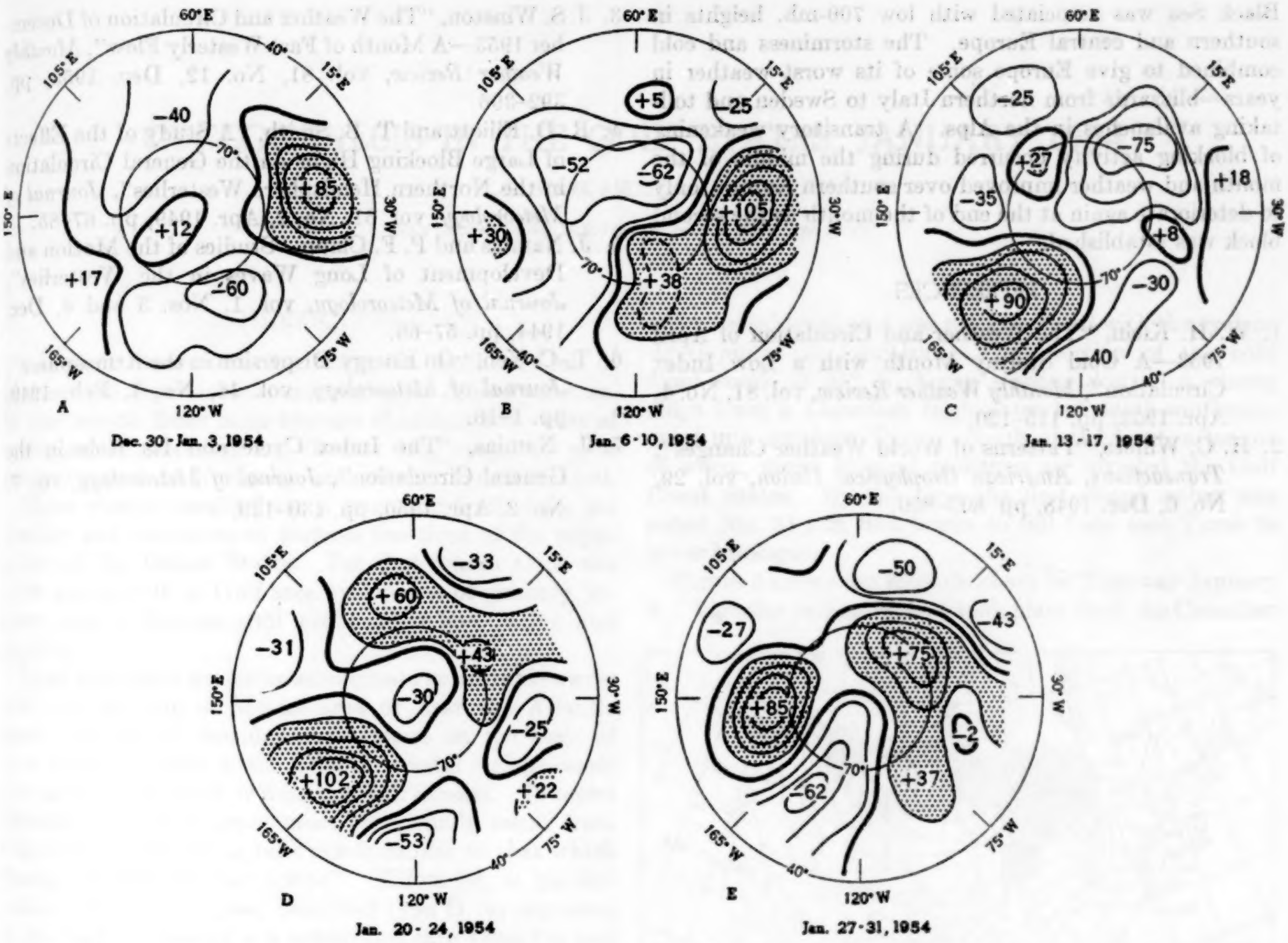

FIGURE 8.—Series of polar projections of 5-day mean 700-mb. height departures from normal (in tens of feet) north of 40° N. Isopleths are for intervals of 200 ft. with positive anomalies greater than 200 ft. shaded. Large positive anomalies appeared in the Atlantic (+850 ft.) early in January and spread rapidly westward across North America to the Pacific where the rate of westward motion diminished appreciably.

and cold Canadian air (Chart I-B). For example a surface front separating these two air masses was located between Boise, Idaho, and Havre, Mont. on 23 different days of the month. As a result Boise had a monthly mean temperature of 37° F. (10° above normal), while Havre had a monthly mean of 0° F. (13° below normal). The difference in daily mean temperatures between these stations was 40° or greater on 16 days of January and reached an extreme of 62° F. on January 23.

Precipitation amounts for the month (Chart III) exceeded normal along the west coast and in the Northern Plains, as well as in the area from Arkansas eastward to the Atlantic. Elsewhere, for the most part, amounts were below normal, with parts of the Central Plains receiving only some 10 percent of the normal. This region was located south of the principal storm track (Chart X) and was dominated by Pacific air masses which were considerably dried out upon crossing the mountains. A few cyclones went through the region, but were too weak and fast moving to be effective in producing significant amounts of precipitation.

In Tennessee and North Carolina, on the other hand, amounts as high as 200 percent of the normal were reported. This precipitation occurred primarily after cold cP outbreaks penetrated the Southern States and were overrun by warm moist Gulf air. The resulting precipitation was copious, occurring in a few storms. Knoxville, for example, received most of its precipitation in two storms which together gave 10.10 inches as compared with its total monthly precipitation of 11.73 inches.

Heavy precipitation along the Pacific Coast occurred as a result of increased cyclonic activity in the eastern Pacific and stronger than normal westerly flow over the coastal ranges. The precipitation was particularly welcome in southern California where droughty conditions had developed. Along the northern border the excess amounts occurred as a large number of cyclones traveled along the mean frontal zone.

The Atlantic block which appeared early in the month and recurred at the end of the month caused cold air from Russia and the Arctic to overspread all Europe. Frequent cyclonic activity from the Gulf of Genoa eastward to the

289649—54——3

Black Sea was associated with low 700-mb. heights in southern and central Europe. The storminess and cold combined to give Europe some of its worst weather in years—blizzards from northern Italy to Sweden and toll-taking avalanches in the Alps. A transitory weakening of blocking activity occurred during the middle of the month and weather improved over southern Europe, only to deteriorate again at the end of the month as the second block was established.

REFERENCES

1. W. H. Klein, "The Weather and Circulation of April 1953—A Cold Stormy Month with a Low Index Circulation", *Monthly Weather Review*, vol. 81, No. 4, Apr. 1953, pp. 115–120.
2. H. C. Willett, "Patterns of World Weather Changes", *Transactions, American Geophysical Union*, vol. 29, No. 6, Dec. 1948, pp. 803–809.
3. J. S. Winston, "The Weather and Circulation of December 1953—A Month of Fast Westerly Flow", *Monthly Weather Review*, vol. 81, No. 12, Dec. 1953, pp. 392–396.
4. R. D. Elliott and T. B. Smith, "A Study of the Effects of Large Blocking Highs on the General Circulation in the Northern Hemisphere Westerlies", *Journal of Meteorology*, vol. 61, No. 2, Apr. 1949, pp. 67–85.
5. J. Namias and P. F. Clapp, "Studies of the Motion and Development of Long Waves in the Westerlies", *Journal of Meteorology*, vol. 1, Nos. 3 and 4, Dec. 1944, pp. 57–66.
6. T.-C. Yeh, "On Energy Dispersion in the Atmosphere", *Journal of Meteorology*, vol. 16, No. 1, Feb. 1949, pp. 1–16.
7. J. Namias, "The Index Cycle and Its Role in the General Circulation", *Journal of Meteorology*, vol. 7, No. 2, Apr. 1950, pp. 130–139.

CYCLOGENESIS IN THE GULF STATES, JANUARY 1954

L. P. STARK AND D. A. RICHTER

WBAN Analysis Center, U. S. Weather Bureau, Washington, D. C.

INTRODUCTION

The Gulf States area (including the northern Gulf of Mexico) is a dependable source region for January storms. In this month there is an average of almost five cases of cyclogenesis, according to Visscher [1], compared with two per month in November and one per month in April.

These storms usually have a pronounced effect on the comfort and commerce of perhaps one-third of the population of the United States. For that reason alone the birth and growth of Gulf area cyclones is of primary interest and a fundamental problem for speculation and inquiry.

Most east coast winter Lows originate as unstable waves either in the Gulf of Mexico area or near the Atlantic coast. Miller [2] classified such storms on the basis of their genesis strictly in the Atlantic coastal region—some over land, others over or near the Gulf Stream. It seems probable that both types must occasionally result from Gulf-bred storms whose behavior is similar to that which George [3] calls "center jumps". Elliott [4], in his discussion of weather types, described type G (cyclogenesis in the Gulf). This type is subdivided into types Ga and Gb, both of which originate in the Gulf area and may eventually mature to east coast storms of major proportions. In his study of Texas-West Gulf cyclones, Saucier [5] suggested two synoptic patterns, the Great Plains trough and the Southwest cold-core Low, from which such cyclones form.

In January 1954 there were three instances of cyclogenesis in the Gulf States area in a period of less than 2 weeks. All three were responsible for widespread precipitation including rain, snowstorms or sleet, and attendant public inconvenience. From that standpoint alone each of those three Lows is worthy of comment. In this study, however, most attention will be given to antecedent synoptic patterns in the lower and mid-troposphere and those features associated with cyclogenesis.

CYCLOGENESIS ON JANUARY 10, 1954

The storm of January 10 (hereafter referred to as Storm I) was first detected at 0630 GMT on that date just south of Shreveport, La. (fig. 2). Twenty-four hours prior to the genesis of Storm I (fig. 1) the parent Low was over southeastern Wisconsin. The Low over west Texas moved southward, and was not associated with the cyclone development in Louisiana. That portion of the cold front south of 35° N. began slowing down. A strong ridge from a Canadian High extended south-southeastward into northern Texas. South of the front, a tongue of warm, moist tropical maritime air invaded the Gulf Coast States. By the time the first closed isobar was noted (fig. 2) rain had begun to fall from east Texas to lower Michigan.

Figure 3 shows the 850-mb. chart for 0300 GMT January 9. Vigorous cold advection took place from the Canadian

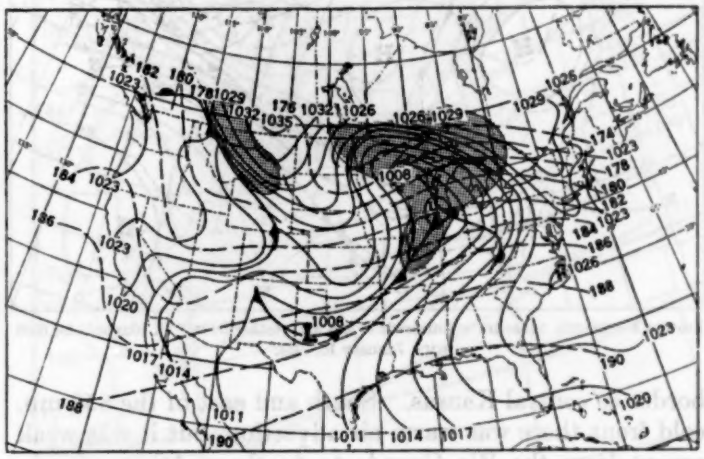

FIGURE 1.—Surface chart for 0630 GMT and 500-mb. contours in hundreds of feet (dashed) for 0300 GMT, January 9, 1954. Shading indicates areas of active precipitation.

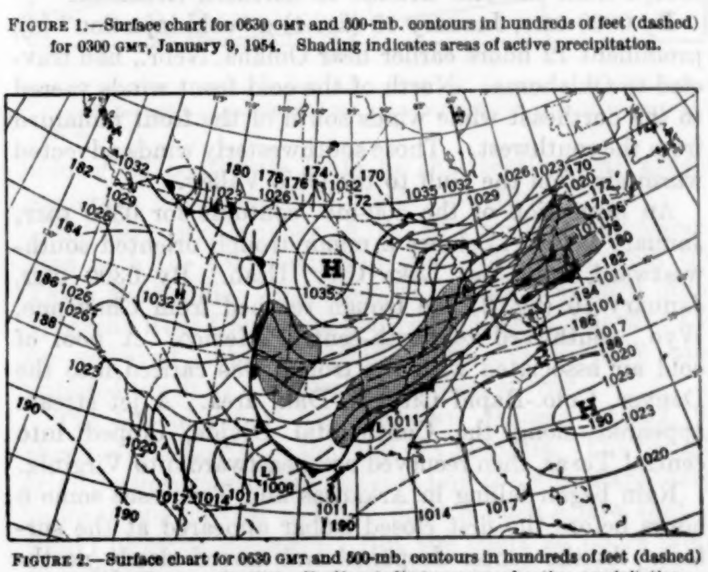

FIGURE 2.—Surface chart for 0630 GMT and 500-mb. contours in hundreds of feet (dashed) for 0300 GMT, January 10, 1954. Shading indicates areas of active precipitation.

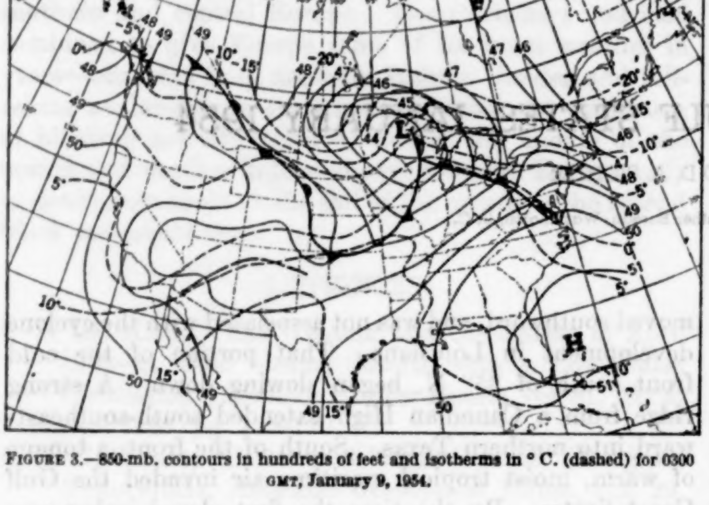

FIGURE 3.—850-mb. contours in hundreds of feet and isotherms in ° C. (dashed) for 0300 GMT, January 9, 1954.

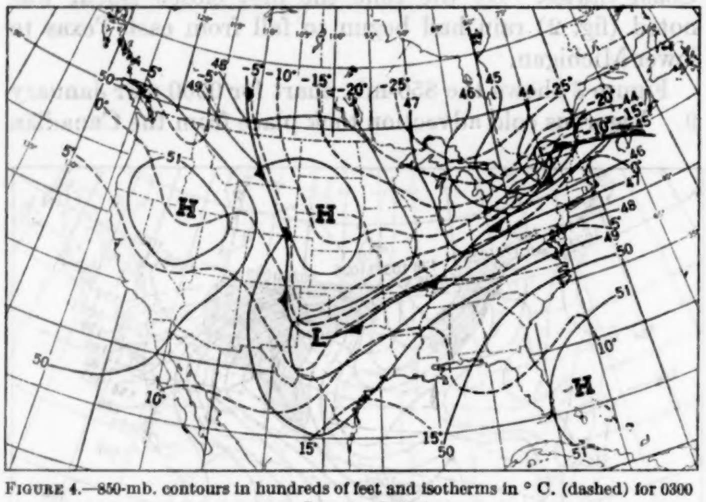

FIGURE 4.—850-mb. contours in hundreds of feet and isotherms in ° C. (dashed) for 0300 GMT, January 10, 1954.

border to central Kansas. South and east of the 850-mb. cold front there was warm air advection, but it was weak except from the Rio Grande to northern Arkansas.

By 0300 GMT, January 10 (fig. 4) a "cold injection" [3], prominent 12 hours earlier near Omaha, Nebr., had traveled to Oklahoma. North of the cold front winds veered to the northeast while winds south of the front remained from the southwest. Those southwesterly winds advected warm air from the Gulf to the Ohio Valley.

An inspection of the 500-mb. contours for 0300 GMT, January 9 (fig. 1) shows a minor trough oriented southwestward from Salt Lake City, Utah. By 0300 GMT, January 10 (fig. 2) the trough reached from Cheyenne, Wyo., southward to north-central Mexico. A pool of cold air associated with the trough was carried into the Denver, Colo.-Rapid City, S. Dak. area. A jet stream appeared along the Continental Divide, dipped into central Texas, then recurved northeastward into Virginia.

Rain began falling in Arkansas and Tennessee some 6 hours before the first closed isobar appeared at the surface. As the center deepened and moved slowly northeastward (fig. 5) the rain changed to freezing rain, sleet,

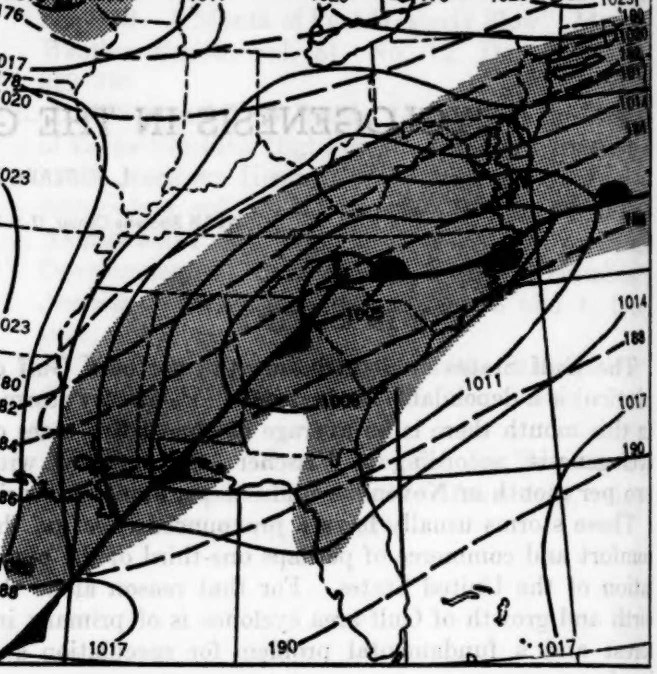

FIGURE 5.—Surface section for 0630 GMT and 500-mb. contours in hundreds of feet (dashed) for 0300 GMT, January 11, 1954. Shading indicates areas of active precipitation.

and snow north of the front. Thunderstorms and substantial rainfall were reported as the southern portion of the front moved eastward replacing and forcing aloft the moist Gulf air. Behind the cold front the surge of Arctic air caused temperatures to drop below freezing along the Gulf Coast from Corpus Christi, Tex., to Mobile, Ala. [6]. As the Low developed further, snow began accumulating. In the Atlantic Coastal States 6 to 10 inches fell from New Jersey northward. One to two inches were measured from West Virginia southwestward to Oklahoma.

CYCLOGENESIS ON JANUARY 15, 1954

On January 14, 24 hours prior to the development of Storm II the surface chart (fig. 6) shows that a quasi-stationary polar front twisted through the Gulf States and northeastward to the Atlantic seaboard. A cold outbreak similar to that found in Storm I was not readily apparent, although a weak cold ridge existed from Iowa to North Dakota. Next day (fig. 7) there was a cold outbreak following the formation of a new wave on the Arctic front, but it did not appear to be directly associated with the Low near Shreveport, La.

A pressure minimum in the Rocky Mountain lee trough (fig. 6) progressed rapidly eastward in 24 hours (fig. 7). Meanwhile the stationary polar front began to move as it was caught in this circulation. Twenty-four-hour pressure falls of 5 to 10 mb. were prevalent in the proximity of the 1,008-mb. center near Shreveport.

The 850-mb. chart for 1500 GMT, January 14 (fig. 8) shows a conspicuous absence of cold air advection east of the Rockies, except that of relatively minor magnitude

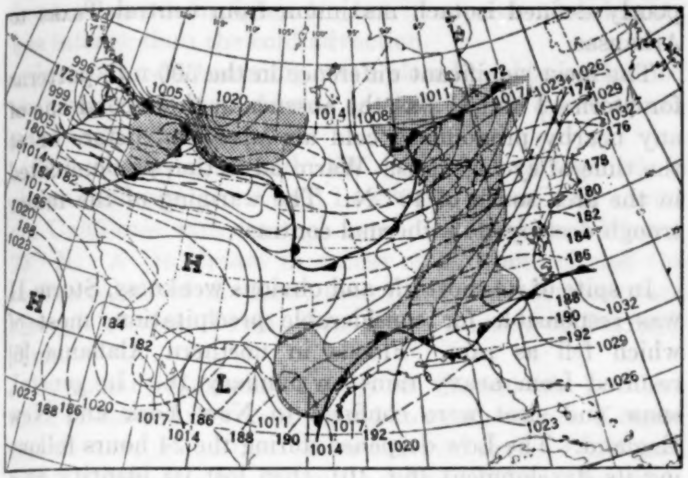

FIGURE 6.—Surface chart 1830 GMT and 500-mb. contours in hundreds of feet (dashed) for 1500 GMT, January 14, 1954. Shading indicates areas of active precipitation.

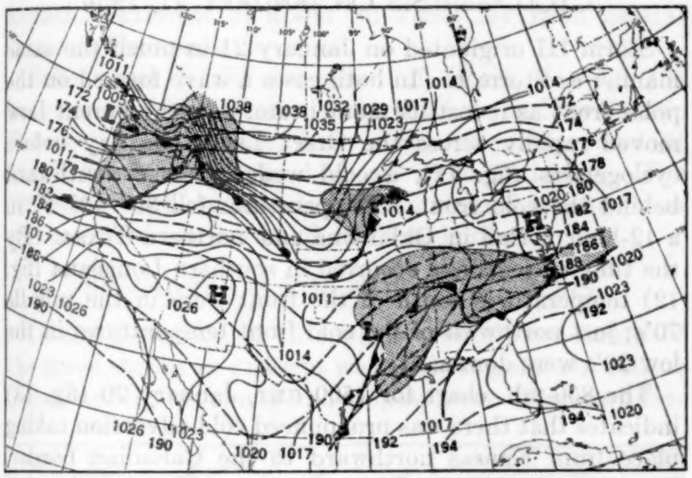

FIGURE 7.—Surface chart for 1830 GMT and 500-mb. contours in hundreds of feet (dashed) for 1500 GMT, January 15, 1954. Shading indicates areas of active precipitation.

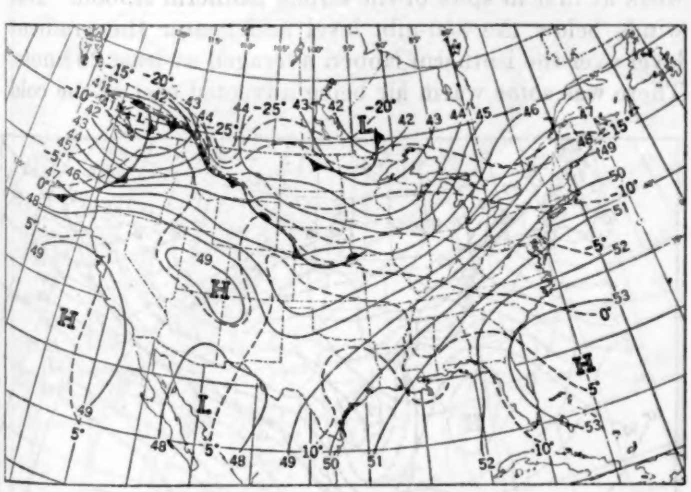

FIGURE 8.—850-mb. contours in hundreds of feet and isotherms in ° C. (dashed) for 1500 GMT, January 14, 1954.

in northern Minnesota and in the eastern Colorado-New Mexico region. A cold injection appears to be forming over northern Montana. Compared with Storm I, the 850-mb. level the day before cyclogenesis in Storm II

289649—54——4

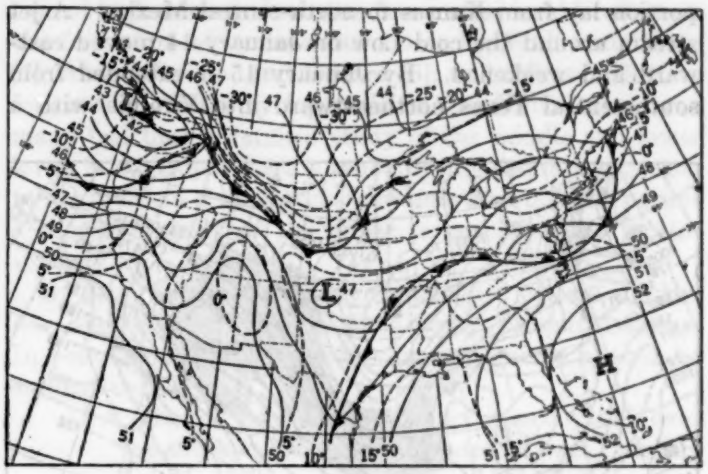

FIGURE 9.—850-mb. contours in hundreds of feet and isotherms in ° C. (dashed) for 1500 GMT, January 15, 1954.

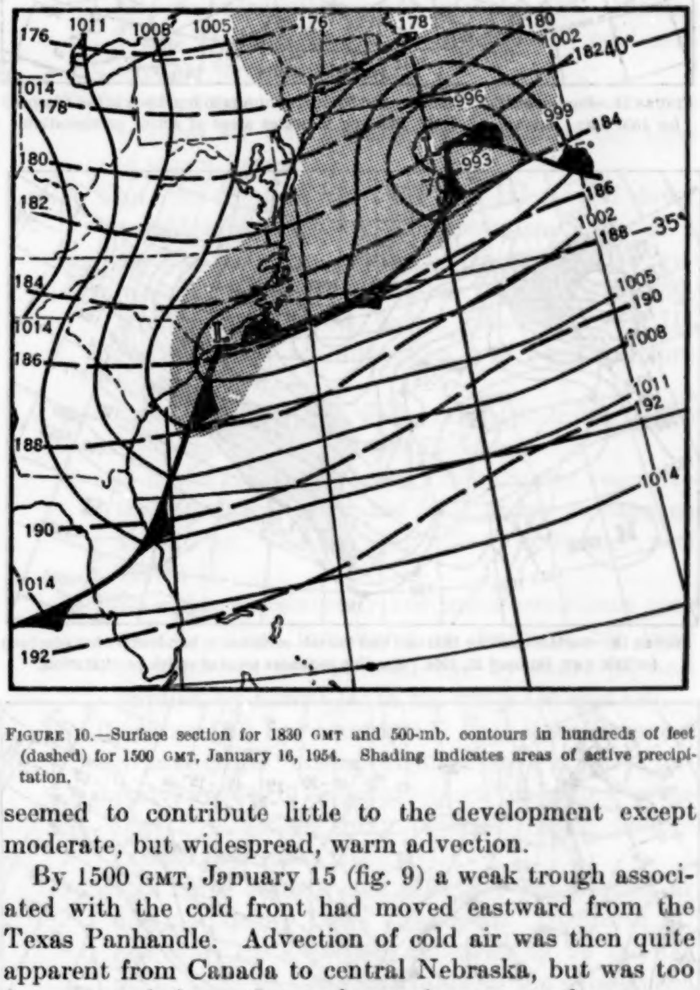

FIGURE 10.—Surface section for 1830 GMT and 500-mb. contours in hundreds of feet (dashed) for 1500 GMT, January 16, 1954. Shading indicates areas of active precipitation.

seemed to contribute little to the development except moderate, but widespread, warm advection.

By 1500 GMT, January 15 (fig. 9) a weak trough associated with the cold front had moved eastward from the Texas Panhandle. Advection of cold air was then quite apparent from Canada to central Nebraska, but was too far removed from the cyclogenetic area to have contributed much as a source of potential energy.

The 500-mb. chart for 1500 GMT, January 14 (fig. 6) shows a cold Low over the Gulf of California. The trough lying northeastward from the cold Low to Canada appeared to be strong enough and imbedded in such a flow that it would progress eastward. But the chart 24 hours later (fig. 7) shows that the northern portion of the trough disappeared in the strong westerly flow; the southern

portion lay from Kansas to north-central Mexico. A jet stream around the cold Low on January 14 moved eastward and weakened. By January 15 it extended from south-central Texas northeastward into Virginia with a poorly defined isotach maximum from central Texas to Arkansas.

The most significant difference in the 500-mb. patterns for Storms I and II was the absence in the second one of any nearby pronounced cold air advection before or at the time of cyclogenesis. Warm advection predominated in the area south of 40° N. The warming of the minor trough destroyed its thermal contrast.

In spite of its short life and obvious weakness, Storm II was responsible for considerable precipitation, most of which fell as rain. Floods in northern Alabama [6] resulted from heavy rains on January 16. In general, snow and sleet were confined to New York and New England. The Low deepened during the 24 hours following its development (fig. 10), then lost its identity as a new Low formed offshore.

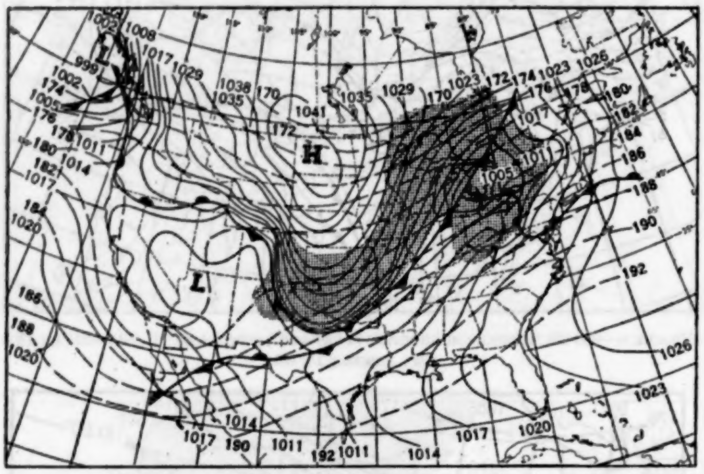

FIGURE 11.—Surface chart for 1830 GMT and 500-mb. contours in hundreds of feet (dashed) for 1500 GMT, January 20, 1954. Shading indicates areas of active precipitation.

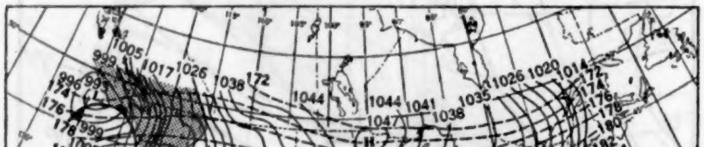

FIGURE 12.—Surface chart for 1830 GMT and 500-mb. contours in hundreds of feet (dashed) for 1500 GMT, January 21, 1954. Shading indicates areas of active precipitation.

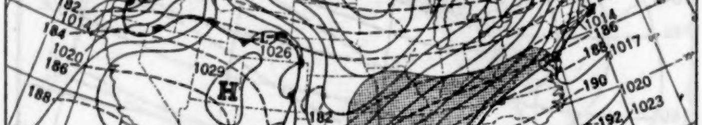

FIGURE 13.—850-mb. contours in hundreds of feet and isotherms in ° C. (dashed) for 1500 GMT, January 20, 1954.

CYCLOGENESIS ON JANUARY 21, 1954

Storm III originated on January 21 in much the same manner as Storm I. In both cases a wave formed on the polar front as it lost its momentum. As the parent Low moved rapidly across the Great Lakes the day before cyclogenesis (fig. 11), a cold wedge pushed southward behind the cold front. Temperatures fell 30°–40° F. in a 12-hour period in Oklahoma and northern Texas. By the time cyclogenesis occurred in southern Louisiana (fig. 12) temperatures south of the front were in the middle 70's; just northwest of the cold front temperatures in the low 20's were dominant.

The 850-mb. chart for 1500 GMT, January 20 (fig. 13) indicates that there was pronounced cold advection taking place from Kansas northward to the Canadian border. There was a cold injection over western Kansas. In view of the light winds at this level, advection may appear weak at first in spite of the strong isotherm ribbon. But winds below the 850-mb. level and nearer the gradient level over the isotherm ribbon averaged at least 20 knots. There was some warm air being advected east of the cold

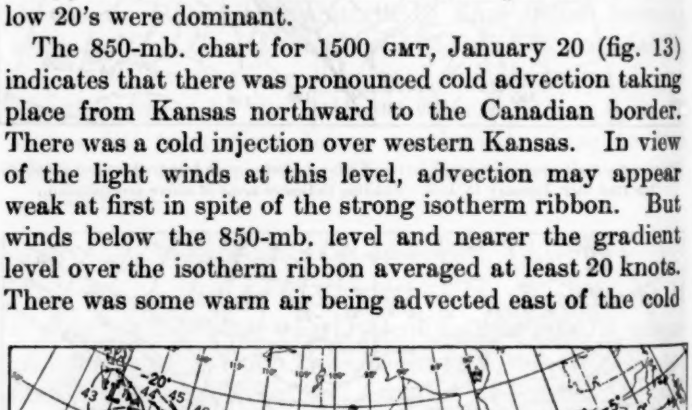

FIGURE 14.—850-mb. contours in hundreds of feet and isotherms in ° C. (dashed) for 1500 GMT, January 21, 1954.

front as shown in figure 13, but it appears considerably less intense than the cold advection.

In another 24 hours (fig. 14) a closed circulation formed over northwestern Arkansas as the cold air drove southward to the Rio Grande.

The pattern at 500-mb. the day before cyclogenesis is shown in figure 11. A cold Low was centered over southern California with a trough extending southward beyond 25° N. A jet stream in excess of 80 knots circled the southern half of the Low, then continued northeastward through western Texas, then across country to Pennsylvania.

By 1500 GMT, January 21 (fig. 12) the 500-mb. Low had filled about 400 feet as it moved to southwestern Kansas. But the trough and Low center contined to move eastward with a resulting fall in 500-mb. height and surface pressure.

The jet stream was oriented northeastward from northern Mexico across the Atlantic coast near Delaware. An isotach maximum of about 80 knots lay from central Texas to Tennessee.

Subsequent to the formation of Storm III (fig. 15) heavy snow fell northward from the Low to New Jersey. Heaviest amounts were observed in eastern Maryland [6] where totals ranged as high as 10 to 12 inches. The 500-mb. trough meanwhile had maintained its sharpness and eastward movement of about 30 knots.

SUMMARY OF SYNOPTIC CONDITIONS

In the discussion of antecedent synoptic conditions of the three storms an attempt was made to point out salient features of the lower and mid-troposphere. The contribution of higher levels doubtless has a considerable effect on the formation of cyclones as shown by Wulf and Obloy [7], Alaka, Jordan, and Renard [8], and others. But for forecasting winter cyclogenesis in the Gulf States area many feel that a detailed study of the middle and lower levels in the troposphere is probably an adequate approach to the problem if the forecasters' time does not also permit a thorough study of the upper troposphere and stratosphere.

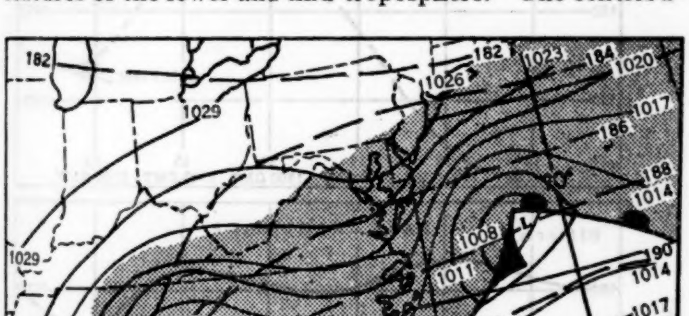

FIGURE 15.—Surface section for 1830 GMT and 500-mb. contours in hundreds of feet (dashed) for 1500 GMT, January 22, 1954. Shading indicates areas of active precipitation.

By now the reader will have catalogued certain similarities and differences in the three storms presented above. In summary, then, the following statements should be emphasized:

1. A 500-mb. cold Low or trough was located over the southwestern United States at least 24 hours before cyclogenesis. The cold troughs moved eastward and were partially responsible for surface pressure falls (except in Storm II). Storms I and II were similar to Saucier's [5] cold-core cyclone formation.
2. An adequate supply of warm, moist, maritime tropical air was present before and at the time of storm formation.
3. The cold front in Storms I and III slowed down considerably before cyclogenesis; in Storm II a stationary front was present for wave formation.
4. Pronounced cold air advection took place at 850- and 500-mb. levels before Storms I and III formed; cold air advection was absent before Storm II formed.
5. The parent Low was well over 1,000 miles to the northeast of the cyclogenetic area.
6. 850-mb. winds in the lower Plains States veered to the northeast after the cold front passage as noted by Visscher [1]. The exception was Storm II.
7. Low index or relatively low index conditions prevailed. That low index is desirable for Gulf cyclogenesis was pointed out by Starr [9] and implied by Elliott [4] in his types Ga and Gb.
8. Bjerknes [10] has commented that it is necessary to have either "unstable frontal wave action or unstable growth of an upper trough" or both in order that cyclogenesis may proceed. Both factors existed in Storms I and III.
9. In all three cases a cold injection was present at 850-mb. before Lows developed. In Storm II, however, the injection appeared to be too far north to be of any importance in the subsequent wave formation.
10. 1,000-500-mb. thickness values increased over the areas of cyclogenesis (fig. 16) while 500-mb. heights generally decreased or were unsteady. The surface pressure falls were a reflection of the height falls and the thickness increases. (See next section.)

11. The activity of the jet stream was essentially the same in the three cases studied. An isotach maximum lay over or slightly to the north of the areas of surface development.

COMMENTS ON FORECASTING CYCLOGENESIS

THE GEORGE METHOD

A method proposed by George [3] was applied to the three January storms to determine whether cyclogenesis would occur and, if so, with what intensity. When used on Storm I the day before development, a center jump appeared likely and cyclogenesis was not favored. Actually, there was a center jump in addition to cyclogenesis of intensity 12 near Shreveport, La.

On Storm II this method indicated cyclogenesis of intensity 5 would occur in southwestern Kansas. A center of intensity 8 was found 24 hours later some 350 miles to the south-southeast even though the cold injection was far north of 38° N. (Cyclogenesis is most favored when the isotherm ribbon is below 38° N.)

In the case of Storm III a forecast development of intensity 6 in central Georgia compared favorably with the actual center of intensity 9 in central Louisiana.

1,000-500-MB. THICKNESS PATTERNS

The departure from normal of the 1,000-500-mb. thickness prior to the development of these storms was studied. A similarity of pattern was evident in all three cases. The greater than normal source of potential energy was delineated by the gradient and geographical location of the centers of plus and minus departures. In Storms I and III the gradient was largest northwest of the cyclogenetic areas; in Storm II the greatest gradient was to the southwest.

There are other ways in which thickness can be used effectively as an aid in forecasting cyclogenesis as proposed by Sutcliffe and Forsdyke [11]. A visual and subjective evaluation of vorticity can be made. If cyclonically curved thickness contours lie upstream from a region of suspected cyclogenesis, one could conclude that cyclonic development is more probable in view of the potential increase in cyclonic thermal vorticity. In the three cases studied here there was an increase in cyclonic curvature of the thickness contours (not reproduced) over the regions of Low formation which could have been projected downstream without apparent difficulty. It was felt that perhaps thickness mean flow charts would have been useful in forecasting the areas of thermal vorticity. Such charts were constructed, but their usefulness was not readily apparent. Linear extrapolation proved of most value.

Another tool can be derived from a consideration of the 1,000-500-mb. thickness patterns. A subjective determination of the greatest possible deepening in an area of likely cyclogenesis can be made by answering the question: What would be the lowest 500-mb. contour and the highest 1,000-500-mb. thickness contour in the suspected area in

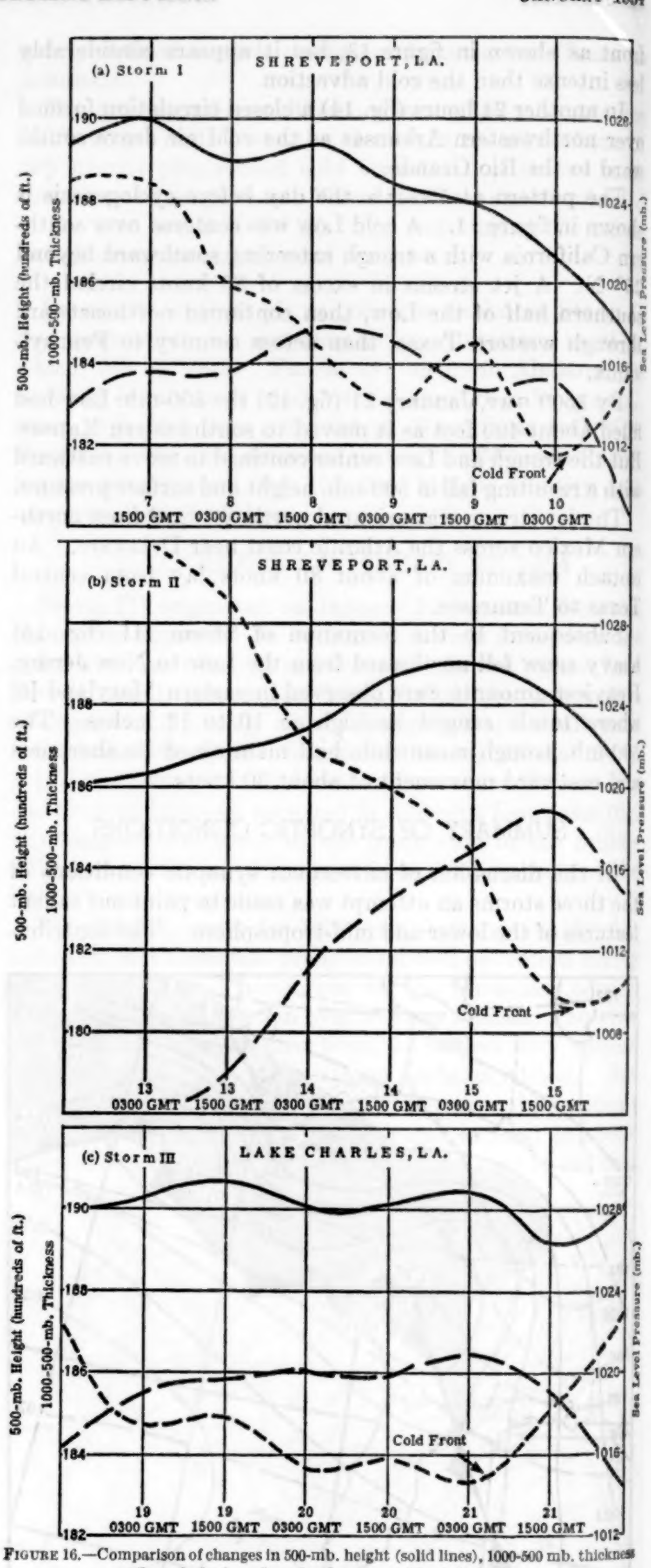

FIGURE 16.—Comparison of changes in 500-mb. height (solid lines), 1000-500 mb. thickness (long dashes), and sea level pressure (short dashes).

24 or 36 hours? In short, a "reasonable" forecast of both thickness and 500-mb. values would result in a reasonable (and consistent) surface prognosis.

The combined contributions of the thickness and 500-mb. changes to the surface pressure changes in the three January storms are graphically illustrated in figure 16. Several prominent features of this figure are:

1. It shows best the effects which falling 500-mb. heights and rising thicknesses have on surface pressure falls
2. Thickness values and 500-mb. heights began falling or fell more rapidly after the cold front passed.
3. In general, thickness values increased as the cold front approached while 500-mb. heights fell.

CONCLUSION

It is felt that cyclogenesis in the Gulf States can be better understood and can be forecast with more confidence and certainty if the George method and thickness considerations are integrated into the pre-forecast synoptic study

ACKNOWLEDGMENTS

The authors are indebted to Messrs. A. K. Showalter, F. W. Burnett, and V. J. Oliver for their comments and criticisms.

REFERENCES

1. H. B. Visscher, *The Formation of Extratropical Cyclones in the Gulf of Mexico and the Resultant Spread of Precipitation*, Eastern Air Lines, Inc., Atlanta, Ga., 1948, 30 pp.
2. J. E. Miller, *Cyclogenesis in the Atlantic Coastal Region of the United States*, Department of Meteorology, College of Engineering, New York University, 1945, 77 pp.
3. J. J. George et al., "Forecasting Relationships Between Upper Level Flow and Surface Meteorological Processes", *Geophysical Research Paper* No. 23, Air Force Cambridge Research Center, Cambridge, Mass., August 1953, pp. 21–50.
4. R. D. Elliott, "Weather Types of North America", *Weatherwise*, vol. 2, No. 5, Oct. 1949, pp. 110–113.
5. W. J. Saucier, "Texas-West Gulf Cyclones", *Monthly Weather Review*, vol. 77, No. 8, Aug. 1949, pp. 219–231.
6. U. S. Weather Bureau, *Weekly Weather and Crop Bulletin, National Summary*, vol. XLI, No. 2, Jan. 11, 1954, No. 3, Jan. 18, 1954, No. 4, Jan. 25, 1954, Washington, D. C.
7. O. R. Wulf and S. J. Obloy, "The Utilization of the Entire Course of Radiosonde Flights in Weather Diagnosis", Department of Meteorology, University of Chicago, *Miscellaneous Report* No. 10, 1944, 110 pp.
8. M. A. Alaka, C. L. Jordan, R. J. Renard, "The Jet Stream" NAVAER 50–IR–249, Department of Meteorology, University of Chicago, June 1, 1953.
9. V. P. Starr, *Basic Principles of Weather Forecasting*, Harper and Brothers, New York, 1942, p. 35.
10. J. Bjerknes, "Extratropical Cyclones", *Compendium of Meteorology*, American Meteorological Society, Boston, Mass., 1951, pp. 577–598.
11. R. C. Sutcliffe and A. G. Forsdyke, "The Theory and Use of Upper Air Thickness Patterns in Forecasting", *Quarterly Journal of the Royal Meteorological Society*, vol. 76, No. 328, Apr. 1950, pp. 189–217.

U. S. GOVERNMENT PRINTING OFFICE: 1954

Chart I. A. Average Temperature (°F.) at Surface, January 1954.

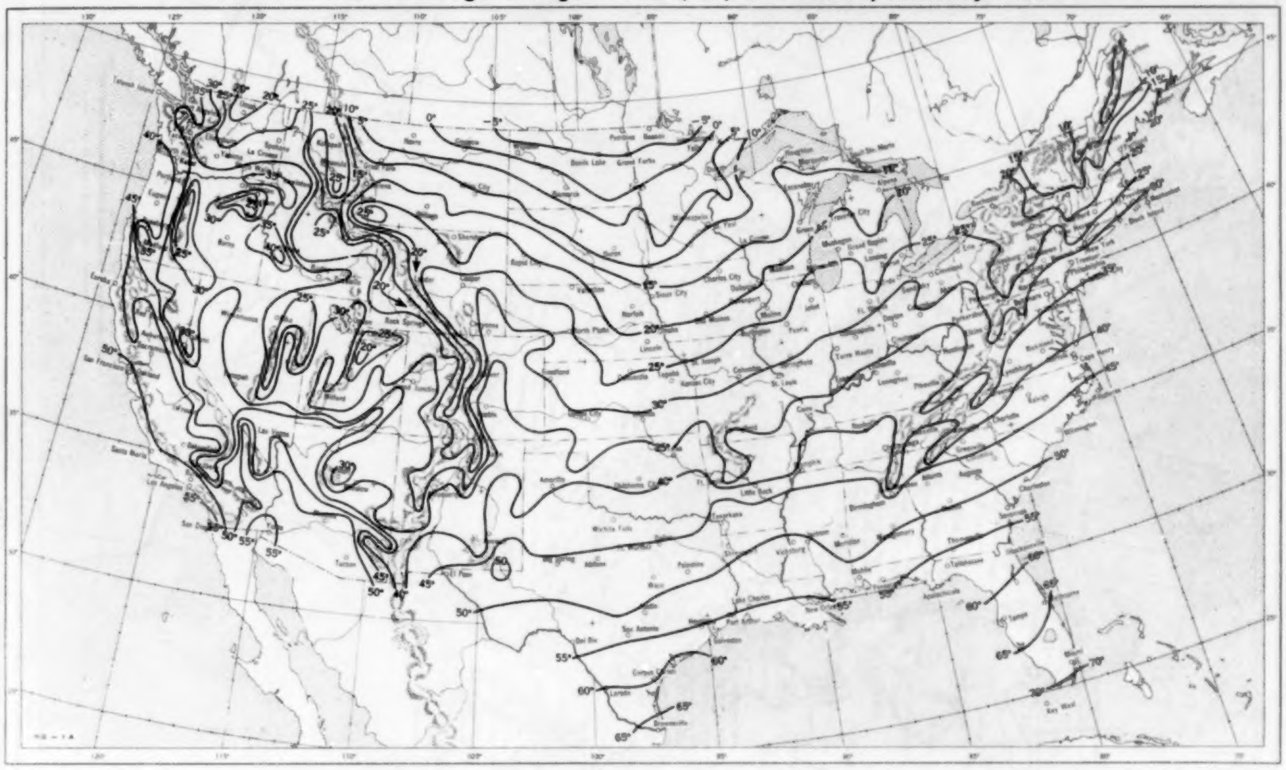

B. Departure of Average Temperature from Normal (°F.), January 1954.

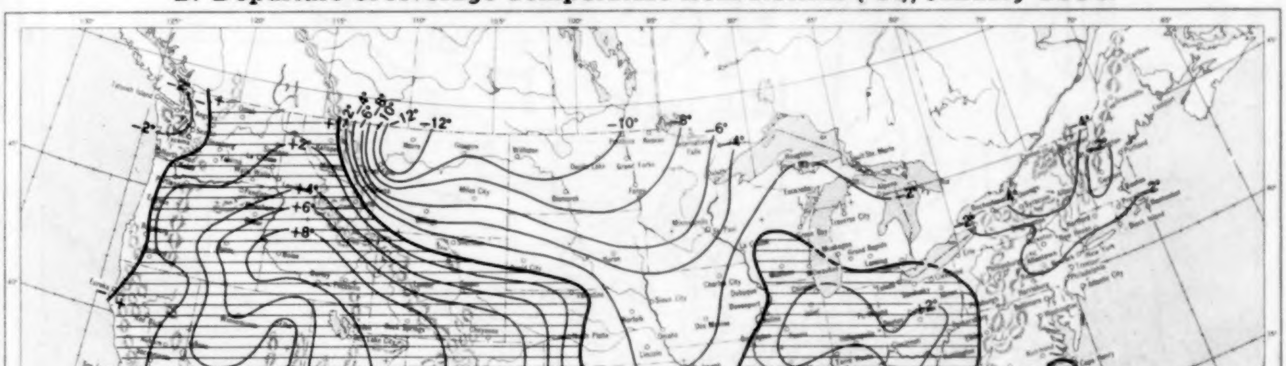

A. Based on reports from 800 Weather Bureau and cooperative stations. The monthly average is half the sum of the monthly average maximum and monthly average minimum, which are the average of the daily maxima and daily minima, respectively.
B. Normal average monthly temperatures are computed for Weather Bureau stations having at least 10 years of record.

Chart II. Total Precipitation (Inches), January 1954.

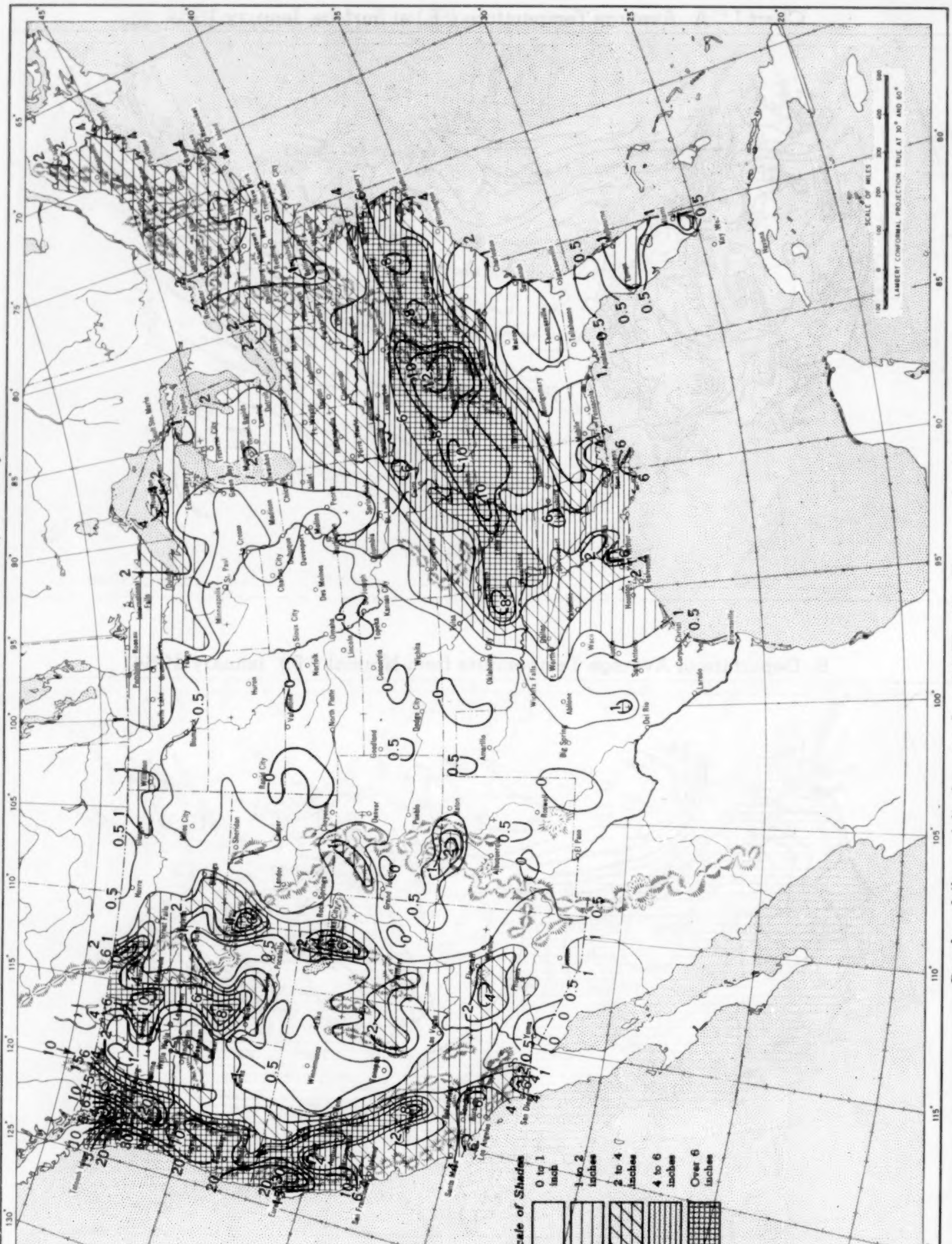

Based on daily precipitation records at 800 Weather Bureau and cooperative stations.

Chart III. A. Departure of Precipitation from Normal (Inches), January 1954.

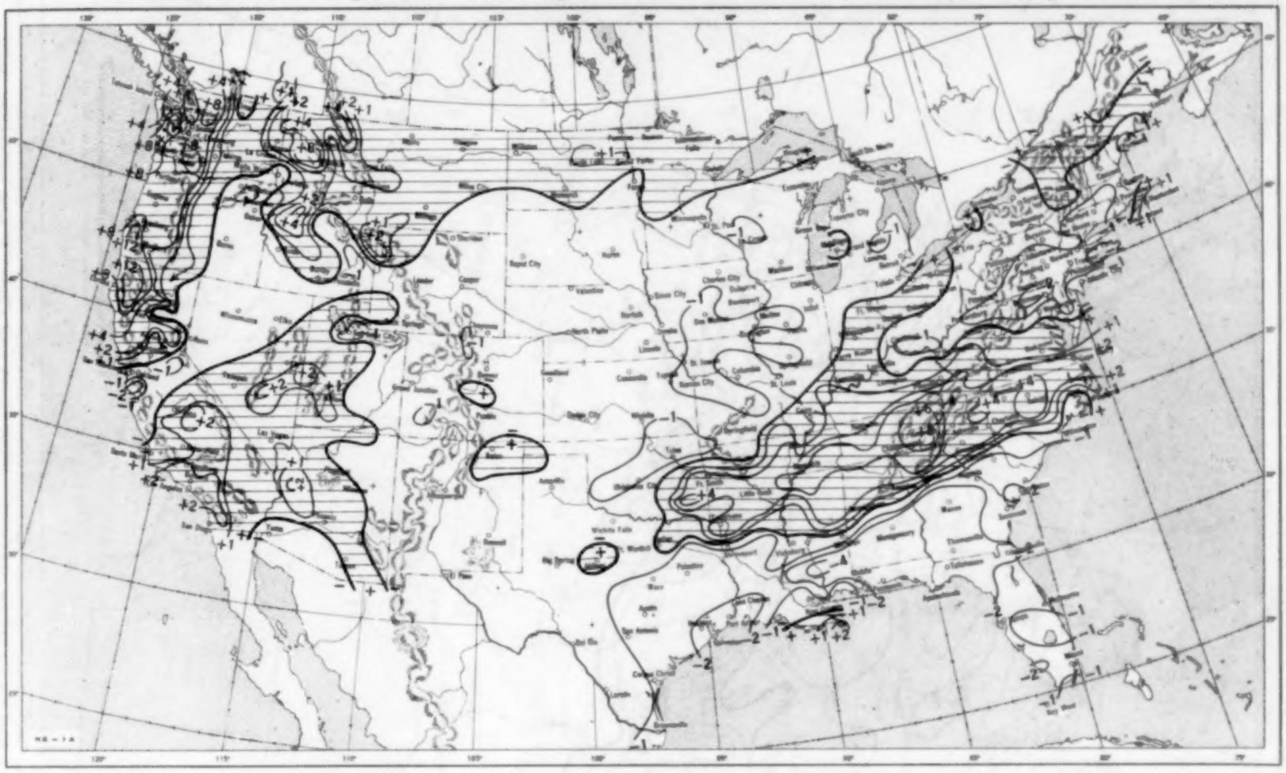

B. Percentage of Normal Precipitation, January 1954.

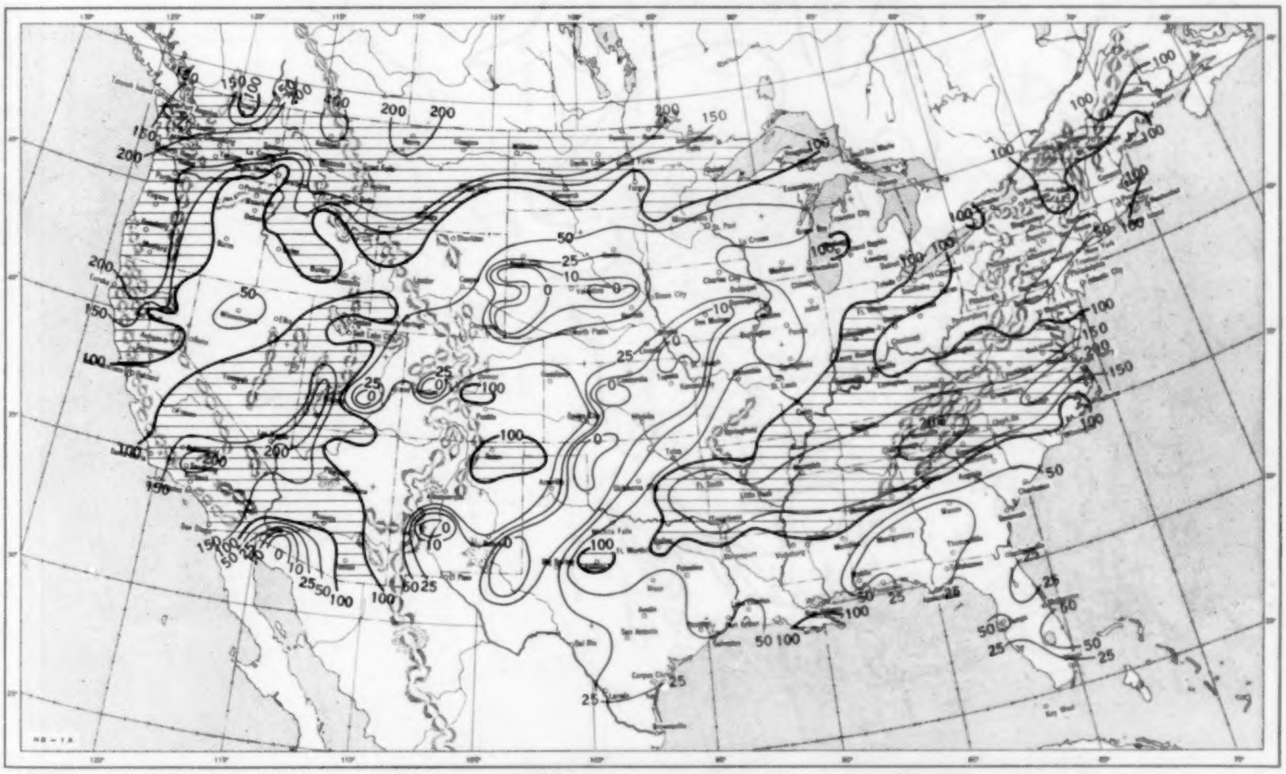

Normal monthly precipitation amounts are computed for stations having at least 10 years of record.

Chart IV. Total Snowfall (Inches), January 1954.

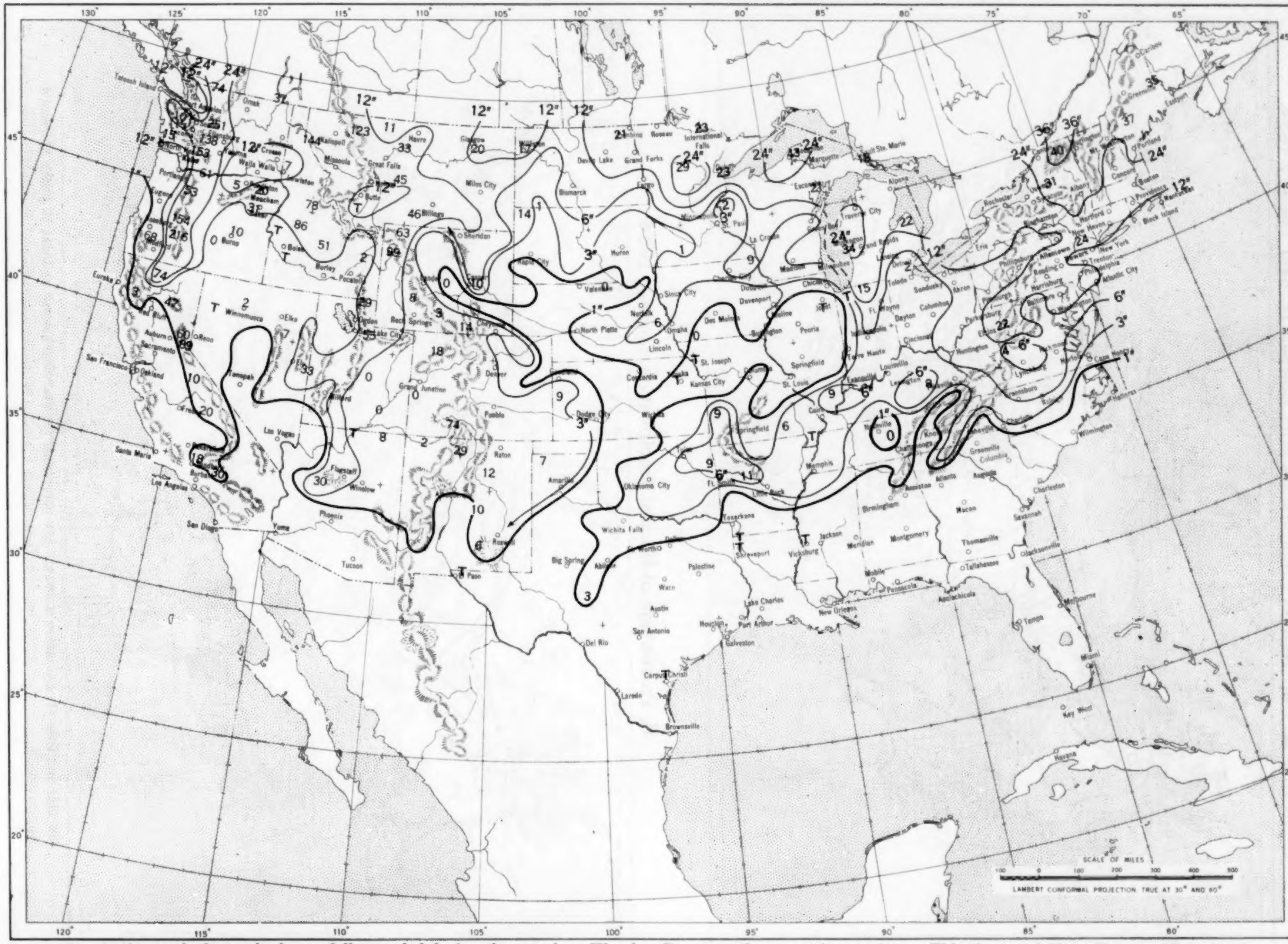

This is the total of unmelted snowfall recorded during the month at Weather Bureau and cooperative stations. This chart and Chart V are published only for the months of November through April although of course there is some snow at higher elevations, particularly in the far West, earlier and later in the year.

Chart V. A. Percentage of Normal Snowfall, January 1954.

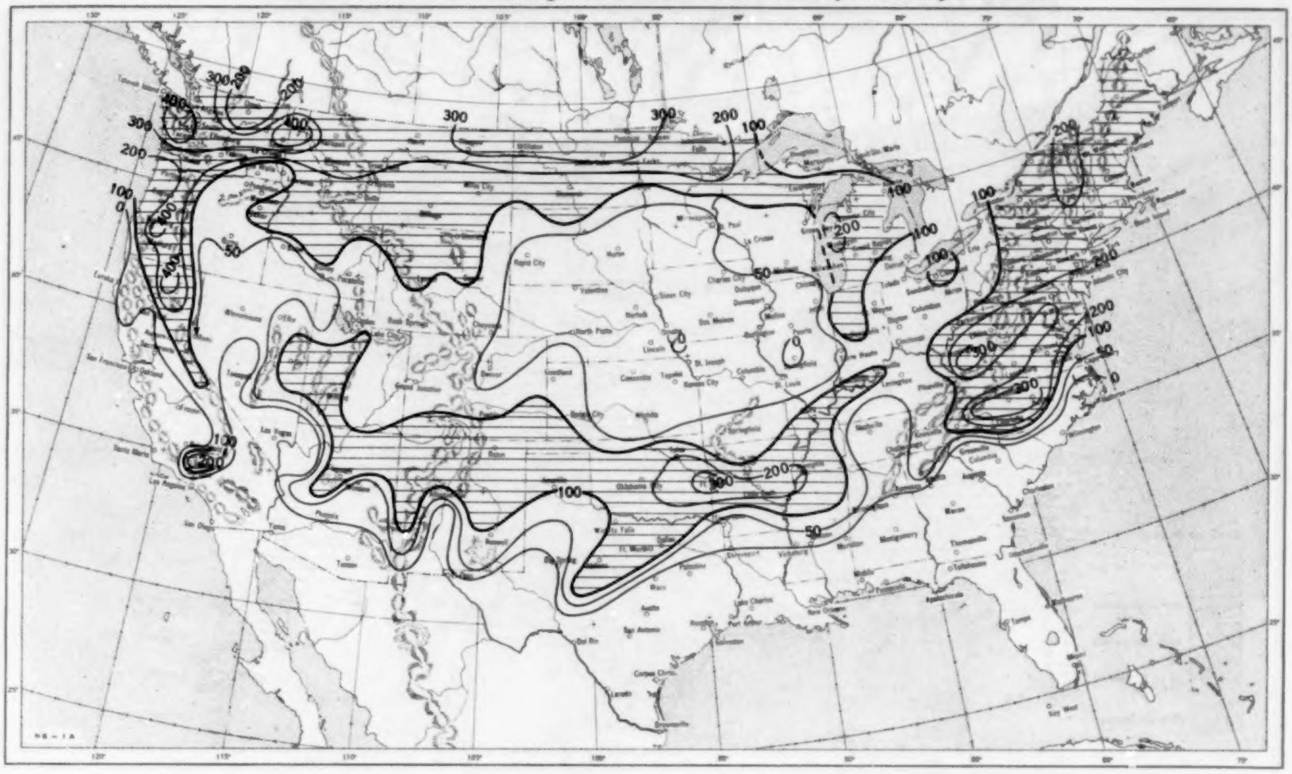

B. Depth of Snow on Ground (Inches), 7:30 a. m. E. S. T., January 26, 1954.

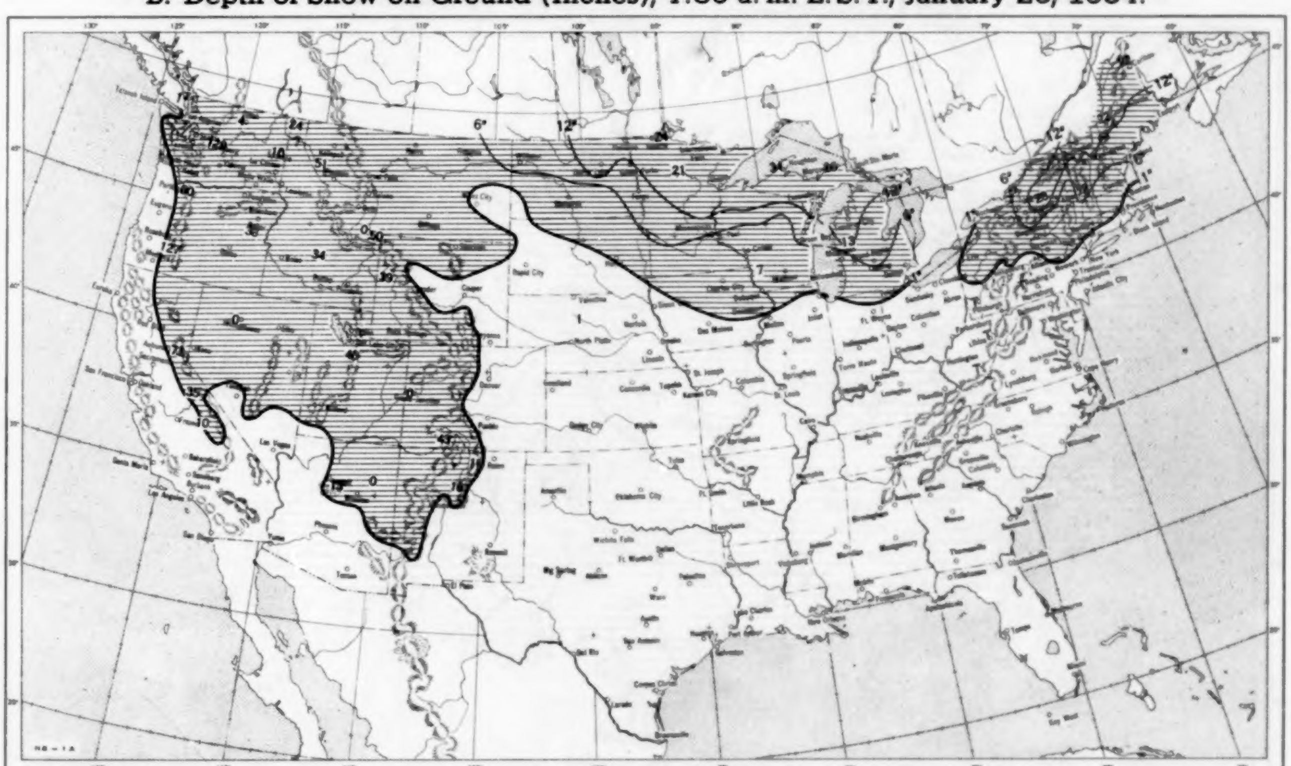

A. Amount of normal monthly snowfall is computed for Weather Bureau stations having at least 10 years of record. B. Shows depth currently on ground at 7:30 a. m. E.S.T., of the Tuesday nearest the end of the month. It is based on reports from Weather Bureau and cooperative stations. Dashed line shows greatest southern extent of snowcover during month.

Chart VI. A. Percentage of Sky Cover Between Sunrise and Sunset, January 1954.

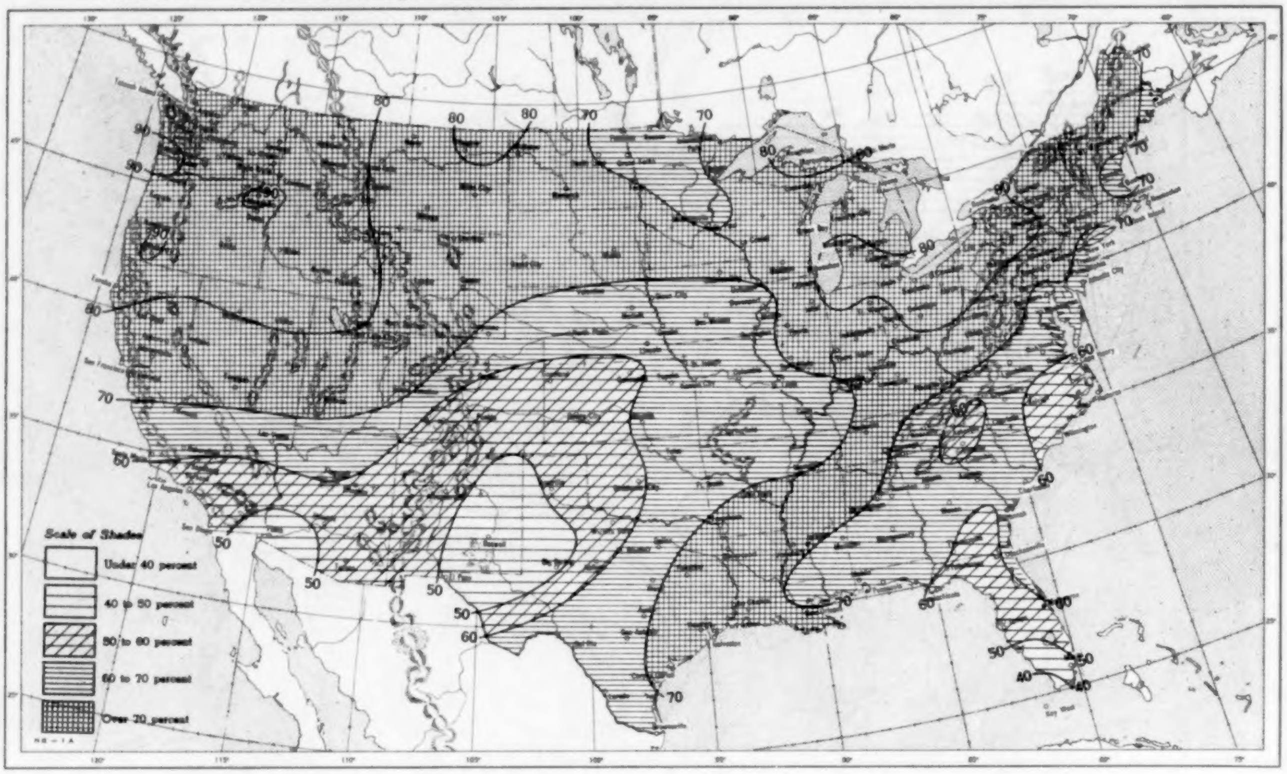

B. Percentage of Normal Sky Cover Between Sunrise and Sunset, January 1954.

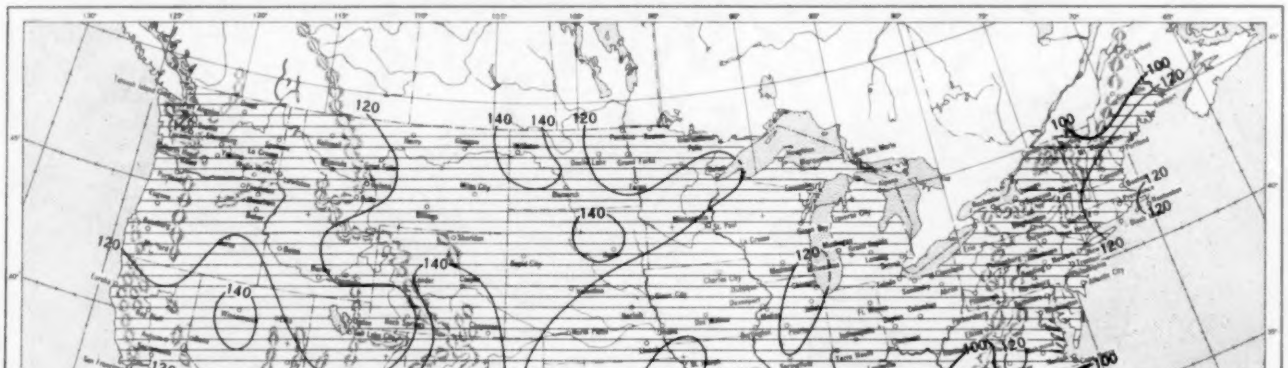

A. In addition to cloudiness, sky cover includes obscuration of the sky by fog, smoke, snow, etc. Chart based on visual observations made hourly at Weather Bureau stations and averaged over the month. B. Computations of normal amount of sky cover are made for stations having at least 10 years of record.

Chart VII. A. Percentage of Possible Sunshine, January 1954.

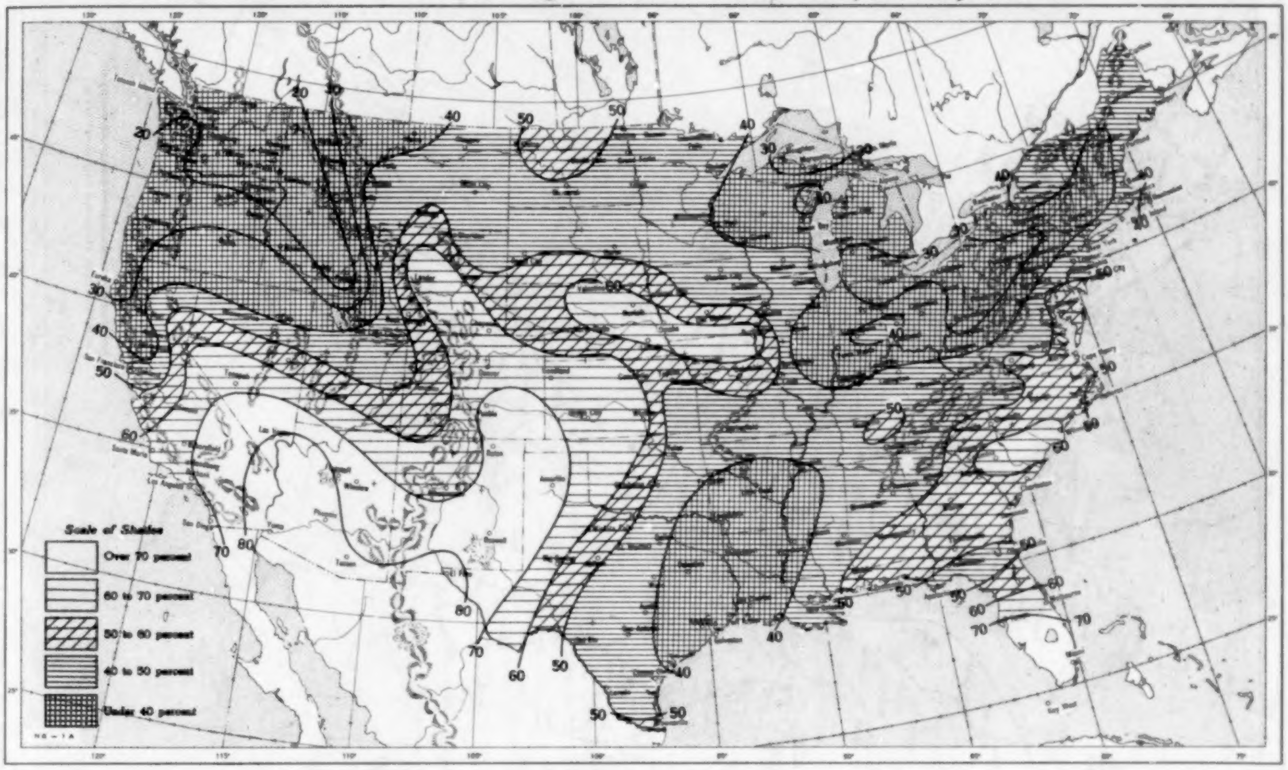

B. Percentage of Normal Sunshine, January 1954.

A. Computed from total number of hours of observed sunshine in relation to total number of possible hours of sunshine during month. B. Normals are computed for stations having at least 10 years of record.

Chart VIII. Average Daily Values of Solar Radiation, Direct + Diffuse, January 1954. Inset: Percentage of Normal Average Daily Solar Radiation, January 1954.

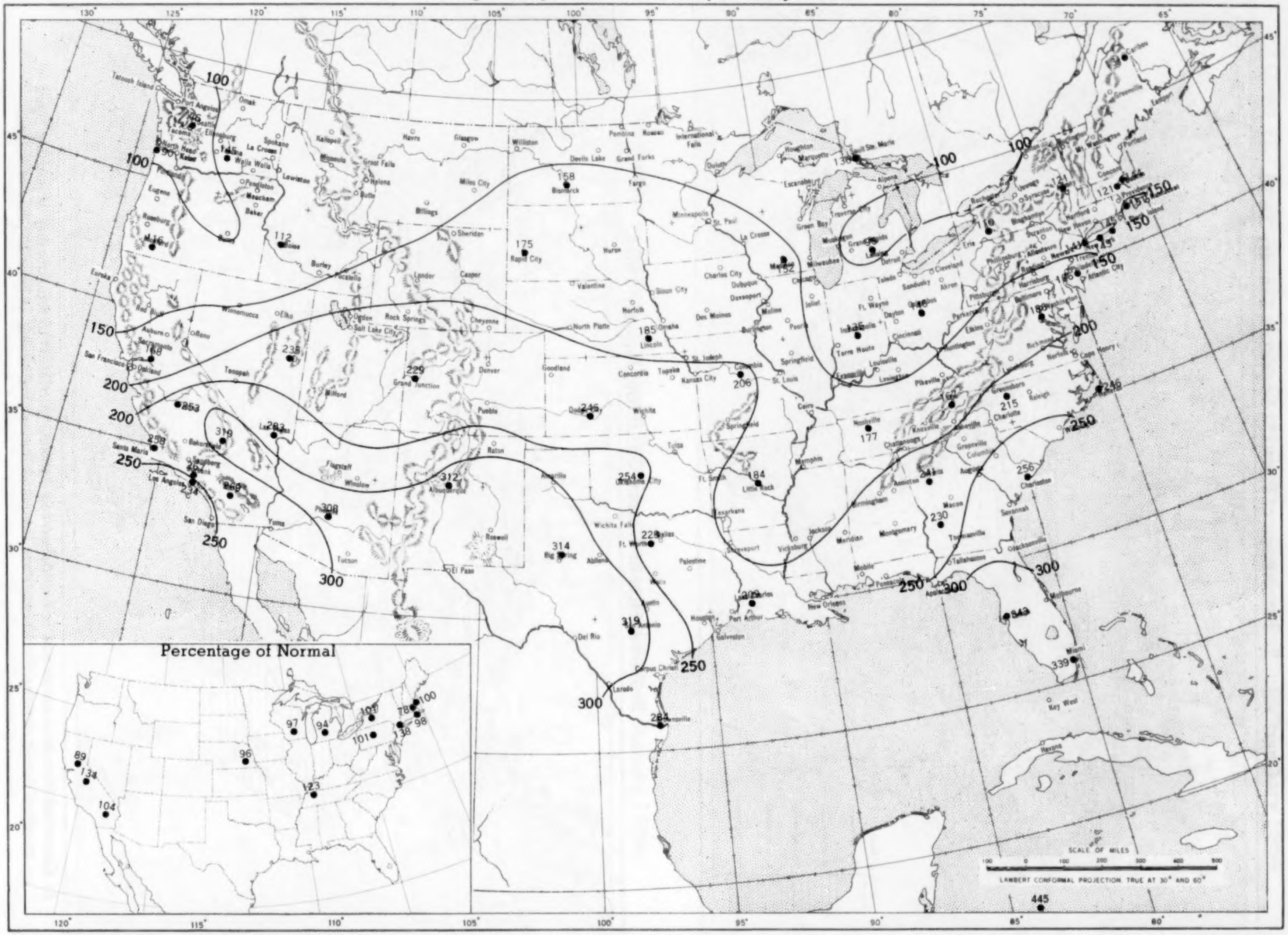

Chart shows mean daily solar radiation, direct + diffuse, received on a horizontal surface in langleys (1 langley = 1 gm. cal. cm. $^{-2}$). Basic data for isolines are shown on chart. Further estimates are obtained from supplementary data for which limits of accuracy are wider than for those data shown. Normals are computed for stations having at least 9 years of record.

Chart IX. Tracks of Centers of Anticyclones at Sea Level, January 1954.

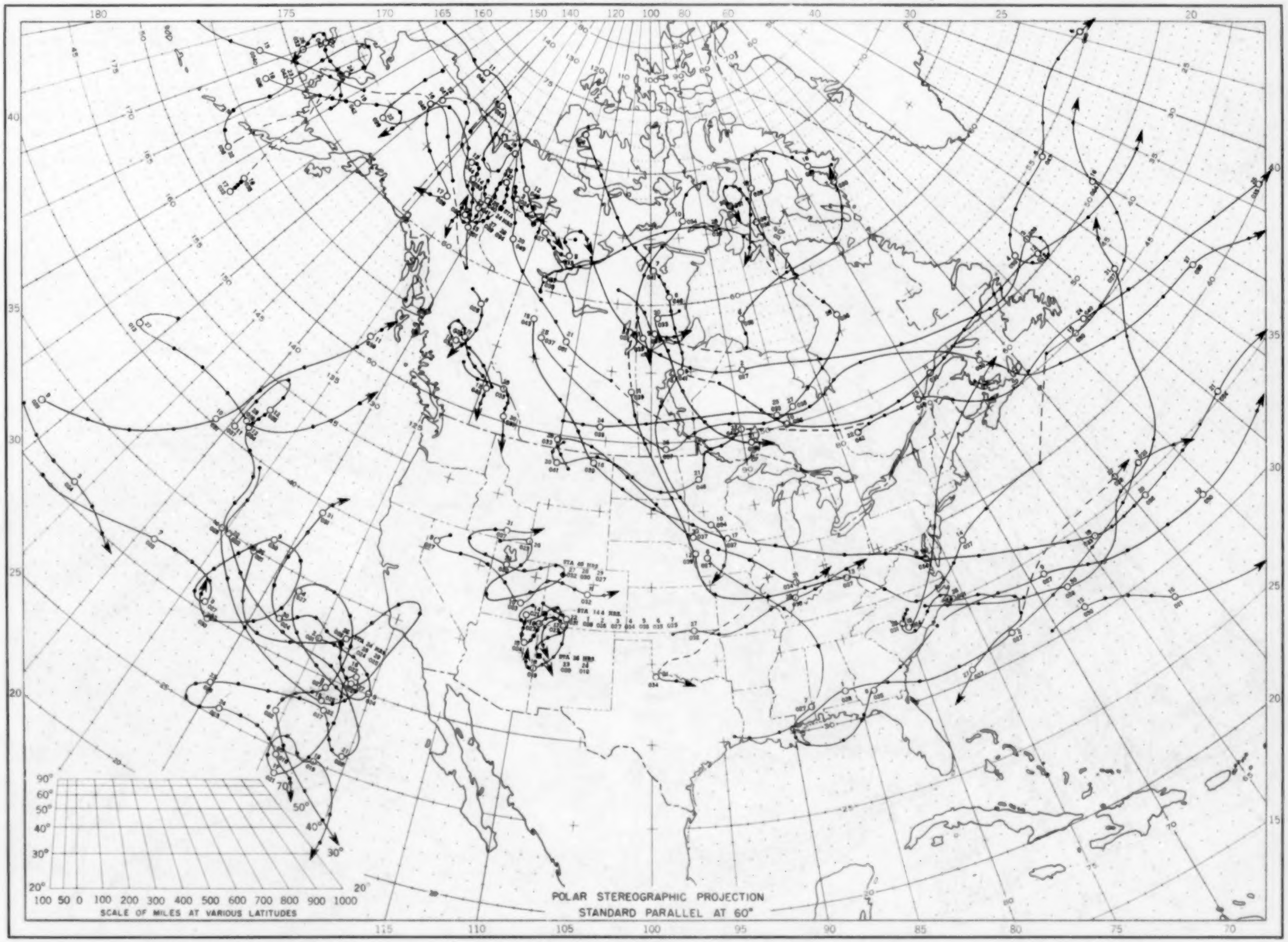

Circle indicates position of center at 7:30 a. m. E. S. T. Figure above circle indicates date, figure below, pressure to nearest millibar. Dots indicate intervening 6-hourly positions. Squares indicate position of stationary center for period shown. Dashed line in track indicates reformation at new position. Only those centers which could be identified for 24 hours or more are included.

Chart X. Tracks of Centers of Cyclones at Sea Level, January 1954.

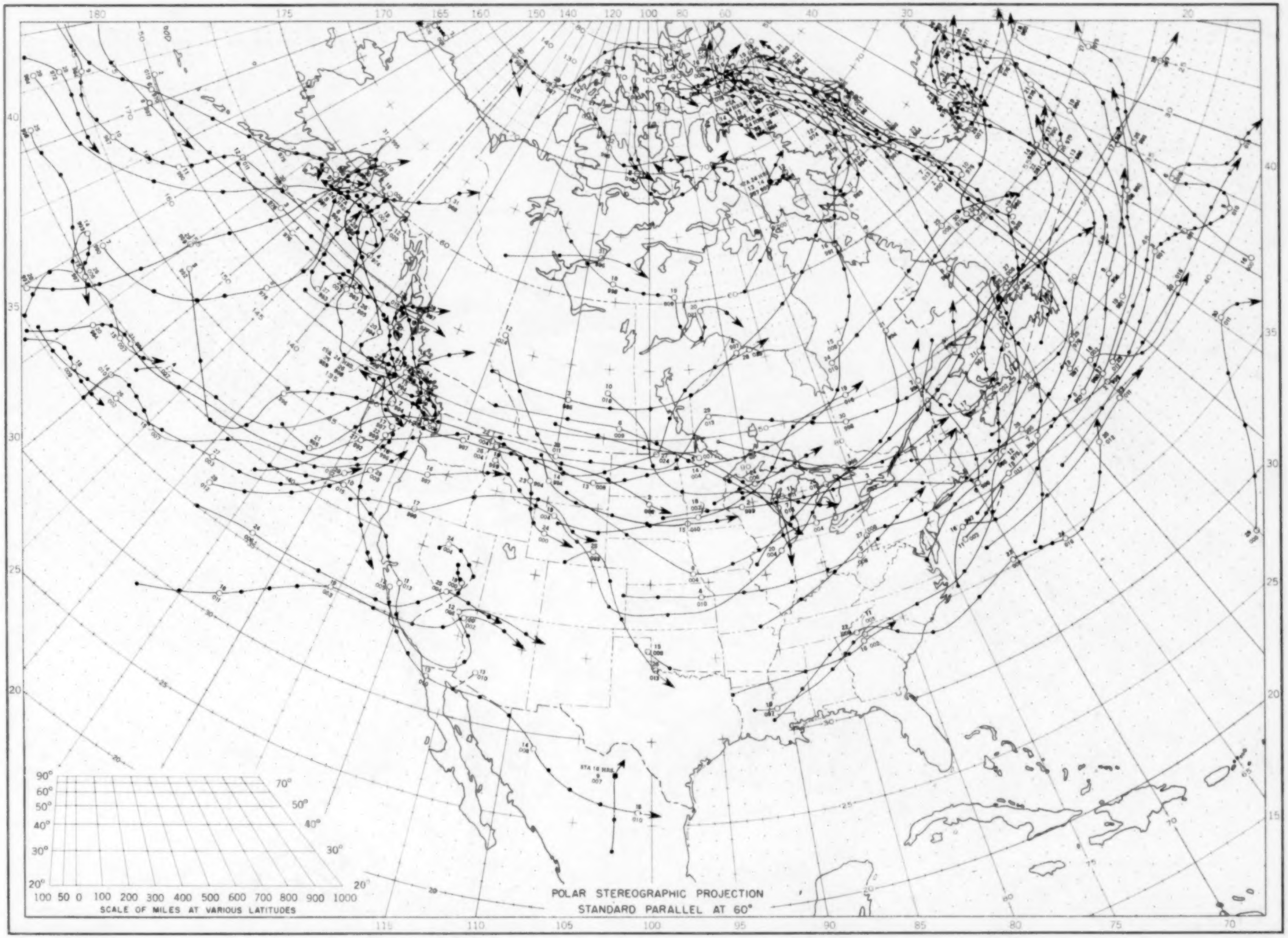

Circle indicates position of center at 7:30 a. m. E. S. T. See Chart IX for explanation of symbols.

Chart XI. Average Sea Level Pressure (mb.) and Surface Windroses, January 1954. Inset: Departure of Average Pressure (mb.) from Normal, January 1954.

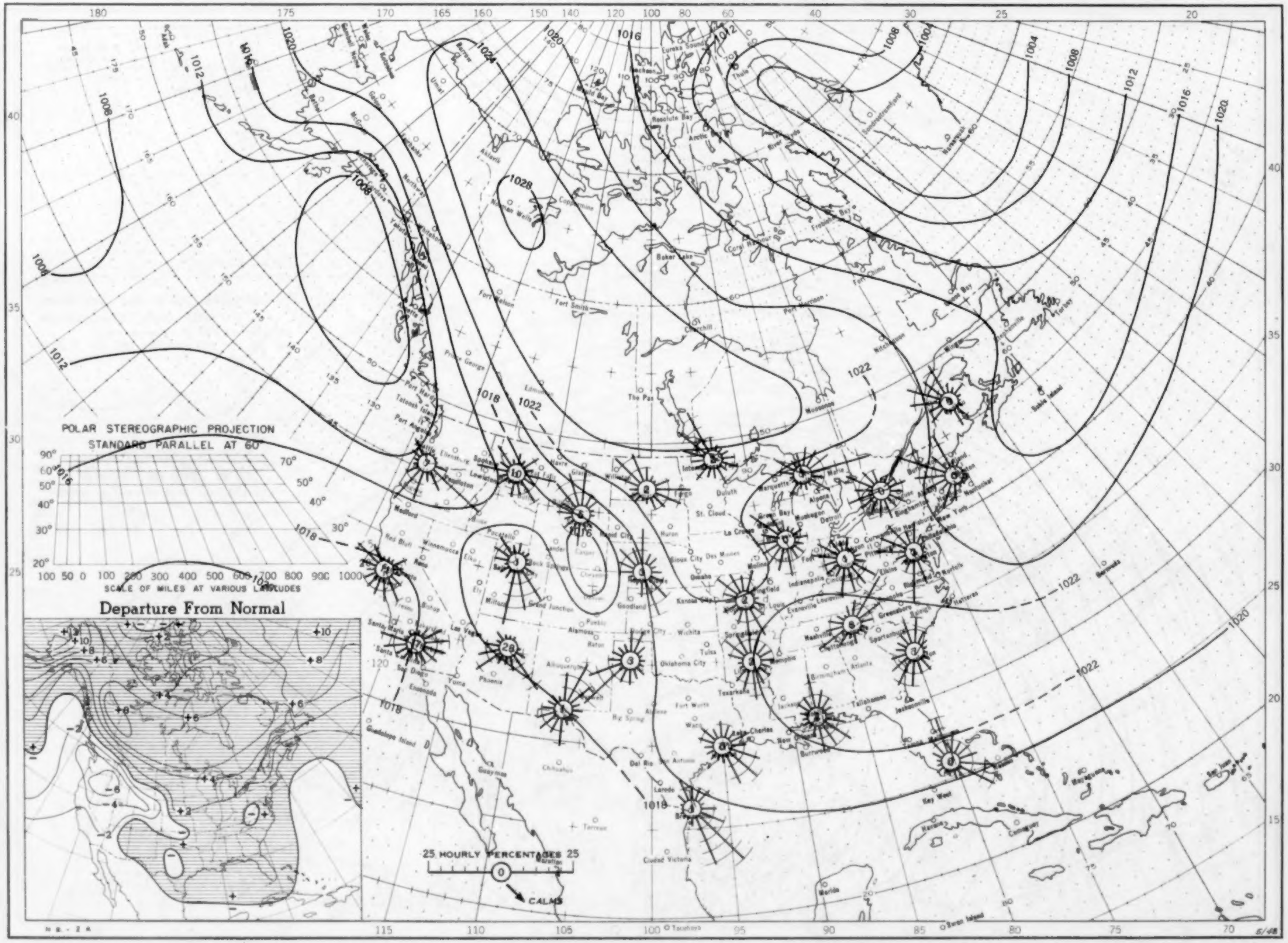

Average sea level pressures are obtained from the averages of the 7:30 a.m. and 7:30 p.m. E.S.T. readings. Windroses show percentage of time wind blew from 16 compass points or was calm during the month. Pressure normals are computed for stations having at least 10 years of record and for 10° intersections in a diamond grid based on readings from the Historical Weather Maps (1899-1939) for the 20 years of most complete data coverage prior to 1940.

Chart XII. Average Dynamic Height in Geopotential Meters (1 g.p.m. = 0.98 dynamic meters) of the 850-mb. Pressure Surface, Average Temperature in °C. at 850 mb., and Resultant Winds at 1500 Meters (m.s.l.), January 1954.

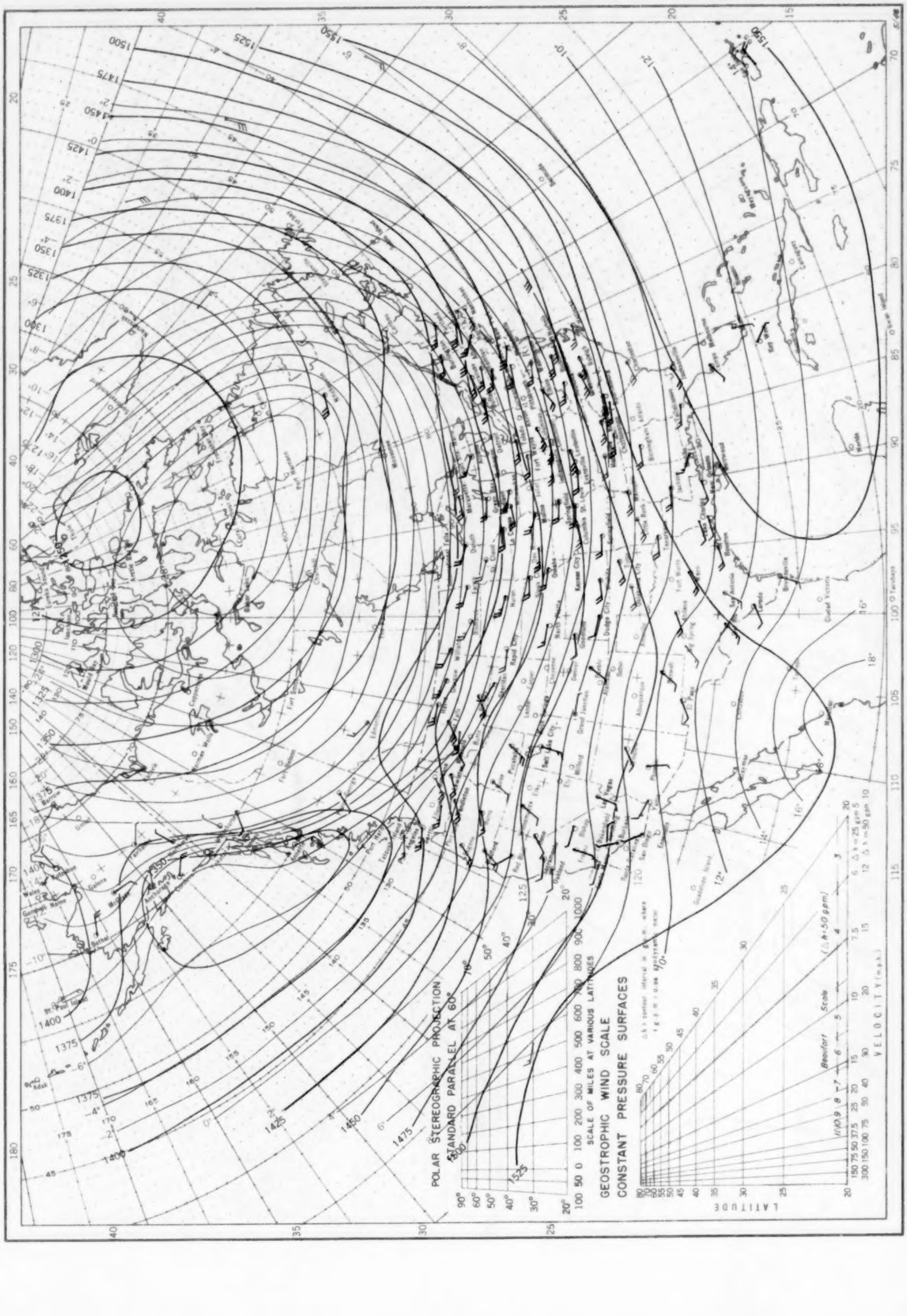

Contour lines and isotherms based on radiosonde observations at 0300 G. M. T. Winds shown in black are based on pilot balloon observations at 2100 G. M. T.; those shown in red are based on rawins taken at 0300 G. M. T. Wind barbs indicate wind speed on the Beaufort scale.

Chart XIII. Average Dynamic Height in Geopotential Meters (1 g.p.m.. = 0.98 dynamic meters) of the 700-mb. Pressure Surface, Average Temperature in °C. at 700 mb., and Resultant Winds at 3000 Meters (m.s.l.), January 1954.

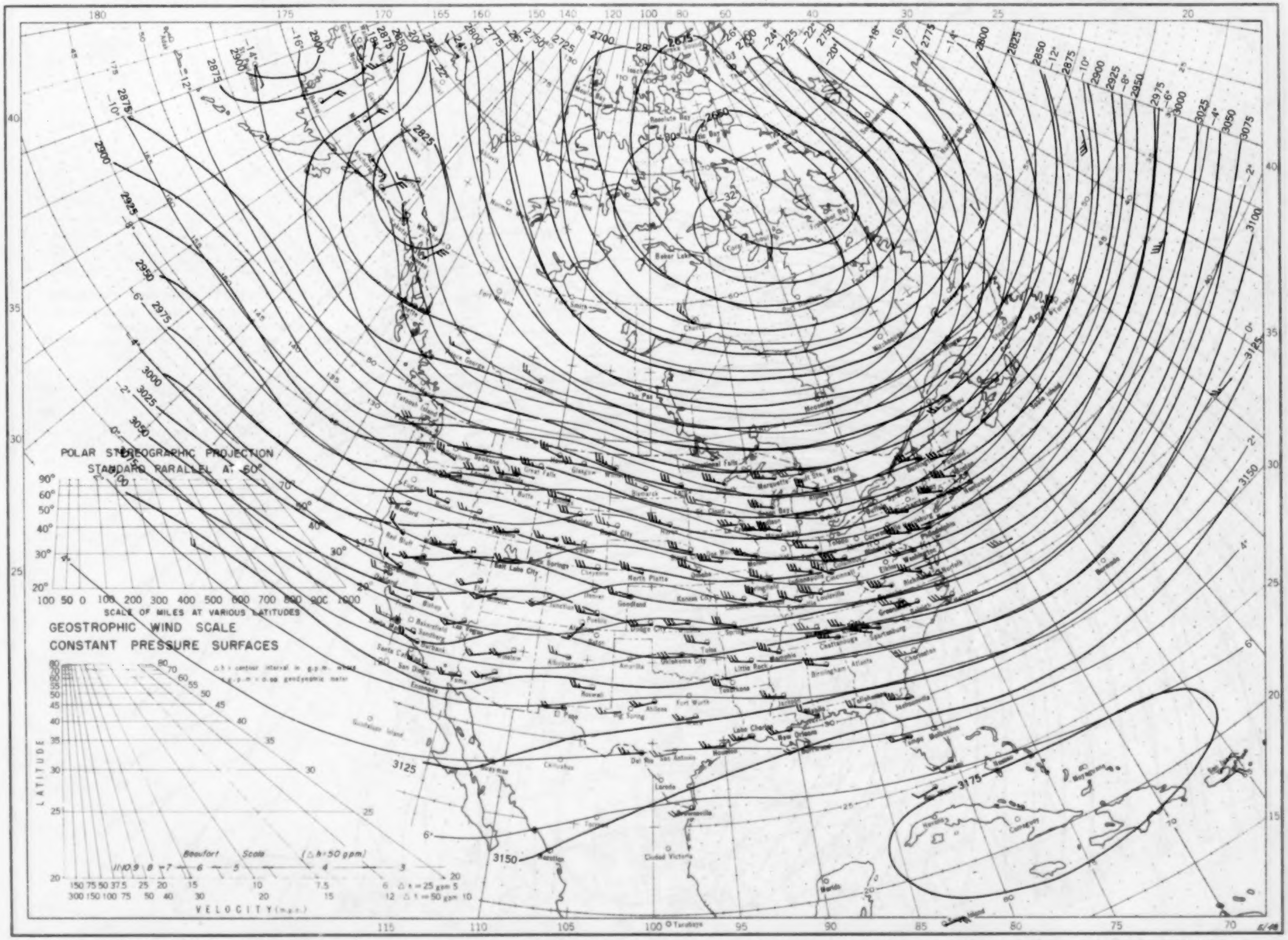

Contour lines and isotherms based on radiosonde observations at 0300 G. M. T. Winds shown in black are based on pilot balloon observations at 2100 G. M. T.; those shown in red are based on rawins taken at 0300 G. M. T. Wind barbs indicate wind speed on the Beaufort scale.

Chart XIV. Average Dynamic Height in Geopotential Meters (1 g.p.m. = 0.98 dynamic meters) of the 500-mb. Pressure Surface, Average Temperature in °C. at 500 mb., and Resultant Winds at 5000 Meters (m.s.l.), January 1954.

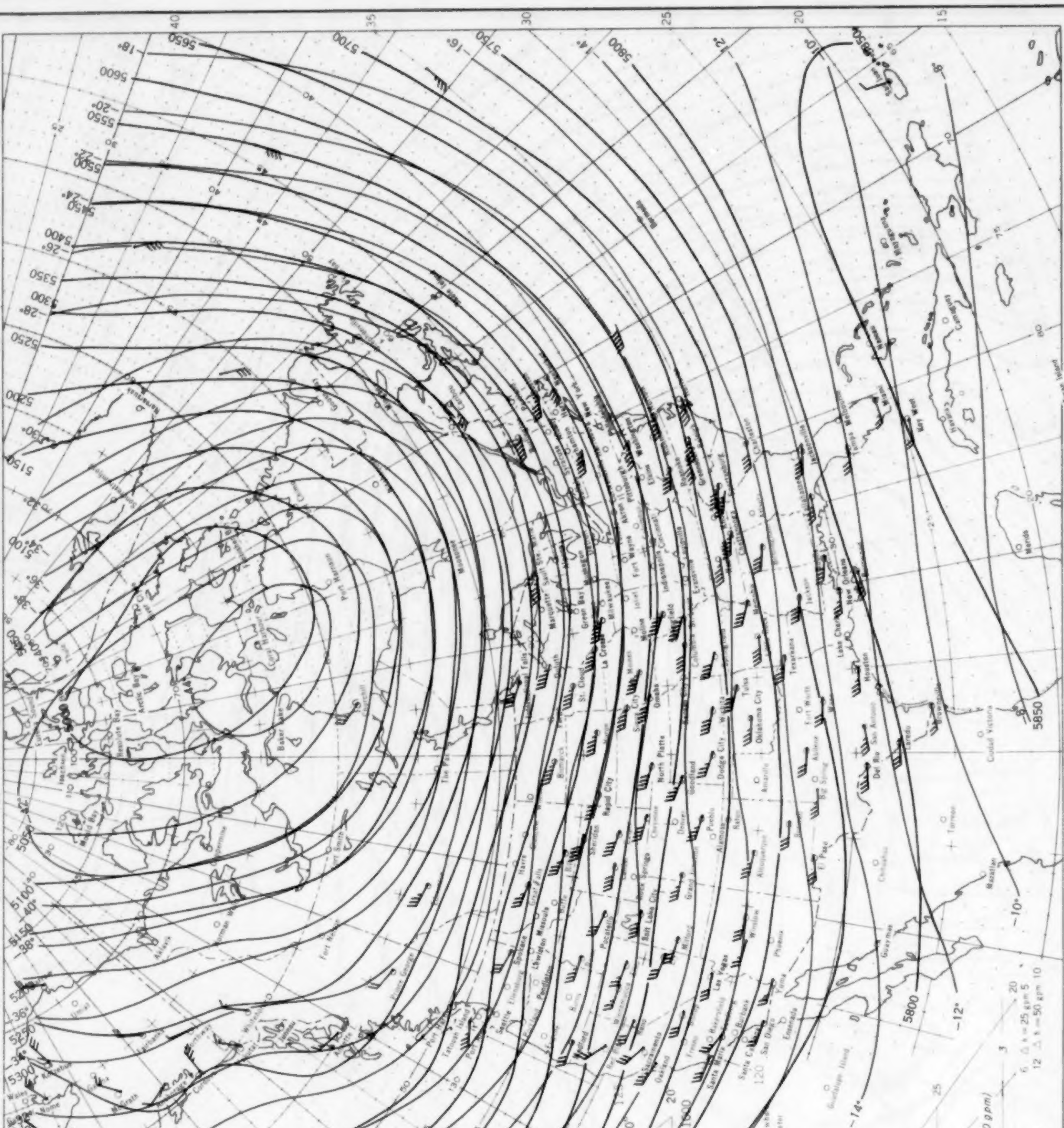

Contour lines and isotherms based on radiosonde observations at 0300 G. M. T. Winds shown in black are based on pilot balloon observations at 2100 G. M. T.; those shown in red are based on rawins at 0300 G. M. T. Wind barbs indicate wind speed on the Beaufort scale.

Chart XV. Average Dynamic Height in Geopotential Meters (1 g.p.m. = 0.98 dynamic meters) of the 300-mb. Pressure Surface, Average Temperature in °C. at 300 mb., and Resultant Winds at 10,000 Meters (m.s.l.), January 1954.

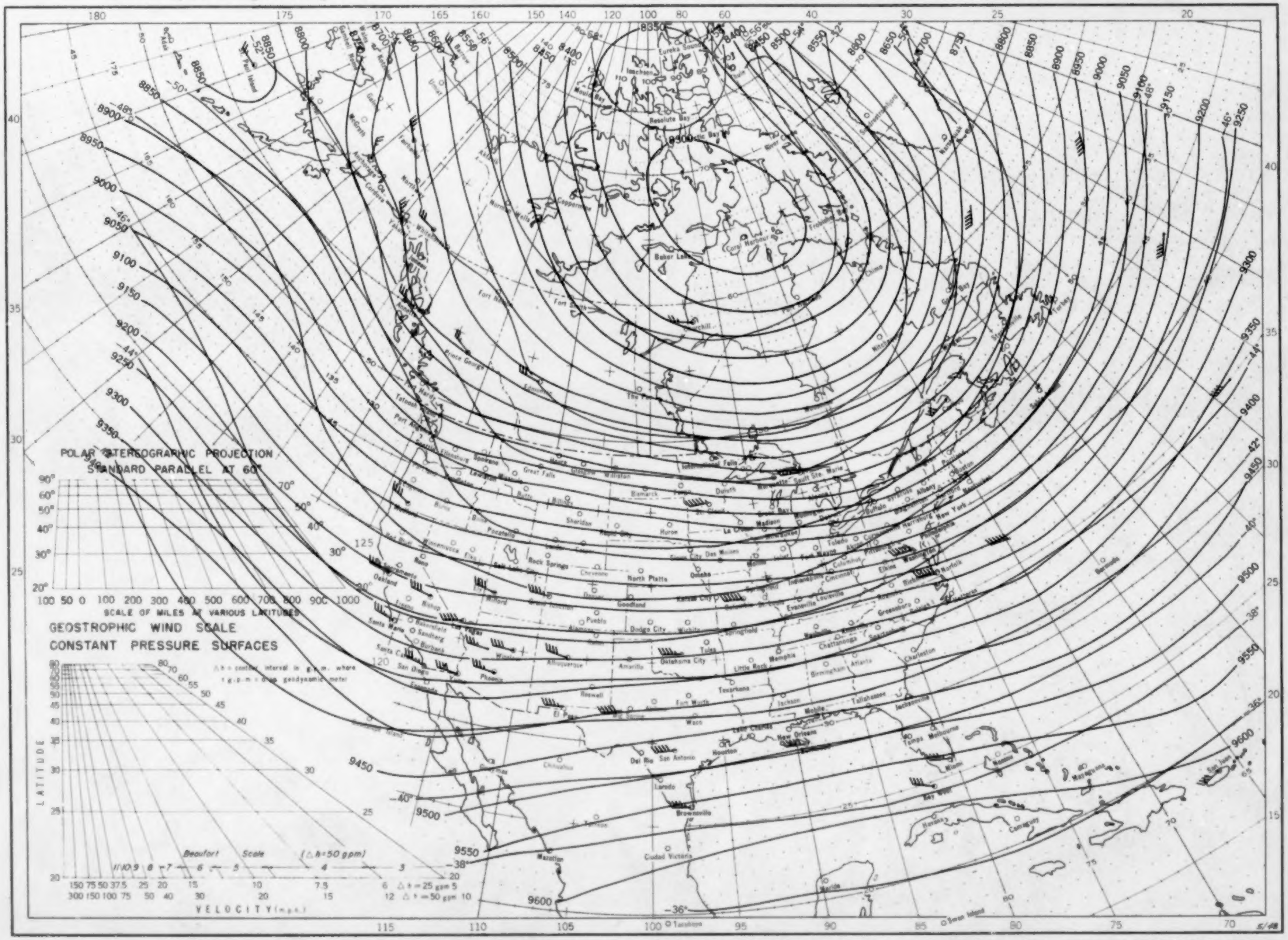

Contour lines and isotherms based on radiosonde observations at 0300 G. M. T. Winds shown in black are based on pilot balloon observations at 2100 G. M. T.; those shown in red are based on rawins at 0300 G. M. T. Wind barbs indicate wind speed on the Beaufort scale.